El Niño

EPS131, Introduction to Physical Oceanography and Climate
EPS 231 Climate dynamics
Dept of Earth and Planetary Sciences, Harvard University
Eli Tziperman

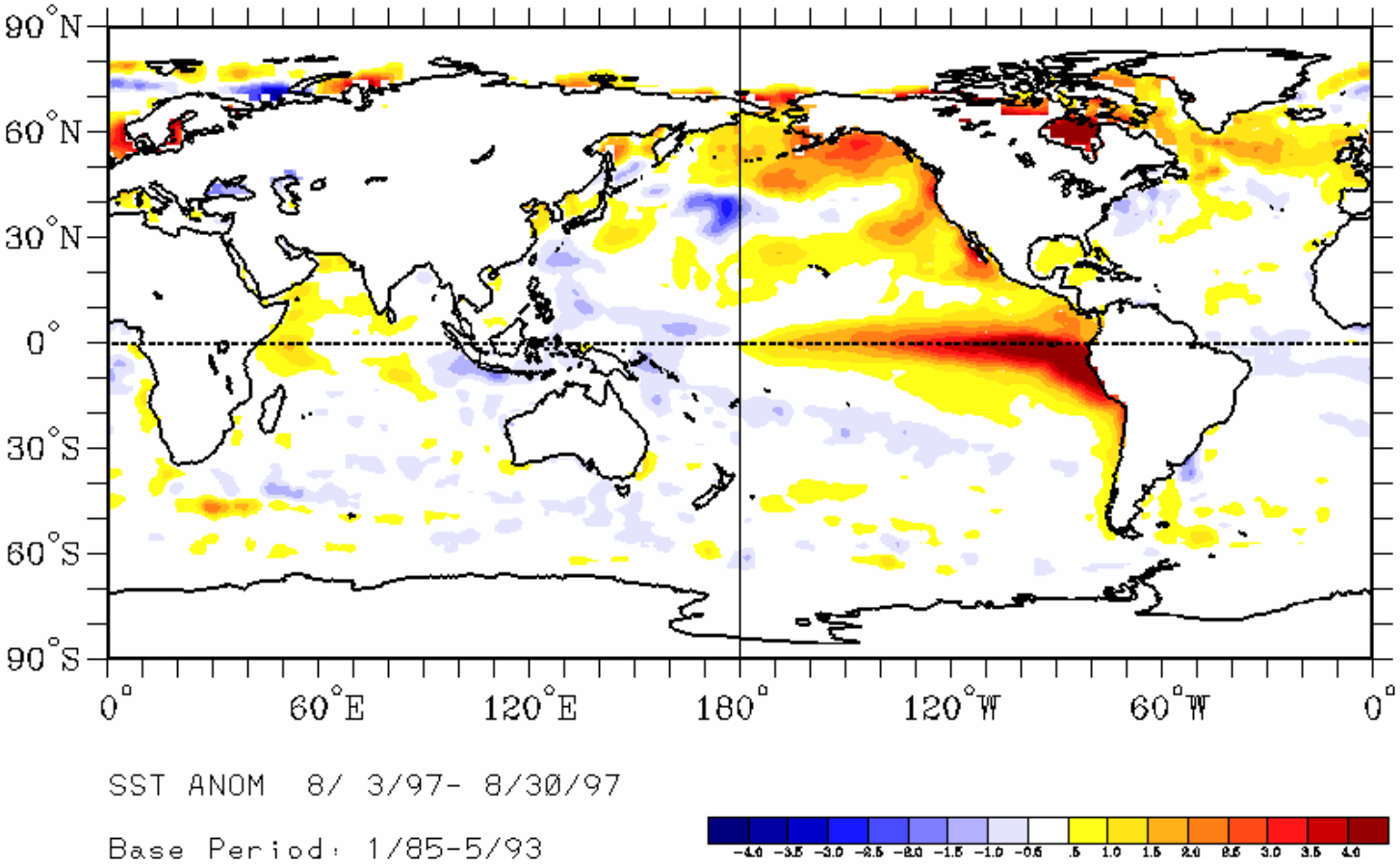

Development of an El Niño event: comparison of two major El Niño events

SST=Sea Surface Temperature

Climatological (long term time-mean) SST in tropical Pacific

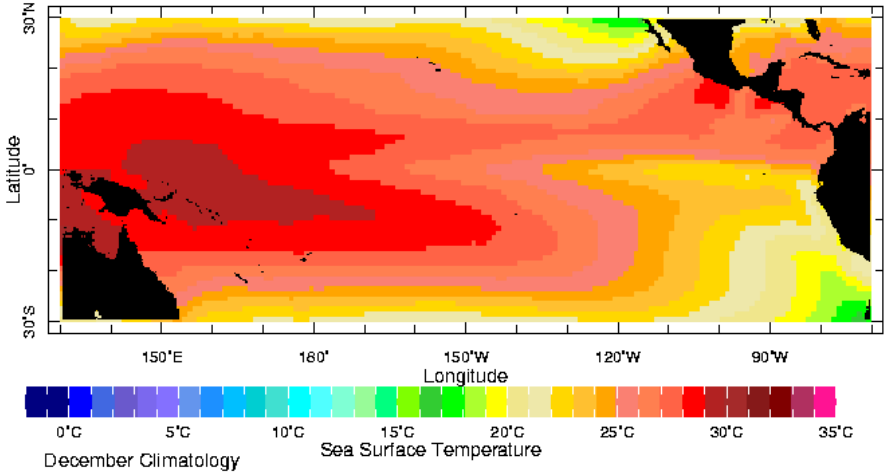

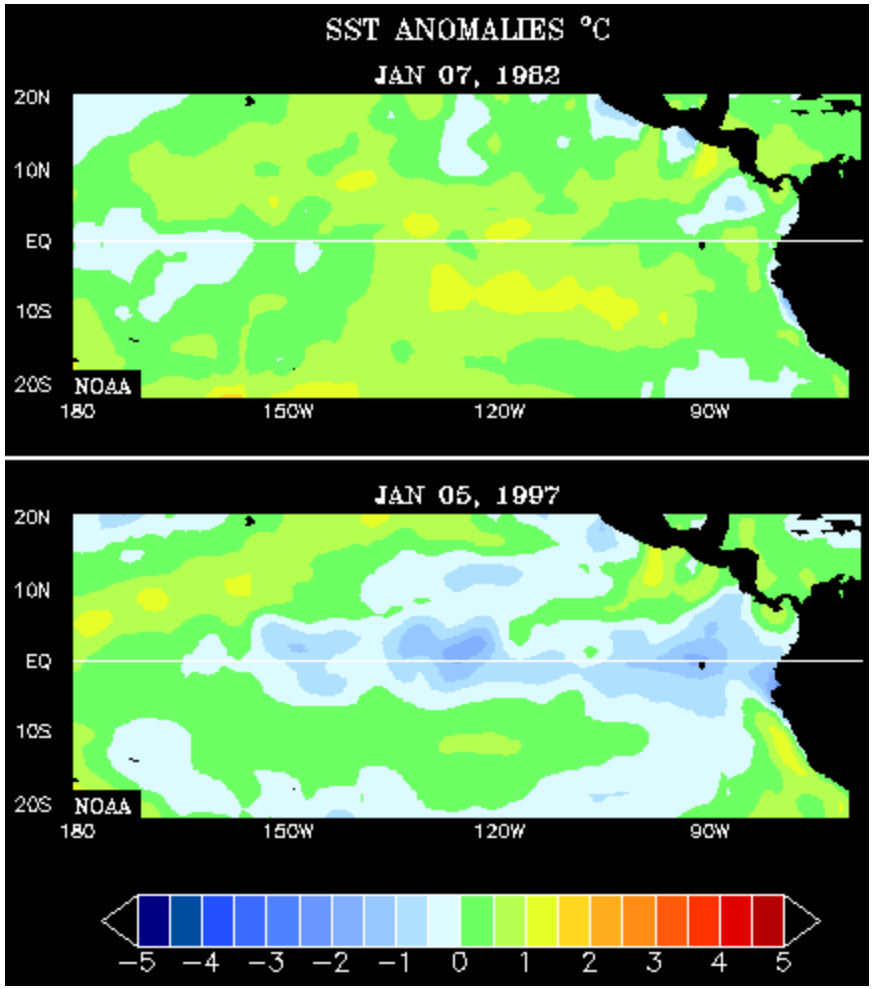

SST: deviation from climatology for 1982 & 1997 events

Development of an El Niño event: comparison of two major El Niño events

SST=Sea Surface Temperature

Climatological (long term time-mean) SST in tropical Pacific

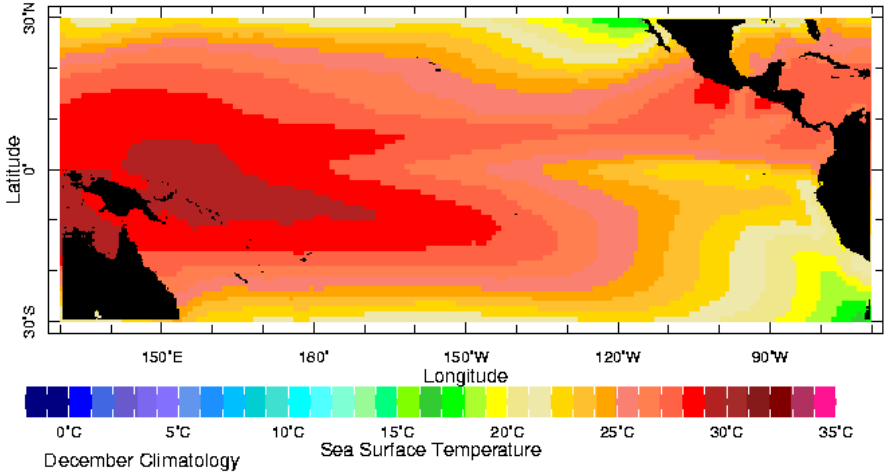

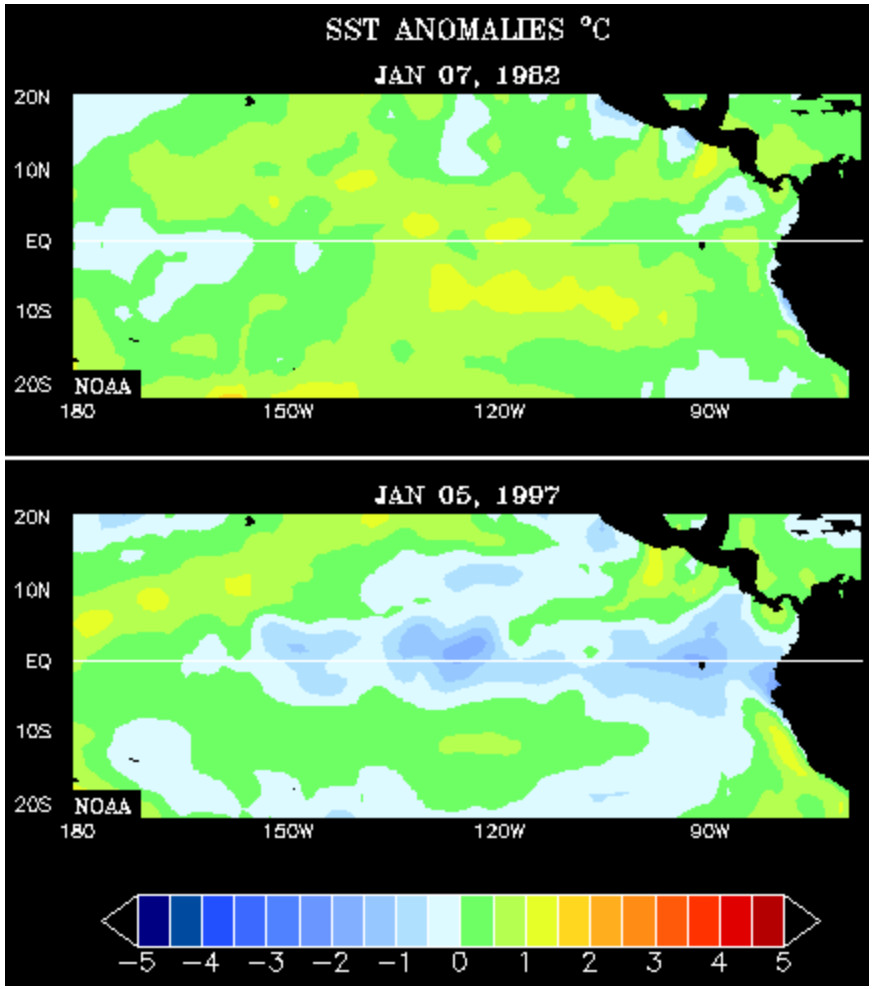

SST: deviation from climatology for 1982 & 1997 events

Development of an El Niño event: comparison of two major El Niño events – 1997, 2015

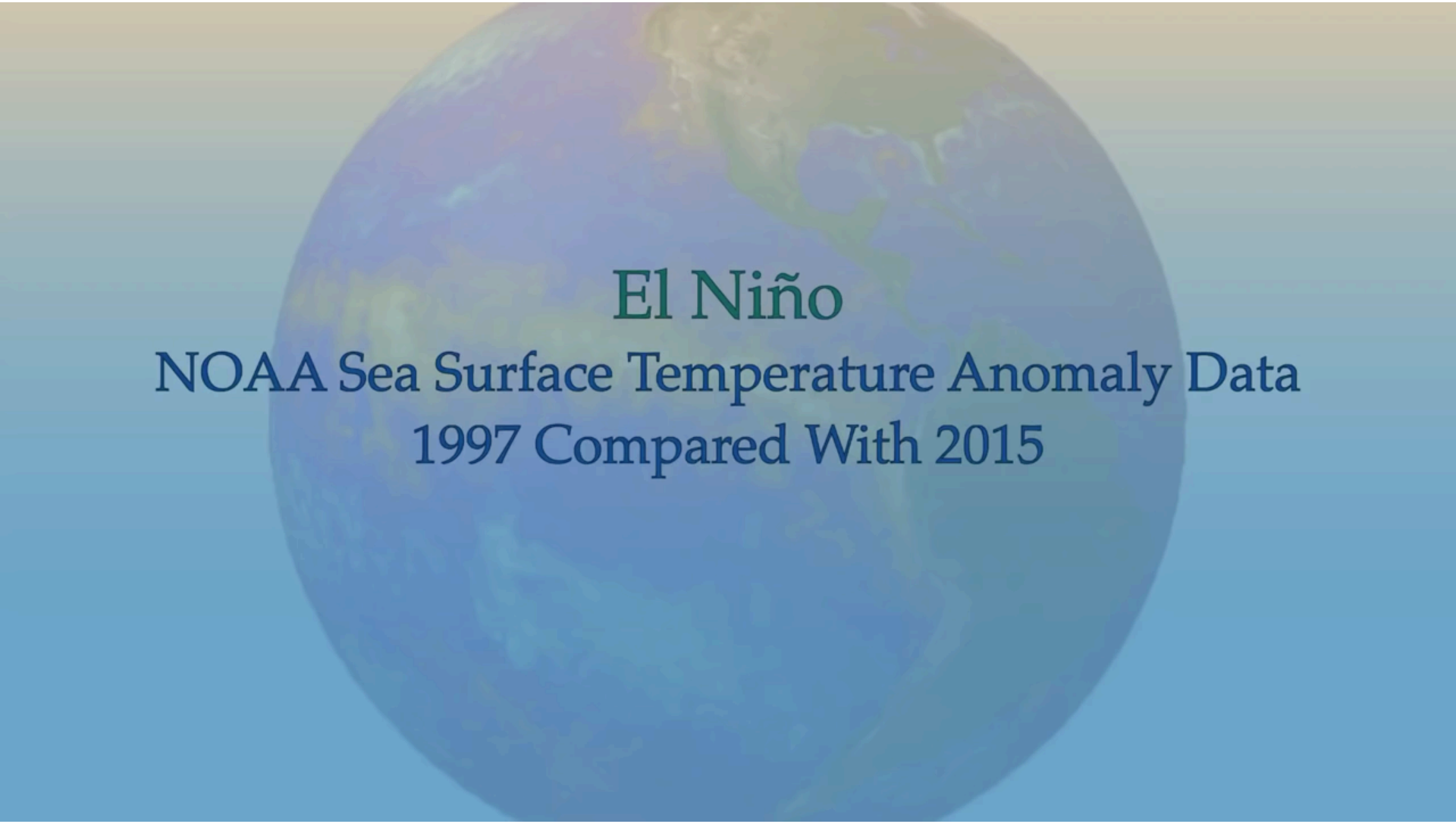

Development of an El Niño event: comparison of two major El Niño events – 1997, 2015

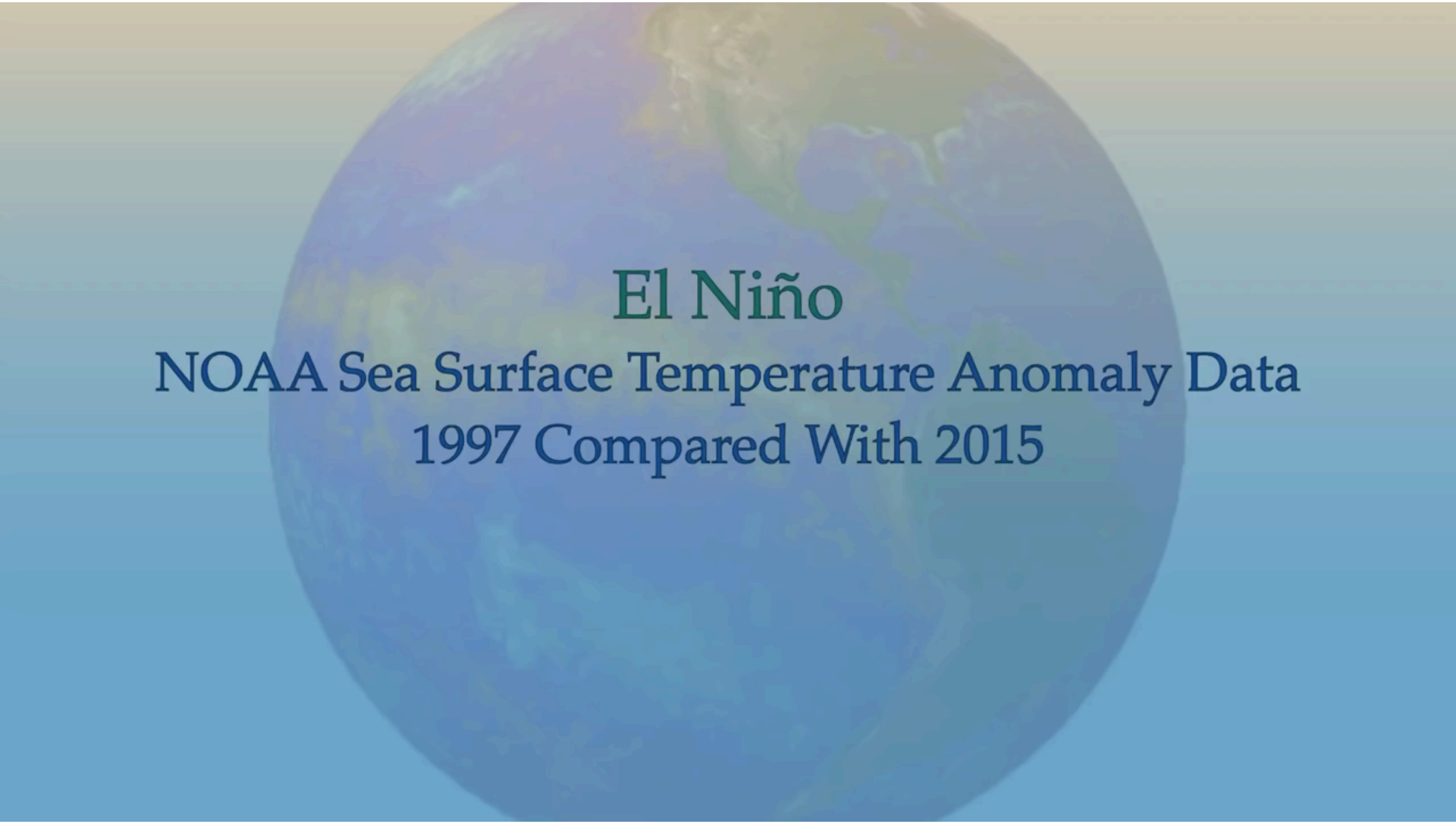

Development of an El Niño event: comparison of two major El Niño events – 1997, 2015

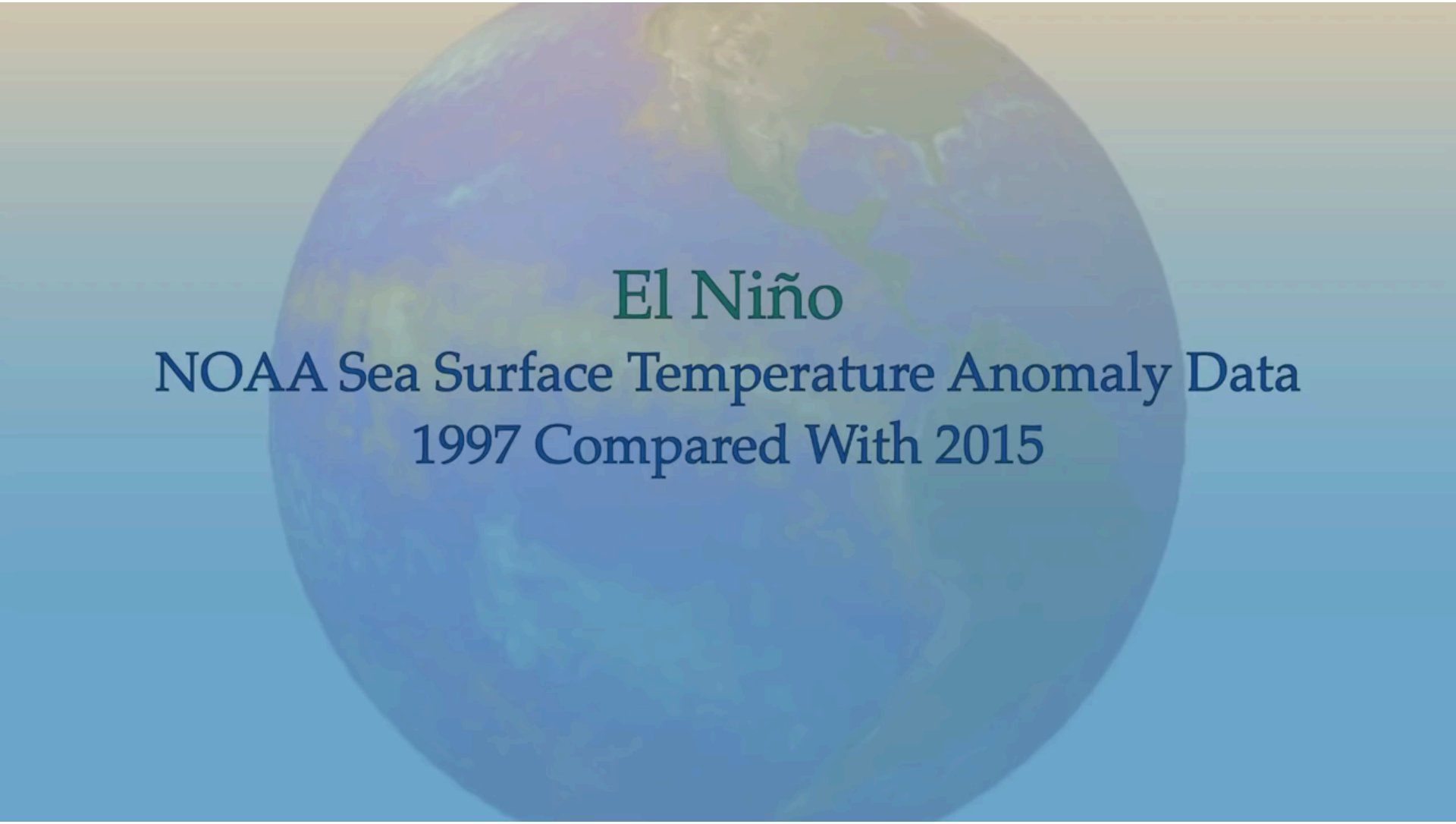

Mechanism: oscillations/transitions between two states: El Niño & La Niña

Transitions between two states

Period: 3–6 years

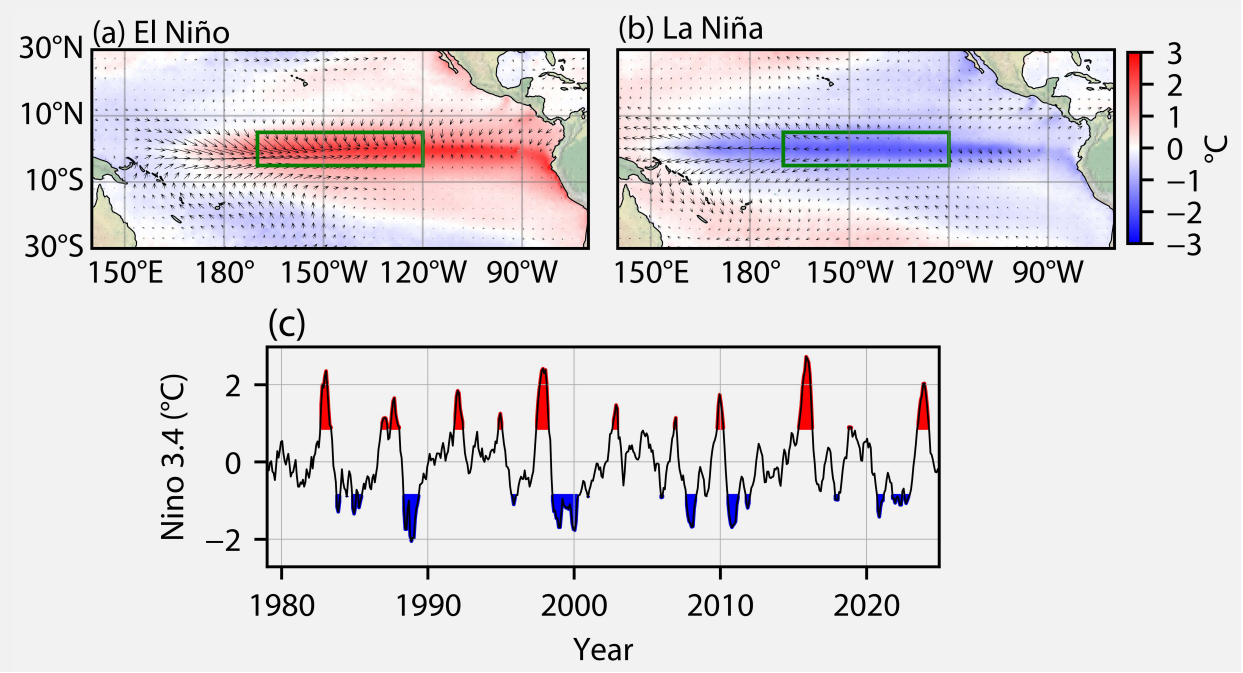

Mechanism: oscillations/transitions between two states: El Niño & La Niña

Transitions between two states

Period: 3–6 years

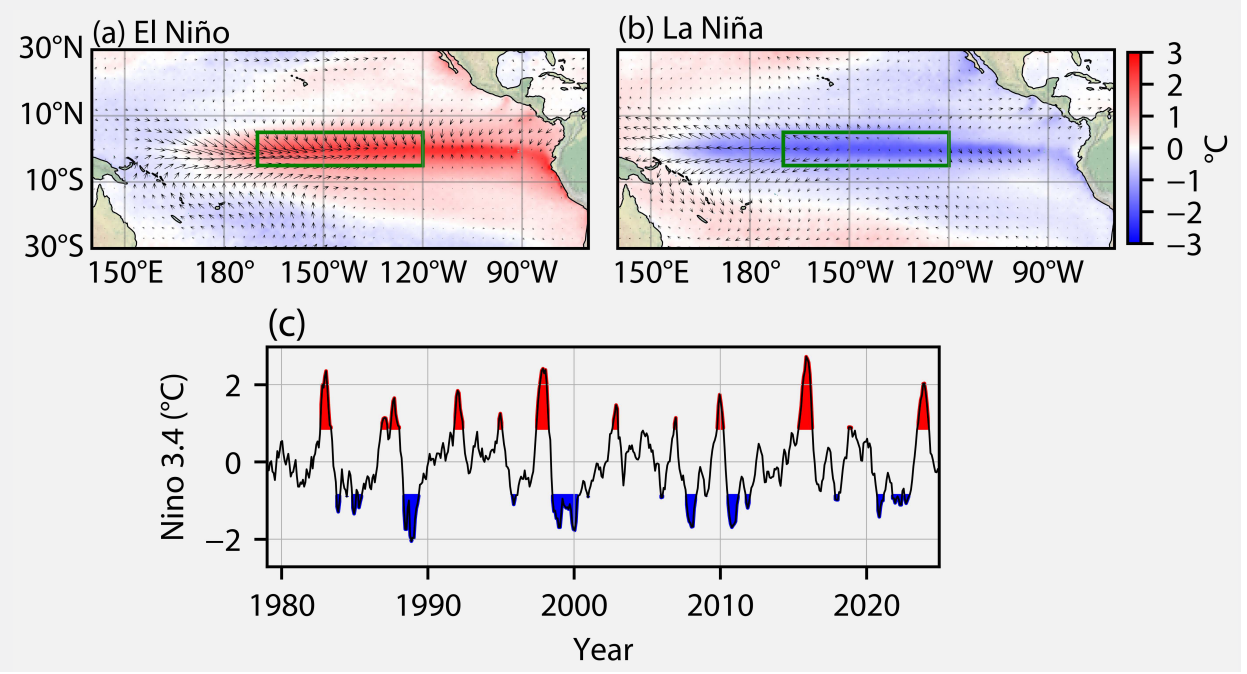

A longer record:

Decadal variability of El Niño Characteristics, possibly due to interaction with mid-latitudes

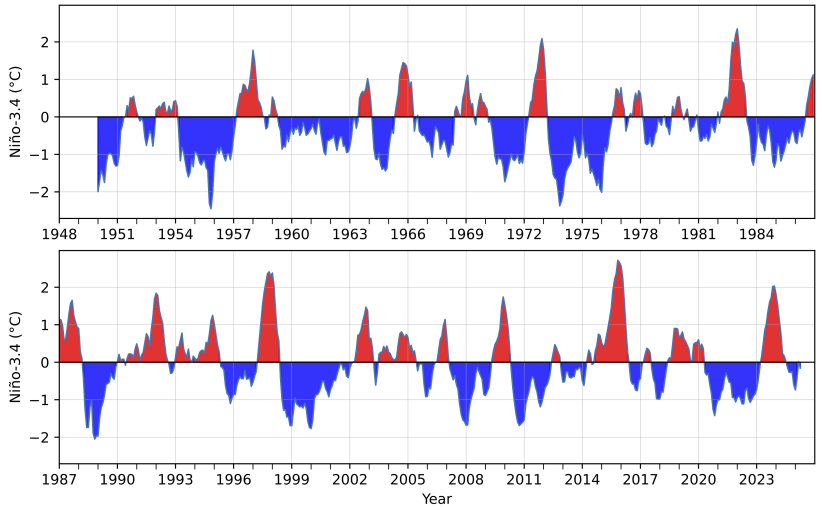

Mechanism: transitions between two states: El Niño & La Niña

El Niño:

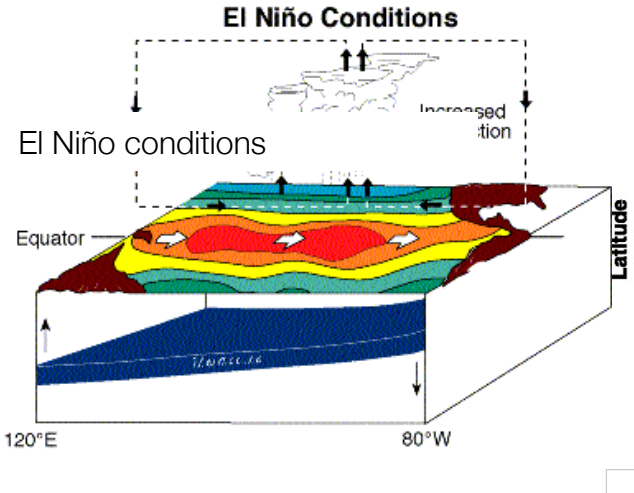

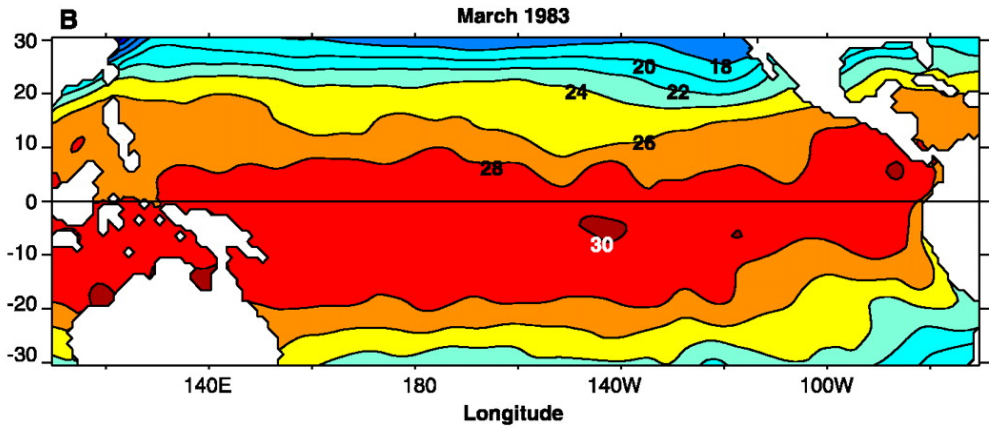

The major players:

Easterly Trade Winds → Thermocline;

Thermocline → sea surface temperature.

Eastward propagating Kelvin waves, westward Rossby Waves

Mechanism: transitions between two states: El Niño & La Niña

El Niño:

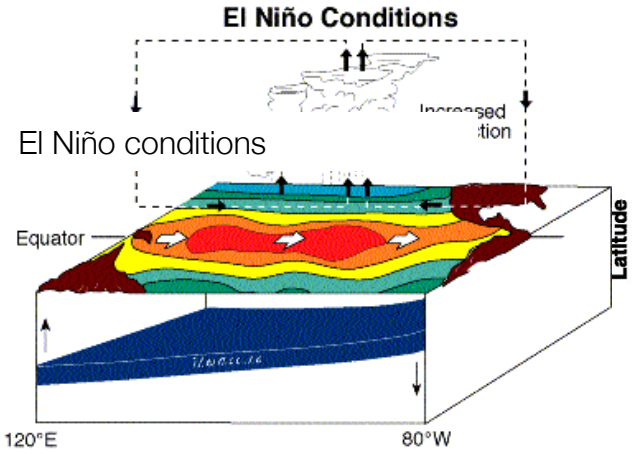

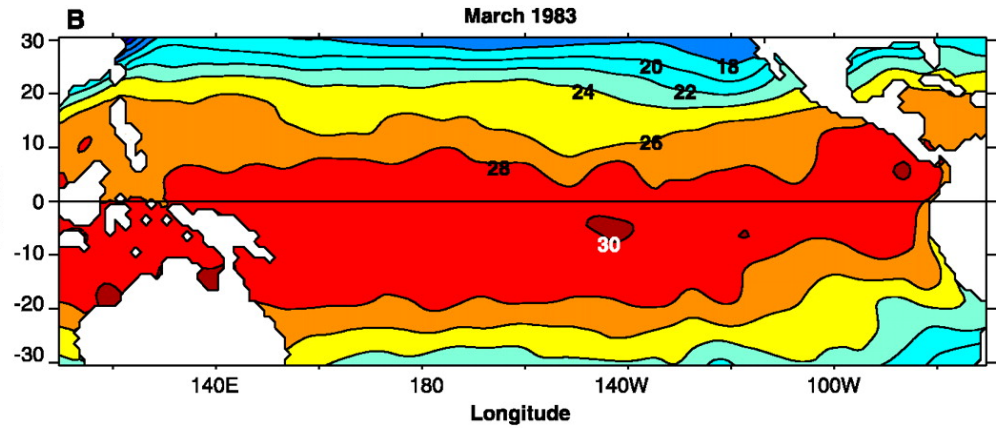

La Niña:

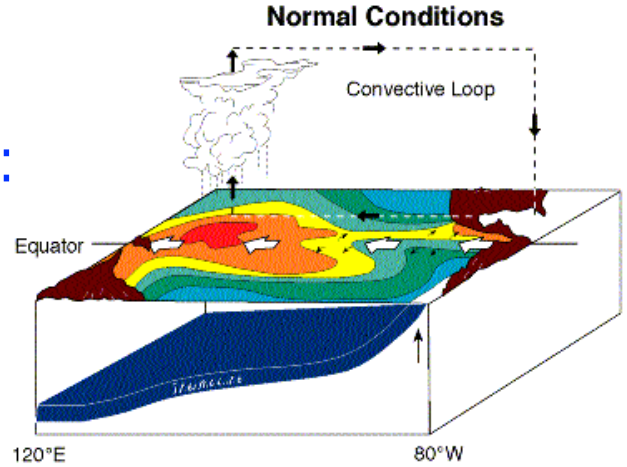

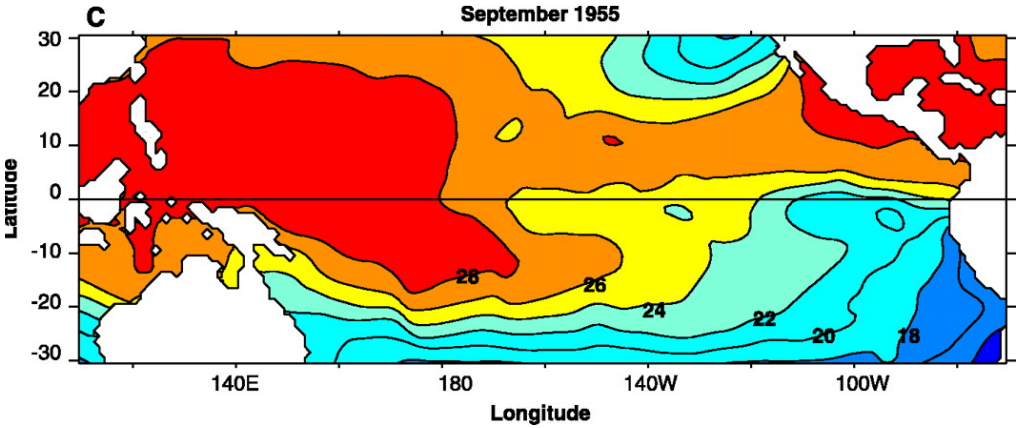

The major players:

Easterly Trade Winds → Thermocline;

Thermocline → sea surface temperature.

Eastward propagating Kelvin waves, westward Rossby Waves

El Niño is a coupled ocean-atmosphere phenomenon

"ENSO": El Niño (warming of ocean) and the Southern Oscillation (in atmospheric pressure difference between Darwin and Tahiti) are well correlated

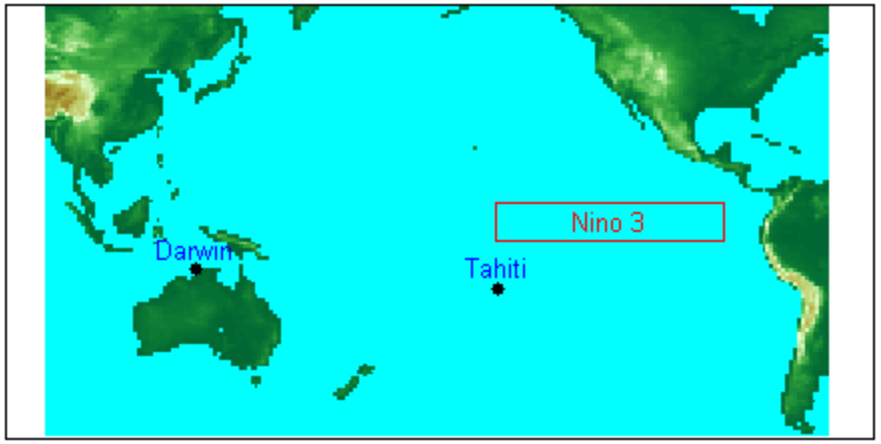

SST (blue) and atmospheric pressure difference (green)

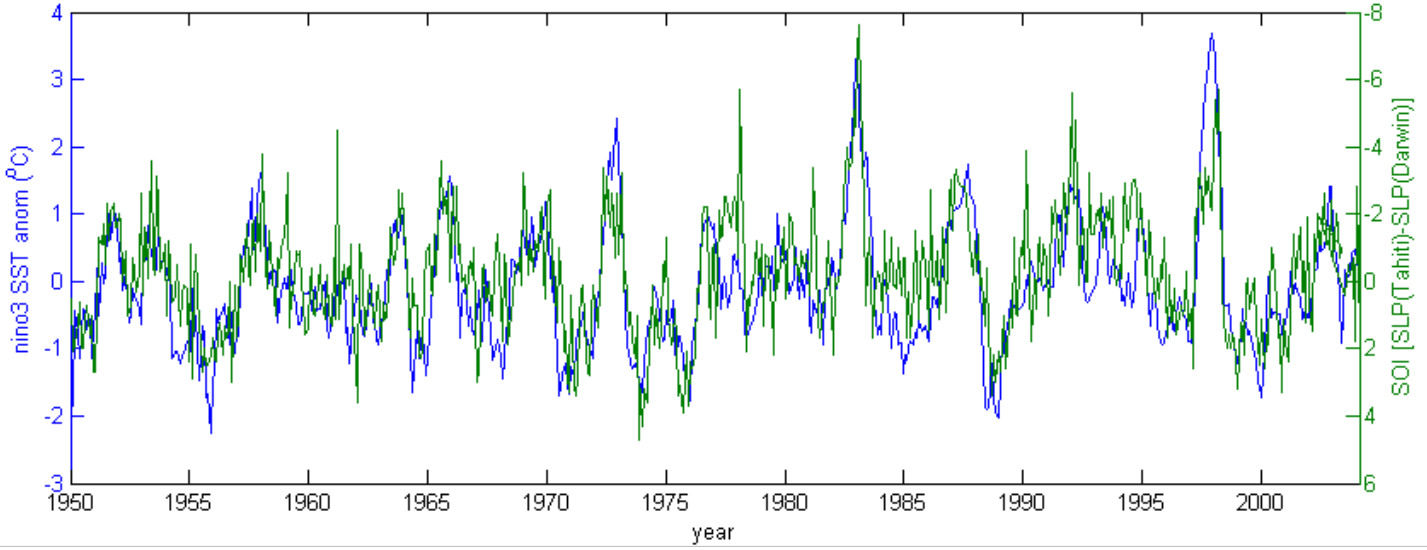

While irregular, all El Niño episodes still look similar, and tend to peak at end of calendar year

Sea surface temperature averaged over the eastern equatorial pacific during several El Niño events, as function of month (over two years):

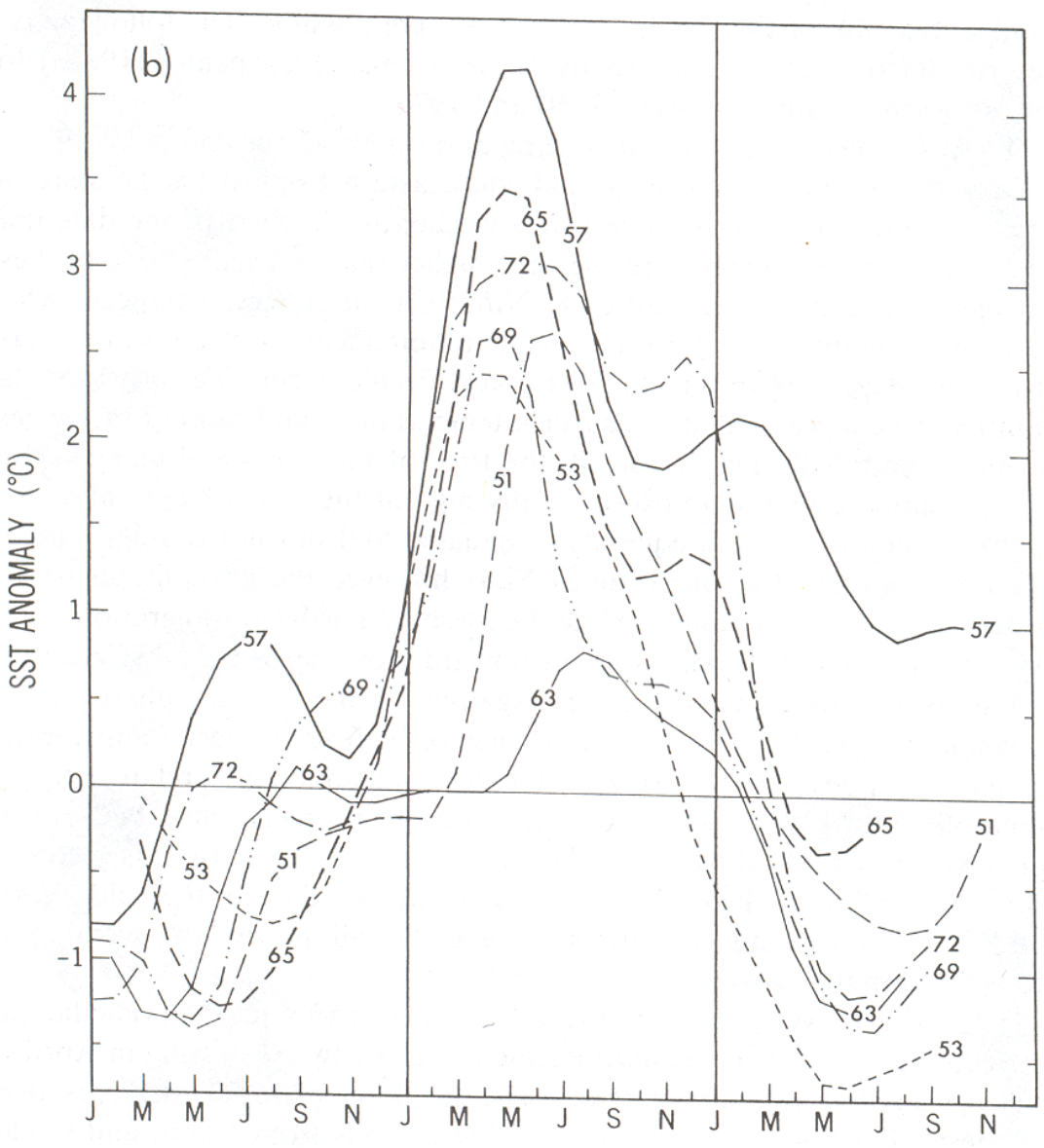

Why do we care: Global impacts

ENSO is the largest inter-annual signal in global climate

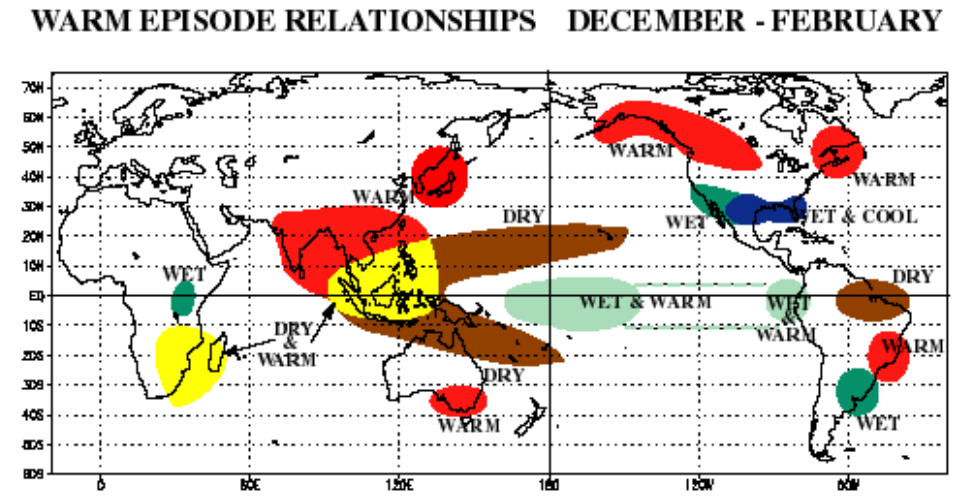

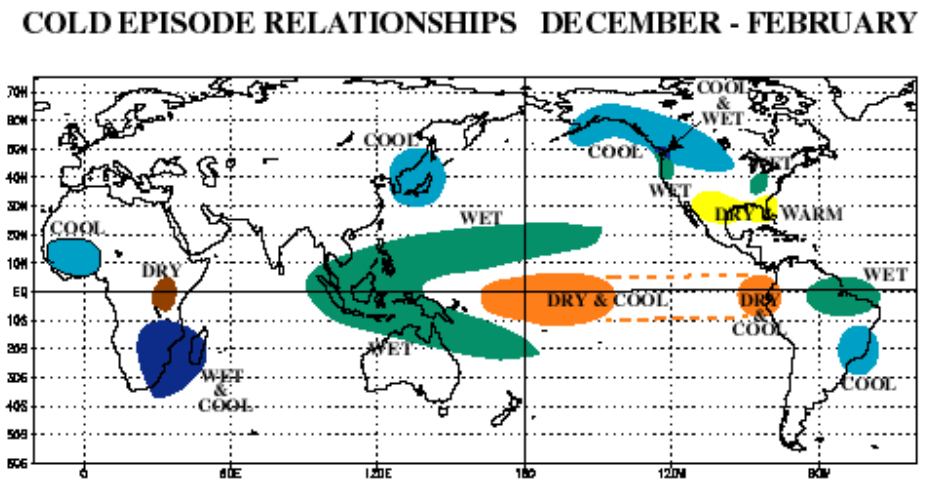

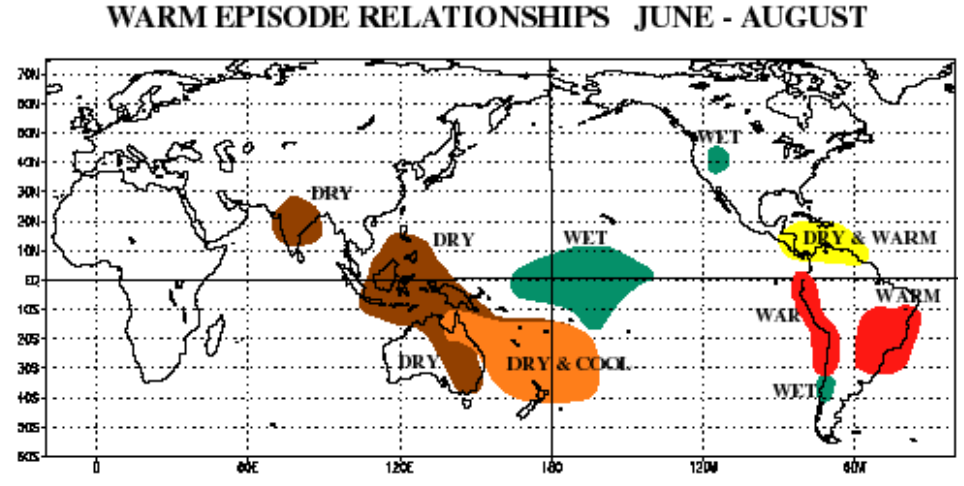

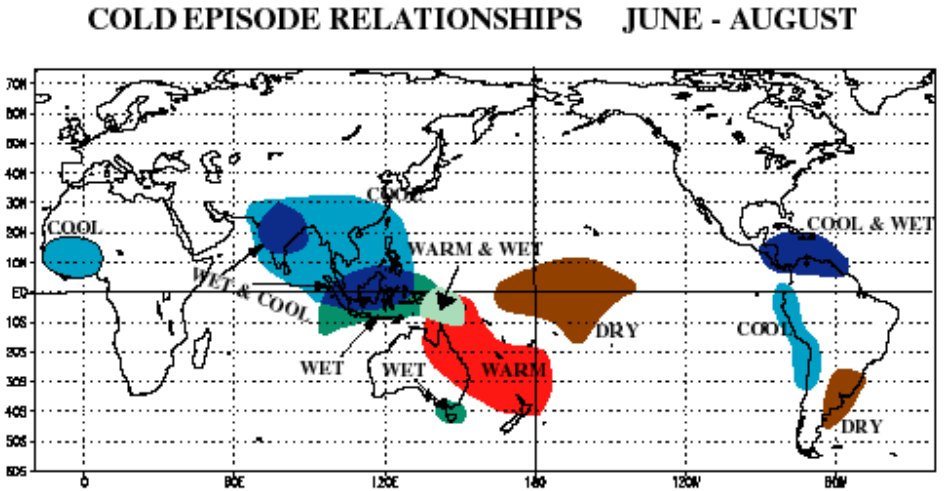

El Niño

Climate Prediction Center
NCEP

La Niña

Climate Prediction Center
NCEP

Why do we care: ENSO's Global climate impacts

Floods

Lakeport, California (1998)

Fires

Australia (1998)

Making Observations: monitoring systems

Satellites:
SST (infrared),
wind speed
(scatterometer),
SSH (altimeter)

Making Observations: monitoring systems

Satellites:
SST (infrared),
wind speed
(scatterometer),
SSH (altimeter)

Moored buoys
temperature
profile, wind
speed, currents

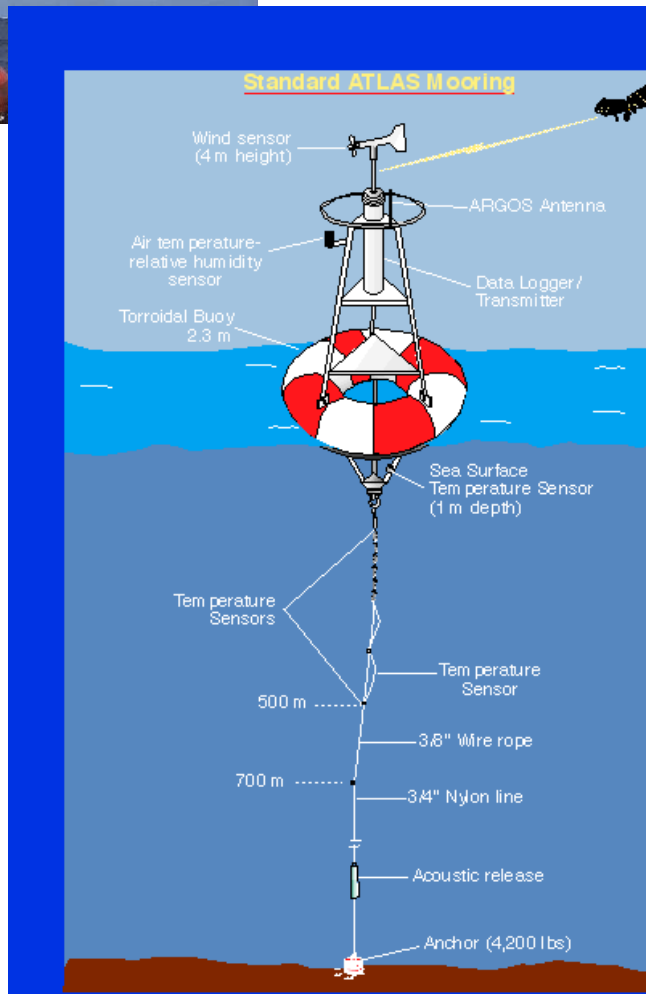

Making Observations: monitoring systems

Satellites:
SST (infrared),
wind speed
(scatterometer),
SSH (altimeter)

Moored buoys
temperature
profile, wind
speed, currents

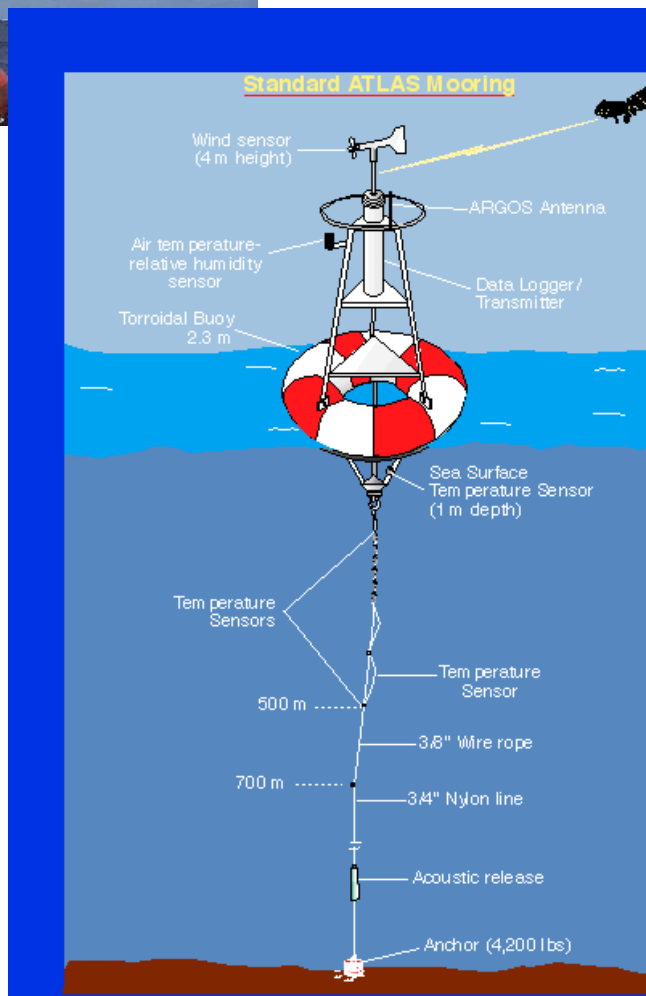

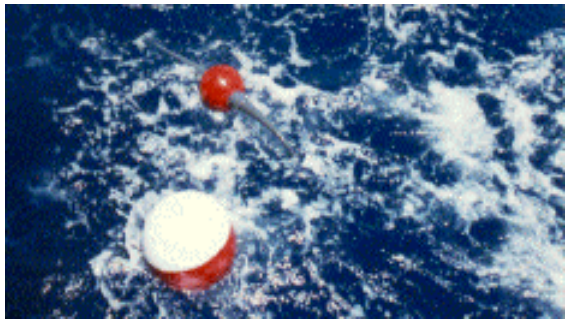

Drifting buoys
SST & surface
currents
“Lagrangian drifters”

Making Observations: monitoring systems

Satellites:
SST (infrared),
wind speed
(scatterometer),
SSH (altimeter)

Moored buoys
temperature
profile, wind
speed, currents

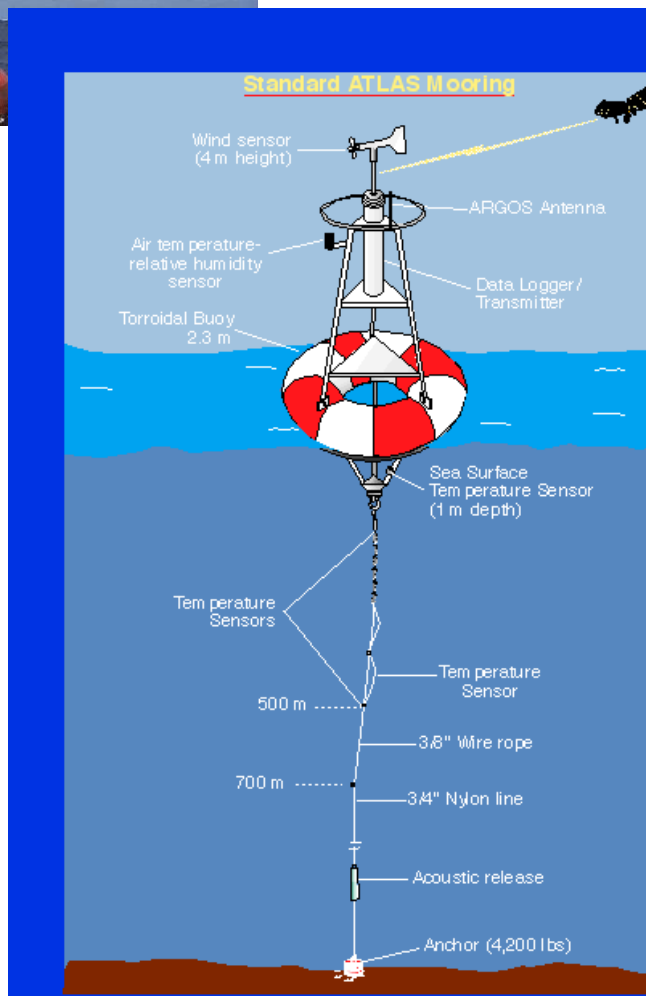

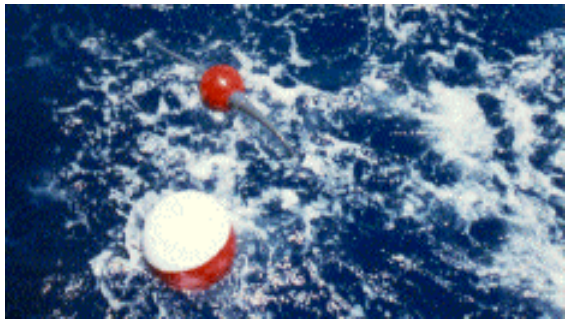

Drifting buoys
SST & surface
currents
“Lagrangian drifters”

Making Observations: monitoring systems

Sate
SST
wind
(scat
SSH

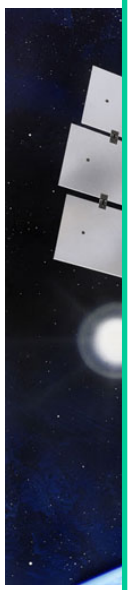

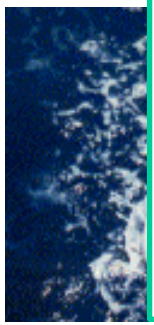

Argo floats

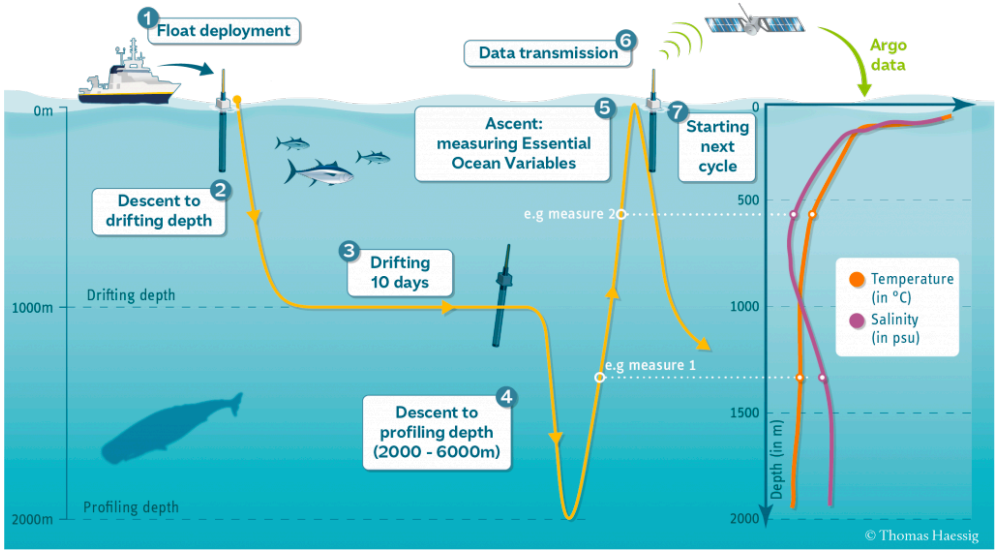

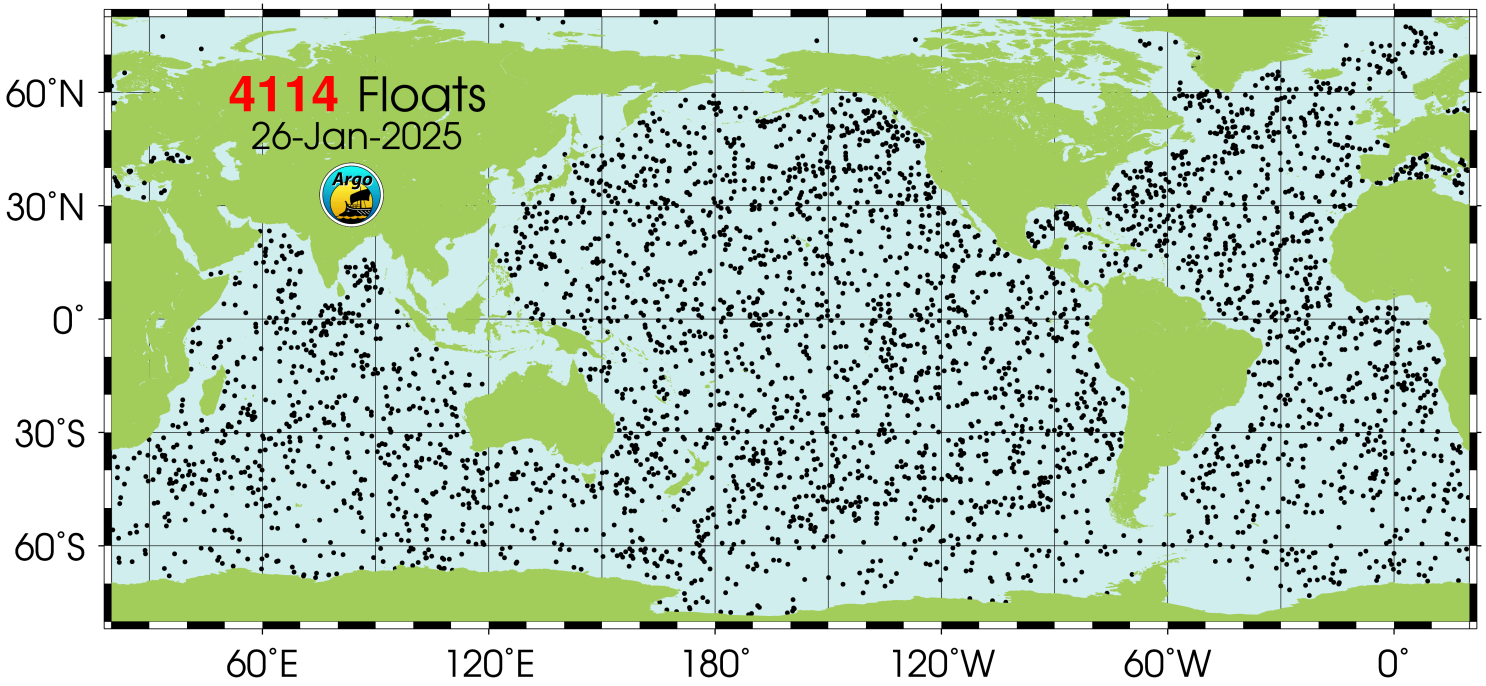

Making Observations: TAO array

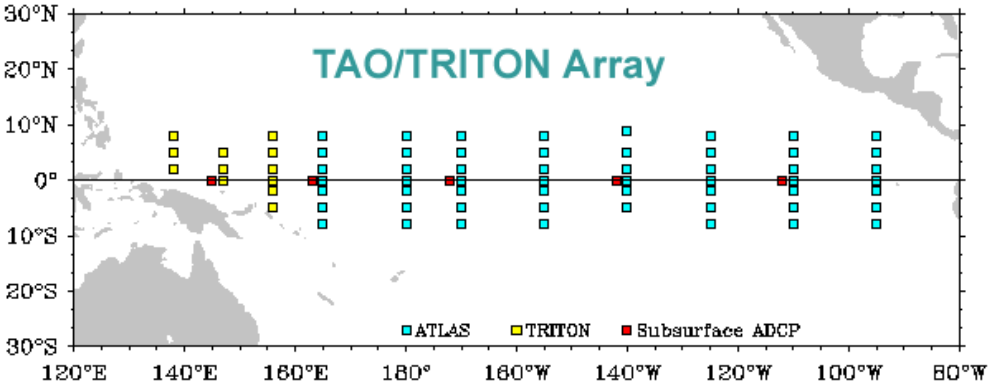

Large observational buoy array, dedicated research vessel, international consortium

Making Observations: TAO array

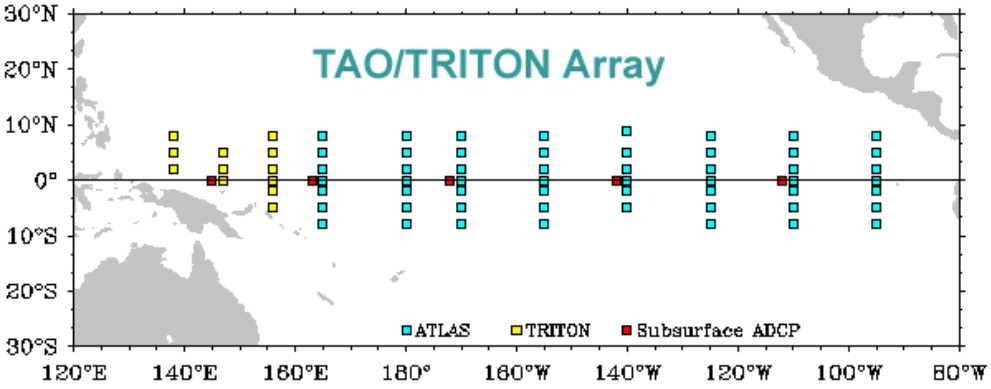

Large observational buc
array, dedicated researc
vessel, international
consortium

Equatorial Sea Surface Temperature (SST) as function of longitude & time [from TAU data]

Same, but deviation of SST from mean

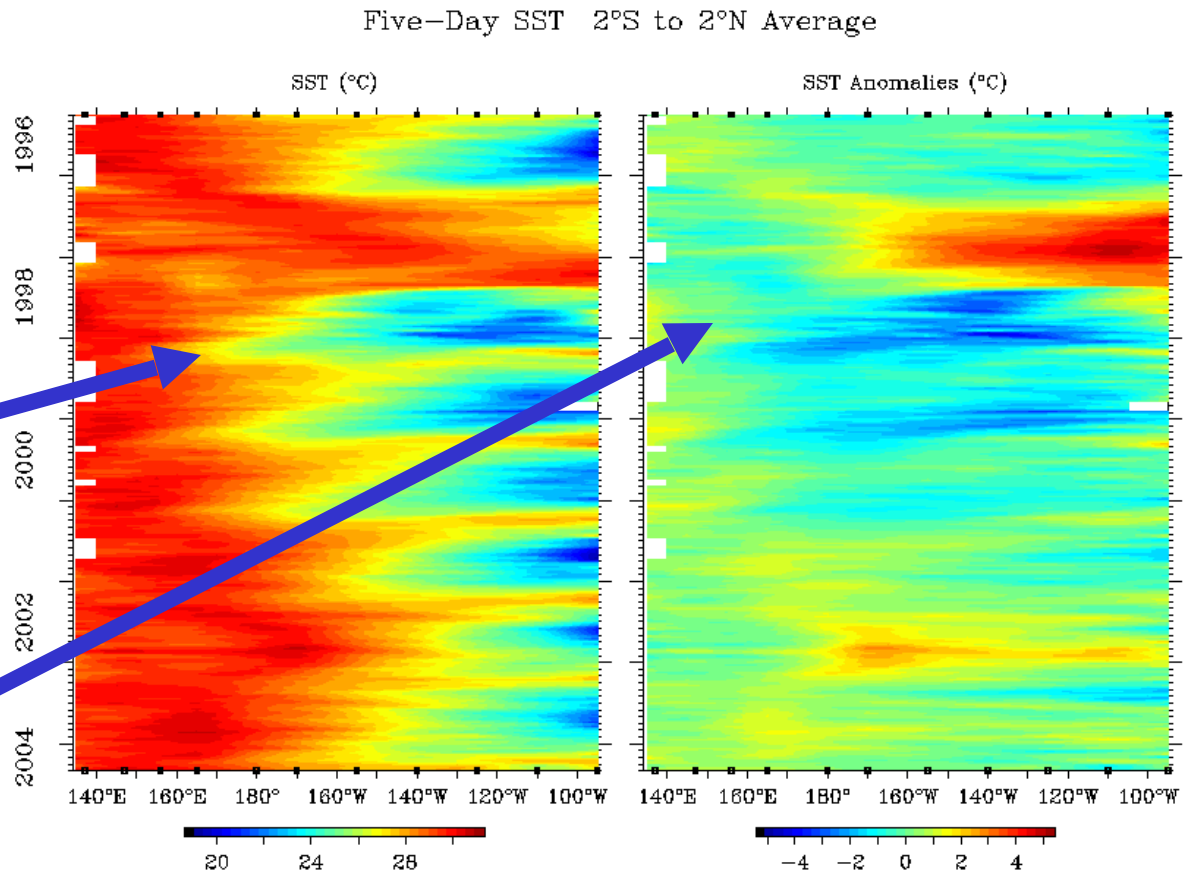

Why do we care: El Niño Impacts, it's not all bad news

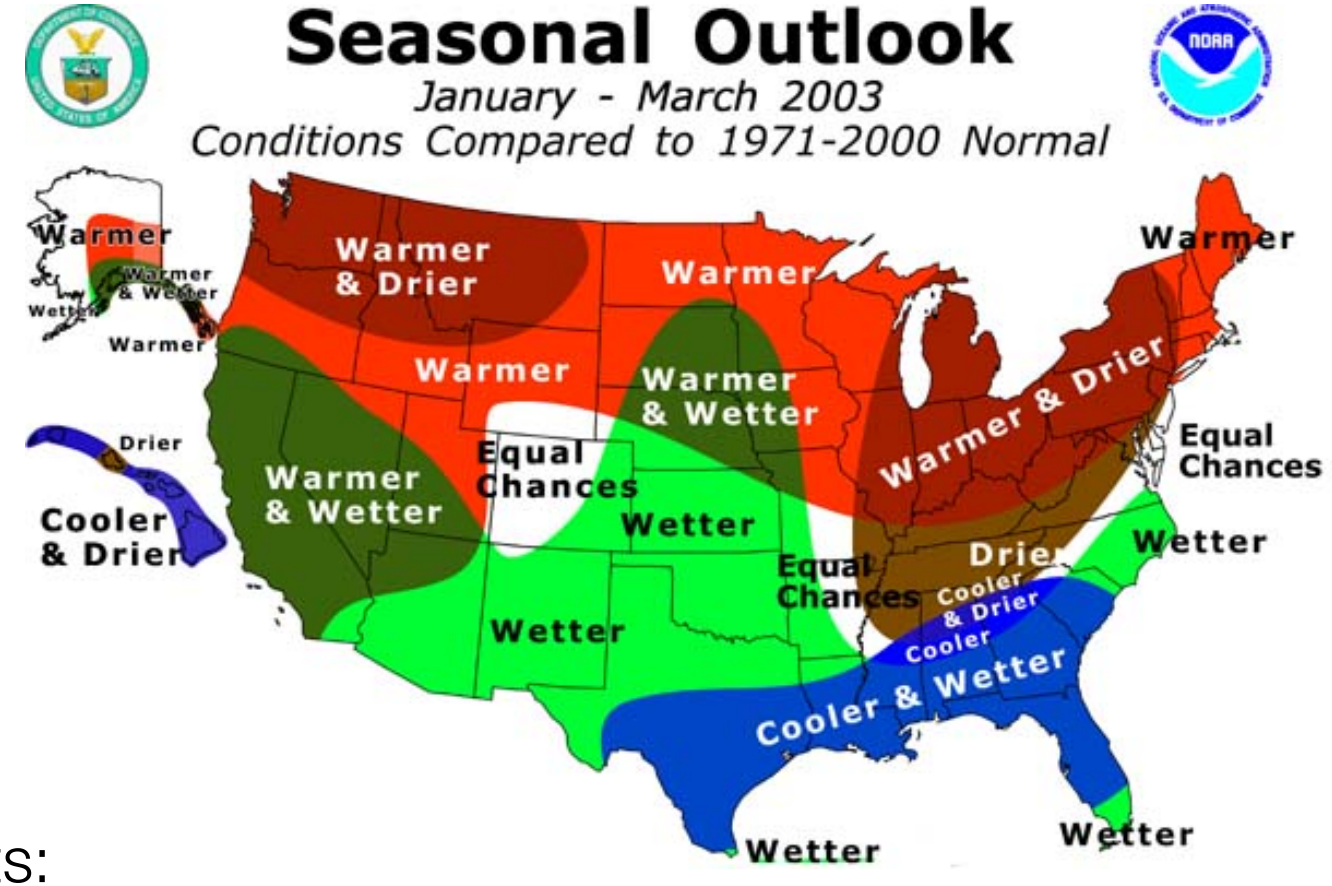

"El Niño's Benefits:
In recent weeks, El Niño has contributed much-needed precipitation to many parched areas of the country. For example, fall and winter storms along the Gulf and East Coasts have nearly ended the drought from Texas to Georgia, and along the entire East Coast."

http://www.noaanews.noaa.gov/stories/s1080.htm

Mechanism, Normal background conditions first:

Zonal wind ➔ Thermocline slope ➔ Warm pool/ cold tongue

State of the ocean during normal conditions:

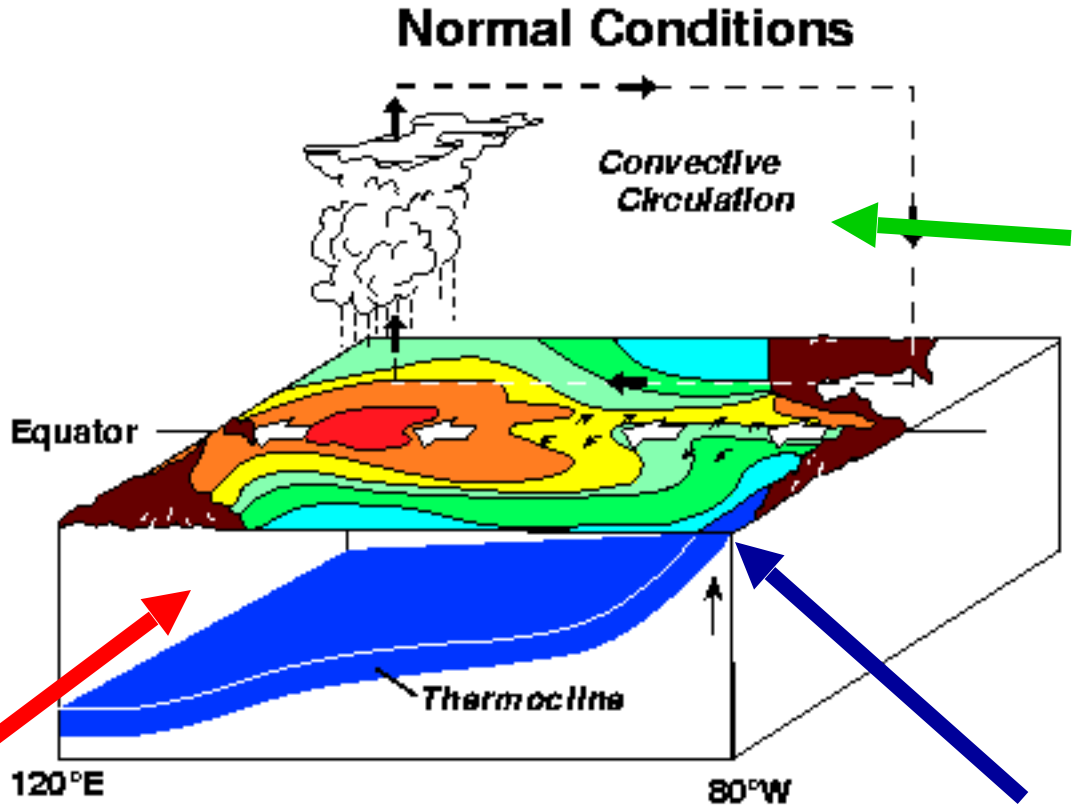

Walker circulation

West Pacific: Deep thermocline, warm pool

East Pacific: Shallow thermocline, cold tongue

Current forecast

EL NIÑO/SOUTHERN OSCILLATION (ENSO) DIAGNOSTIC DISCUSSION

issued by

CLIMATE PREDICTION CENTER/NCEP/NWS, 9 April 2026

ENSO Alert System Status: Final La Niña Advisory / El Niño Watch

Synopsis: ENSO-neutral conditions are present and are favored through April-June 2026 (80% chance). In May-July 2026, El Niño is likely to emerge (61% chance) and persist through at least the end of 2026.

https://www.cpc.ncep.noaa.gov/products/analysis_monitoring/enso_advisory/ensodisc.pdf

Current forecast

EL NIÑO/SOUTHERN OSCILLATION (ENSO) DIAGNOSTIC DISCUSSION

issued by

CLIMATE PREDICTION CENTER/NCEP/NWS, 9 April 2026

ENSO Alert System Status: Final La Niña Advisory / El Niño Watch

Synopsis: ENSO-neutral conditions are present and are favored through April-June 2026 (80% chance). In May-July 2026, El Niño is likely to emerge (61% chance) and persist through at least the end of 2026.

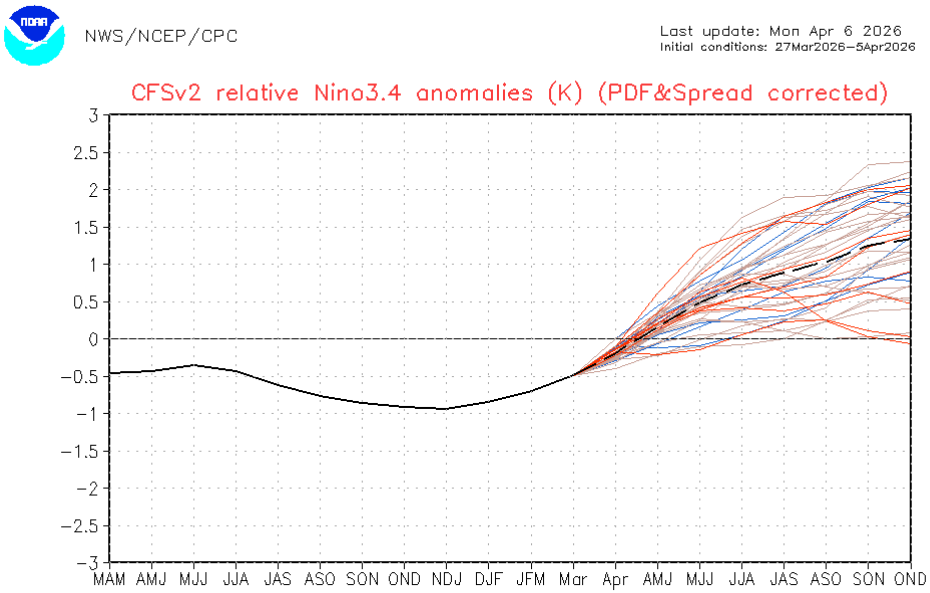

https://www.cpc.ncep.noaa.gov/products/analysis_monitoring/enso_advisory/ensodisc.pdf

Current forecast

EL NIÑO/SOUTHERN OSCILLATION (ENSO) DIAGNOSTIC DISCUSSION

issued by

CLIMATE PREDICTION CENTER/NCEP/NWS, 9 April 2026

ENSO Alert System Status: Final La Niña Advisory / El Niño Watch

Synopsis: ENSO-neutral conditions are present and are favored through April-June 2026 (80% chance). In May-July 2026, El Niño is likely to emerge (61% chance) and persist through at least the end of 2026.

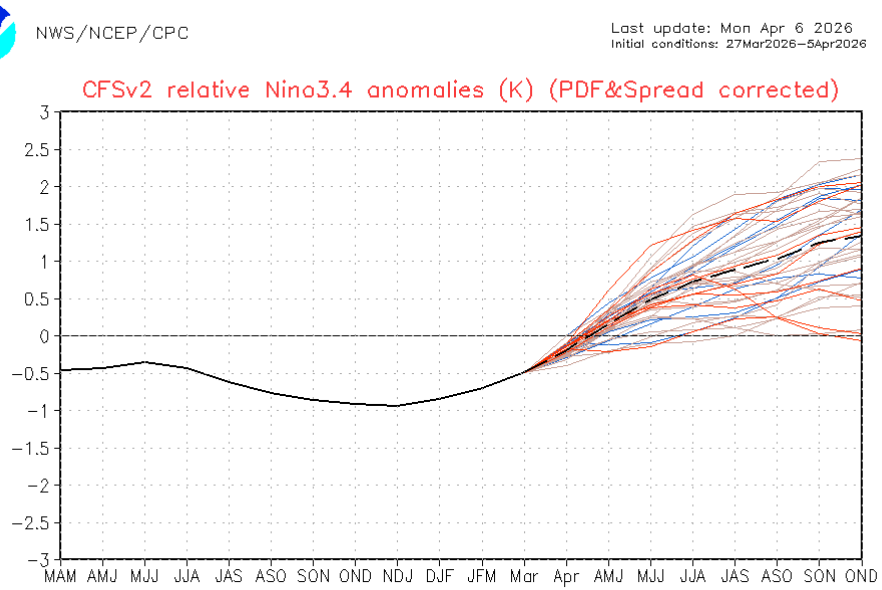

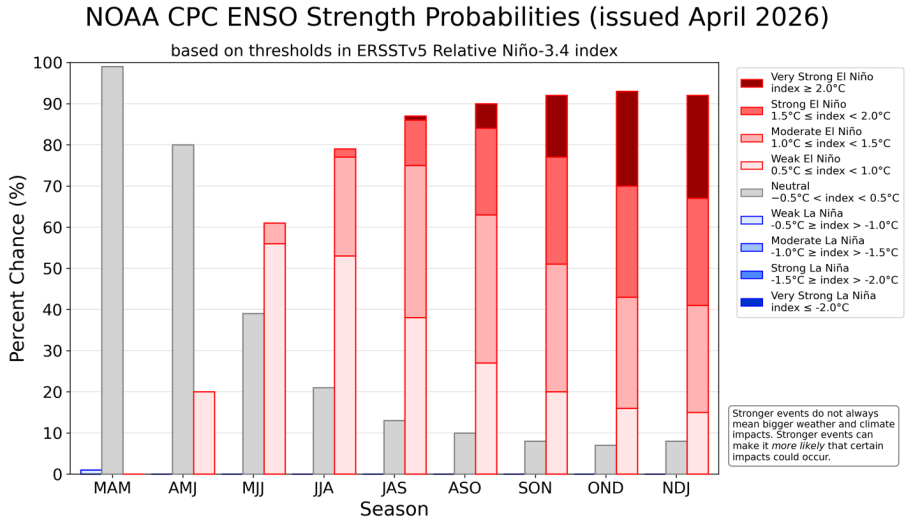

https://www.cpc.ncep.noaa.gov/products/analysis_monitoring/enso_advisory/ensodisc.pdf

Outline of notes: Delay Oscillator

1. Kelvin wave reminder
2. Notes: equatorial Kelvin wave
3. Rossby wave reminder
4. Ekman pumping reminder
5. Delayed oscillator mechanism (next few slides)

Notes:

1. Shallow water equations and the equatorial beta plane (section 1.2.1, equations 1–3)
2. Equatorial Kelvin wave (section 1.2.3)
3. Equatorial Rossby/Poincare/Yanai waves (section 1.2.3)

Equatorial wave modes

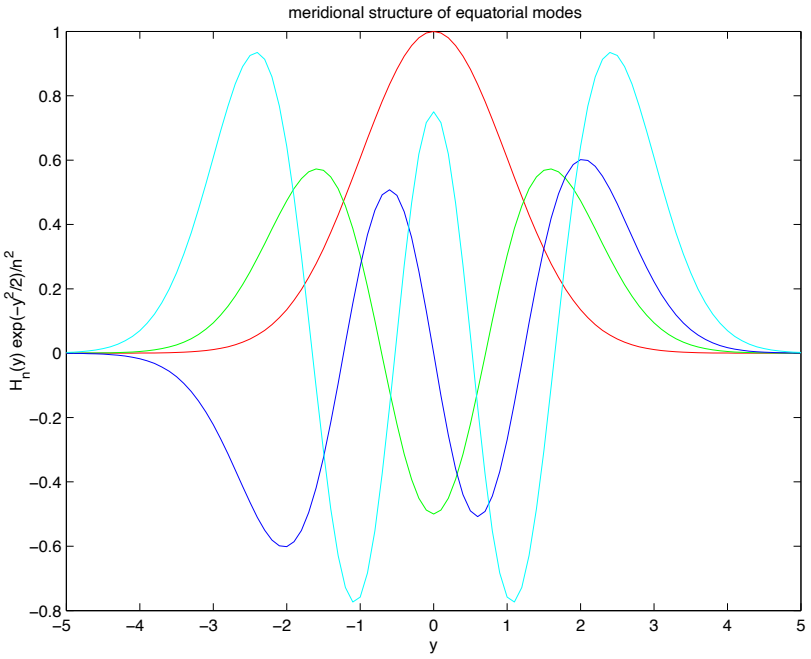

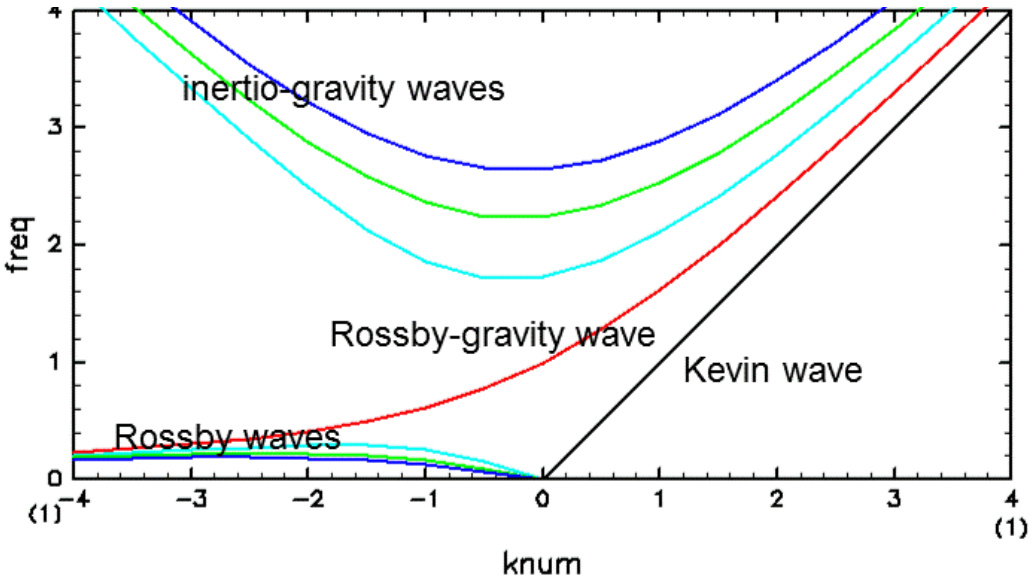

The latitudinal structure of the first few equatorial modes: $H_n(y)\exp(-y^2/2)/n^2$.

graduate level

Observations of **atmospheric** Equatorial wave modes

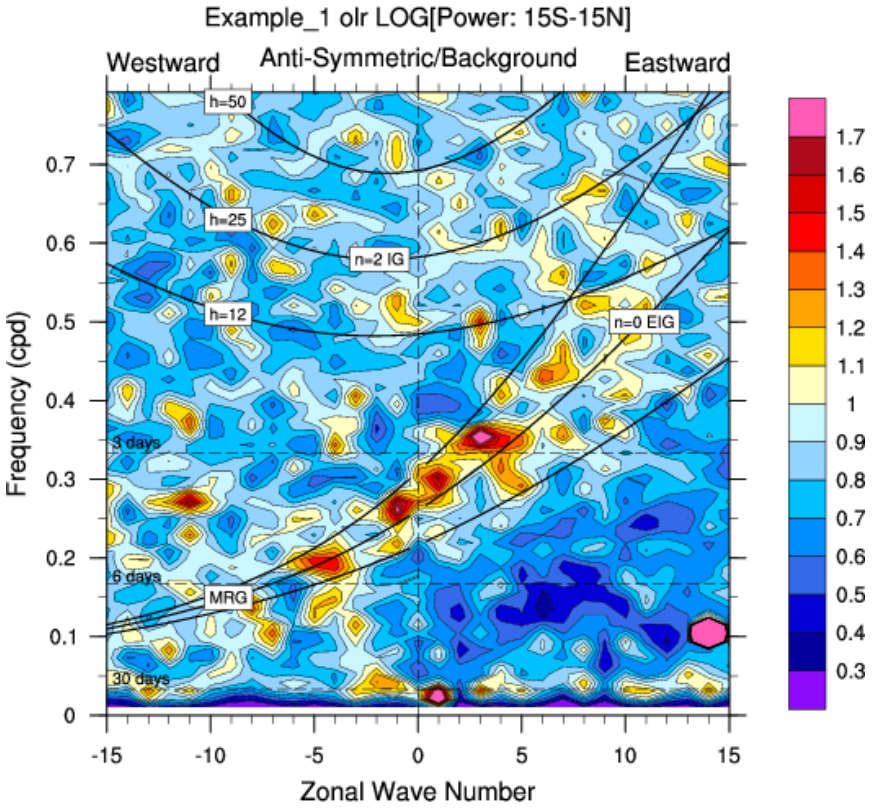

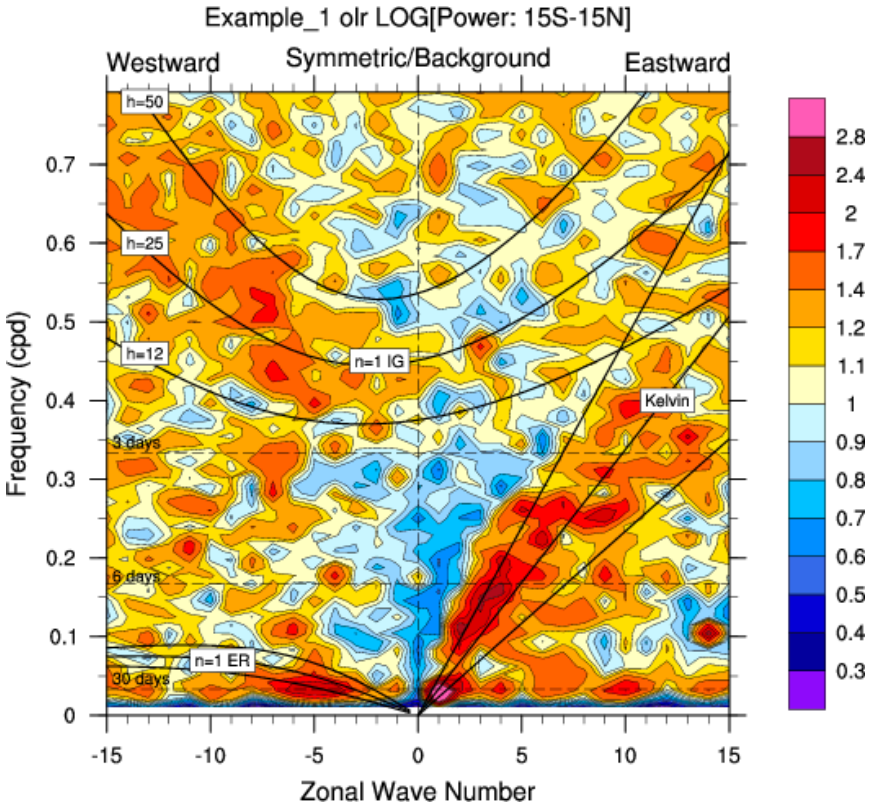

Atmospheric equatorial waves

(Wheeler-Kiladis Space-Time Spectra)

https://www.ncl.ucar.edu/Applications/space_time.shtml

graduate level

Observations of **atmospheric** Equatorial wave modes

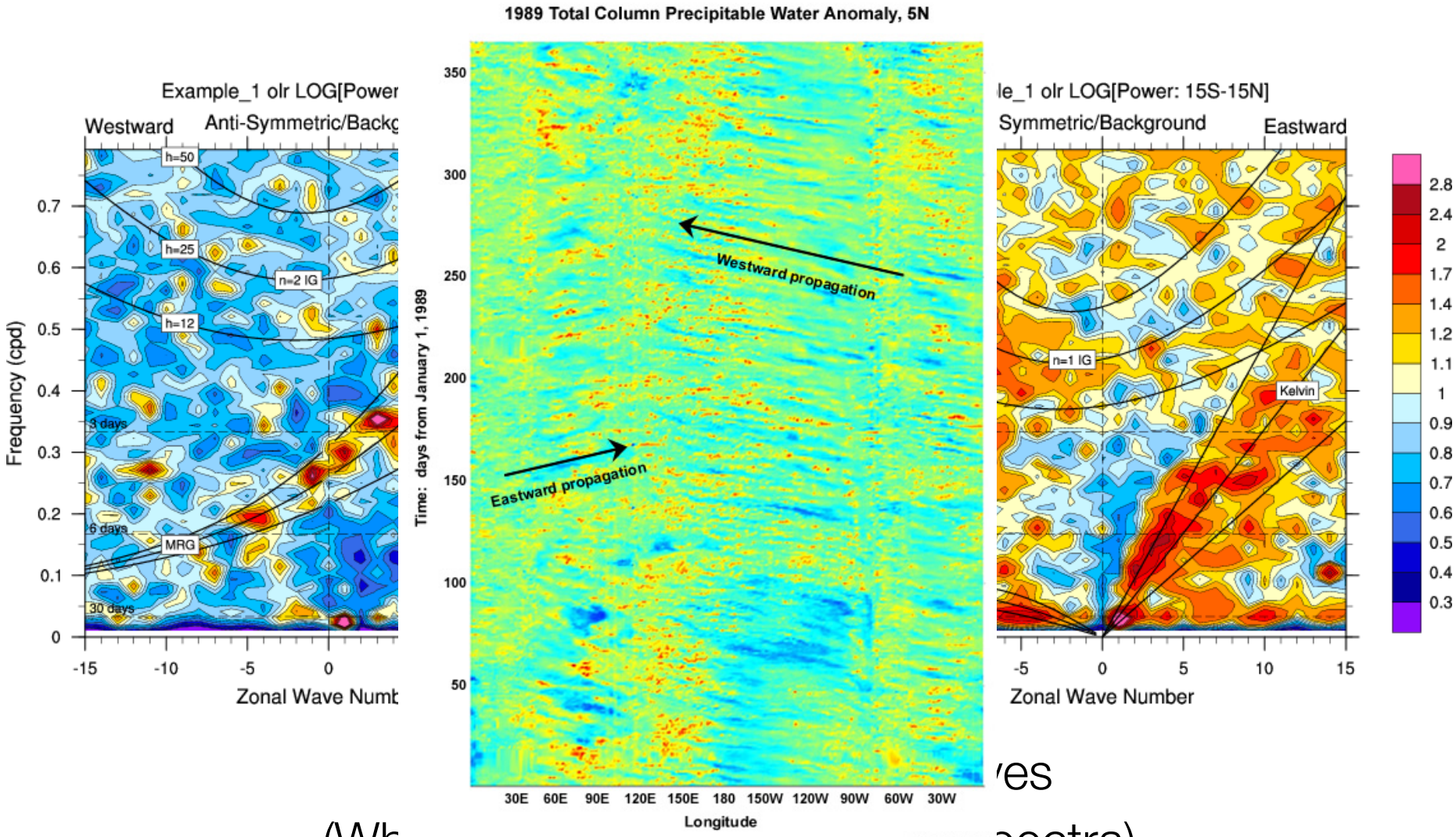

(Wheeler-Kiladis Space-Time Spectra)

https://www.ncl.ucar.edu/Applications/space_time.shtml

graduate level

Mechanism: Kelvin & Rossby waves, and the delayed oscillator (Schopf & Suarez, Battisti 1988)

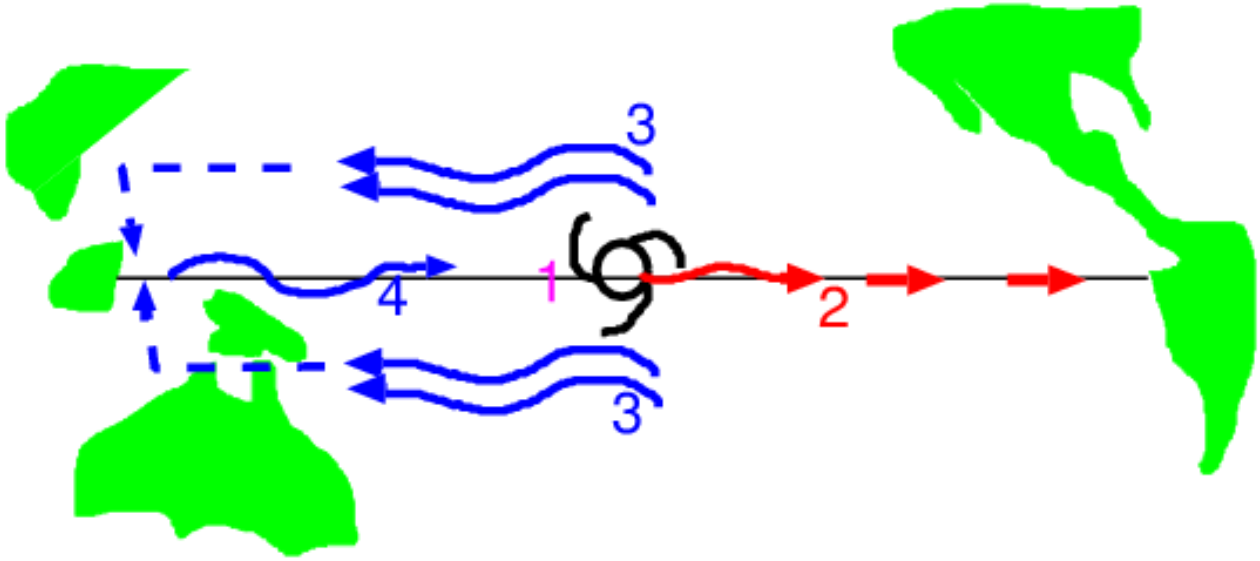

1. An initial weakening of trades
2. Warm Kelvin wave, positive feedback, El Niño peaks
3. Cold Rossby waves making their way to the west pacific
4. Reflecting from western boundary, ending the event, start a cooling
5. All repeats with opposite signs…

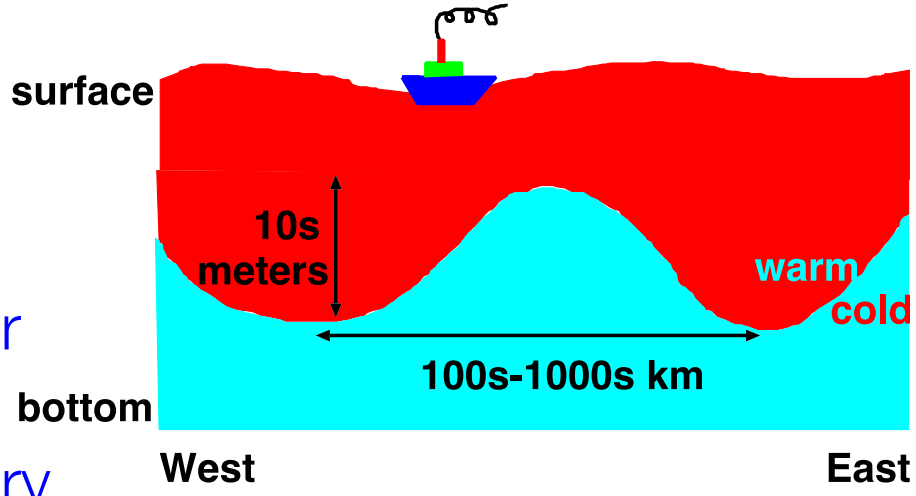

Kelvin and Rossby waves and boundary reflections

1. Force ocean with a westerly wind stress pulse

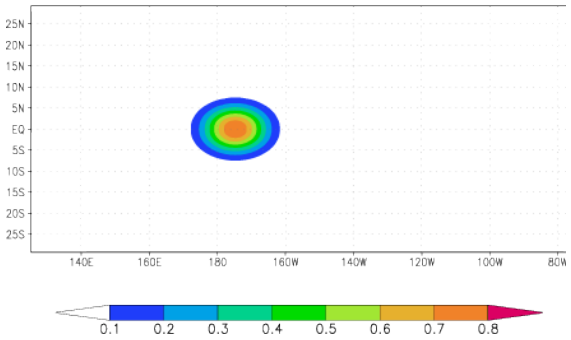

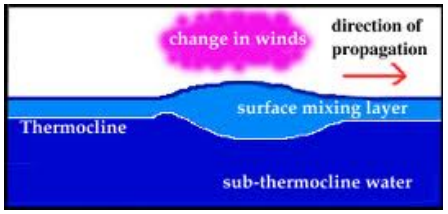

Kelvin wave schematic

2. Warm Kelvin waves propagate east along equator ➔ Event starts!

3. Cold Rossby waves propagate west at higher latitude & reflect eastward as Kelvin waves ➔ Event ends

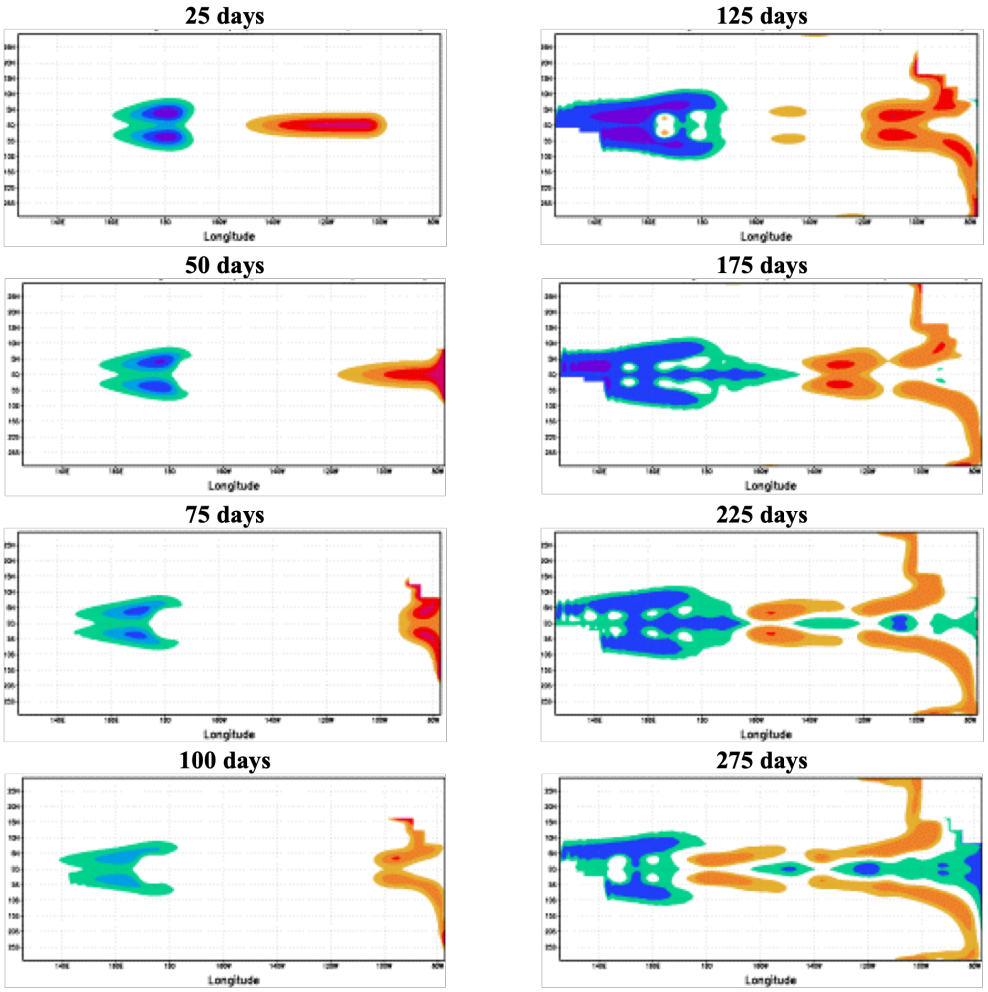

http://iri.columbia.edu/climate/ENSO/theory/

notes

delayed oscillator derivation

use also next side

Delayed oscillator equations

East Pacific temperature, *T(t),* depends on thermocline depth there:

$$\frac{dT(t)}{dt} = \hat{a}h_{eq}(x_c, t - \frac{1}{2}\tau_K) + \hat{b}h_{off-eq}(x_c, t - [\frac{1}{2}\tau_R + \tau_K]) - cT(t)^3$$

Schopf & Suarez 1989

graduate level

Delayed oscillator equations

East Pacific temperature, *T(t),* depends on thermocline depth there:

$$\frac{dT(t)}{dt} = \hat{a}h_{eq}(x_c, t - \frac{1}{2}\tau_K) + \hat{b}h_{off-eq}(x_c, t - [\frac{1}{2}\tau_R + \tau_K]) - cT(t)^3$$

$$\frac{dT(t)}{dt} = \bar{a}\tau_{eq}(x_c, t - \frac{1}{2}\tau_K) - \bar{b}\tau_{eq}(x_c, t - [\frac{1}{2}\tau_R + \tau_K]) - cT(t)^3$$

Schopf & Suarez 1989

graduate level

Delayed oscillator equations

East Pacific temperature, *T(t),* depends on thermocline depth there:

$$\frac{dT(t)}{dt} = \hat{a}h_{eq}(x_c, t - \frac{1}{2}\tau_K) + \hat{b}h_{off-eq}(x_c, t - [\frac{1}{2}\tau_R + \tau_K]) - cT(t)^3$$

wind at eq, x_c, directly affects h

$$\frac{dT(t)}{dt} = \bar{a}\tau_{eq}(x_c, t - \frac{1}{2}\tau_K) - \bar{b}\tau_{eq}(x_c, t - [\frac{1}{2}\tau_R + \tau_K]) - cT(t)^3$$

Schopf & Suarez 1989

graduate level

Delayed oscillator equations

East Pacific temperature, *T(t),* depends on thermocline depth there:

$$\frac{dT(t)}{dt} = \hat{a}h_{eq}(x_c, t - \frac{1}{2}\tau_K) + \hat{b}h_{off-eq}(x_c, t - [\frac{1}{2}\tau_R + \tau_K]) - cT(t)^3$$

wind at eq, x_c, directly affects h

$$h_{\text{off-eq}} \propto -w^{Ekman}_{\text{off-eq}} \propto -\text{curl}(\tau_{\text{off-eq}}) \approx \partial_y \tau^{(x)}_{\text{off-eq}} \approx (\tau^{(x)}_{\text{off-eq}} - \tau^{(x)}_{\text{eq}})/L \propto -\tau^{(x)}_{\text{eq}}.$$

$$\frac{dT(t)}{dt} = \bar{a}\tau_{eq}(x_c, t - \frac{1}{2}\tau_K) - \bar{b}\tau_{eq}(x_c, t - [\frac{1}{2}\tau_R + \tau_K]) - cT(t)^3$$

Schopf & Suarez 1989

graduate level

Delayed oscillator equations

East Pacific temperature, *T(t),* depends on thermocline depth there:

$$\frac{dT(t)}{dt} = \hat{a}h_{eq}(x_c, t - \frac{1}{2}\tau_K) + \hat{b}h_{off-eq}(x_c, t - [\frac{1}{2}\tau_R + \tau_K]) - cT(t)^3$$

wind at eq, x_c, directly affects h

$$h_{\text{off-eq}} \propto -w^{Ekman}_{\text{off-eq}} \propto -\text{curl}(\tau_{\text{off-eq}}) \approx \partial_y \tau^{(x)}_{\text{off-eq}} \approx (\tau^{(x)}_{\text{off-eq}} - \tau^{(x)}_{\text{eq}})/L \propto -\tau^{(x)}_{\text{eq}}.$$

$$\frac{dT(t)}{dt} = \bar{a}\tau_{eq}(x_c, t - \frac{1}{2}\tau_K) - \bar{b}\tau_{eq}(x_c, t - [\frac{1}{2}\tau_R + \tau_K]) - cT(t)^3$$

$$\frac{dT(t)}{dt} = aT(t - \frac{1}{2}\tau_K) - bT(t - [\frac{1}{2}\tau_R + \tau_K]) - cT(t)^3$$

Schopf & Suarez 1989

graduate level

Delayed oscillator equations

East Pacific temperature, *T(t),* depends on thermocline depth there:

$$\frac{dT(t)}{dt} = \hat{a}h_{eq}(x_c, t - \frac{1}{2}\tau_K) + \hat{b}h_{off-eq}(x_c, t - [\frac{1}{2}\tau_R + \tau_K]) - cT(t)^3$$

wind at eq, x_c, directly affects h

$$h_{\text{off-eq}} \propto -w^{Ekman}_{\text{off-eq}} \propto -\text{curl}(\tau_{\text{off-eq}}) \approx \partial_y \tau^{(x)}_{\text{off-eq}} \approx (\tau^{(x)}_{\text{off-eq}} - \tau^{(x)}_{\text{eq}})/L \propto -\tau^{(x)}_{\text{eq}}.$$

$$\frac{dT(t)}{dt} = \bar{a}\tau_{eq}(x_c, t - \frac{1}{2}\tau_K) - \bar{b}\tau_{eq}(x_c, t - [\frac{1}{2}\tau_R + \tau_K]) - cT(t)^3$$

$$-\tau^{(x)}_{\text{eq}}(t - [\frac{1}{2}\tau_R + \tau_K])/L \propto -T(t - [\frac{1}{2}\tau_R + \tau_K]).$$

$$\frac{dT(t)}{dt} = aT(t - \frac{1}{2}\tau_K) - bT(t - [\frac{1}{2}\tau_R + \tau_K]) - cT(t)^3$$

Schopf & Suarez 1989

graduate level

Delayed oscillator equations

East Pacific temperature, *T(t),* depends on thermocline depth there:

$$\frac{dT(t)}{dt} = \hat{a}h_{eq}(x_c, t - \frac{1}{2}\tau_K) + \hat{b}h_{off-eq}(x_c, t - [\frac{1}{2}\tau_R + \tau_K]) - cT(t)^3$$

wind at eq, x_c, directly affects h

$$h_{\text{off-eq}} \propto -w^{Ekman}_{\text{off-eq}} \propto -\text{curl}(\tau_{\text{off-eq}}) \approx \partial_y \tau^{(x)}_{\text{off-eq}} \approx (\tau^{(x)}_{\text{off-eq}} - \tau^{(x)}_{\text{eq}})/L \propto -\tau^{(x)}_{\text{eq}}.$$

$$\frac{dT(t)}{dt} = \bar{a}\tau_{eq}(x_c, t - \frac{1}{2}\tau_K) - \bar{b}\tau_{eq}(x_c, t - [\frac{1}{2}\tau_R + \tau_K]) - cT(t)^3$$

$$-\tau^{(x)}_{\text{eq}}(t - [\frac{1}{2}\tau_R + \tau_K])/L \propto -T(t - [\frac{1}{2}\tau_R + \tau_K]).$$

$$\frac{dT(t)}{dt} = aT(t - \frac{1}{2}\tau_K) - bT(t - [\frac{1}{2}\tau_R + \tau_K]) - cT(t)^3$$

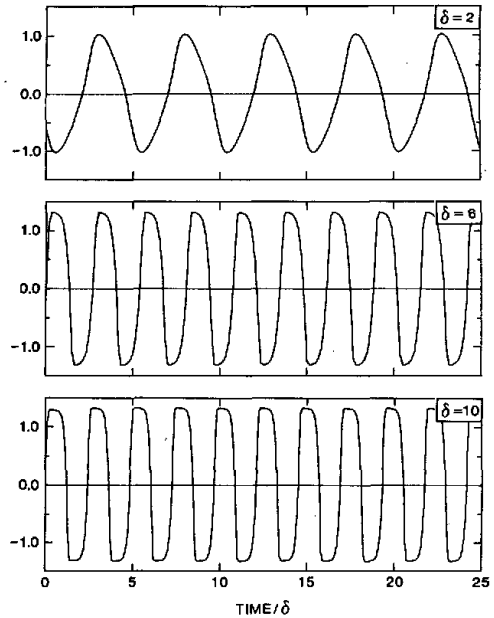

FIG. 4. Behavior of the nonlinear oscillator. (a) $\alpha = 0.75$, $\delta = 2$, (b) $\alpha = 0.75$, $\delta = 6$, and (c) $\alpha = 0.75$, $\delta = 10$. The time axis is scaled in units of the delay.

Schopf & Suarez 1989

graduate level

Delay oscillator mechanism (Schopf-Suarez, Battisti, 1989)

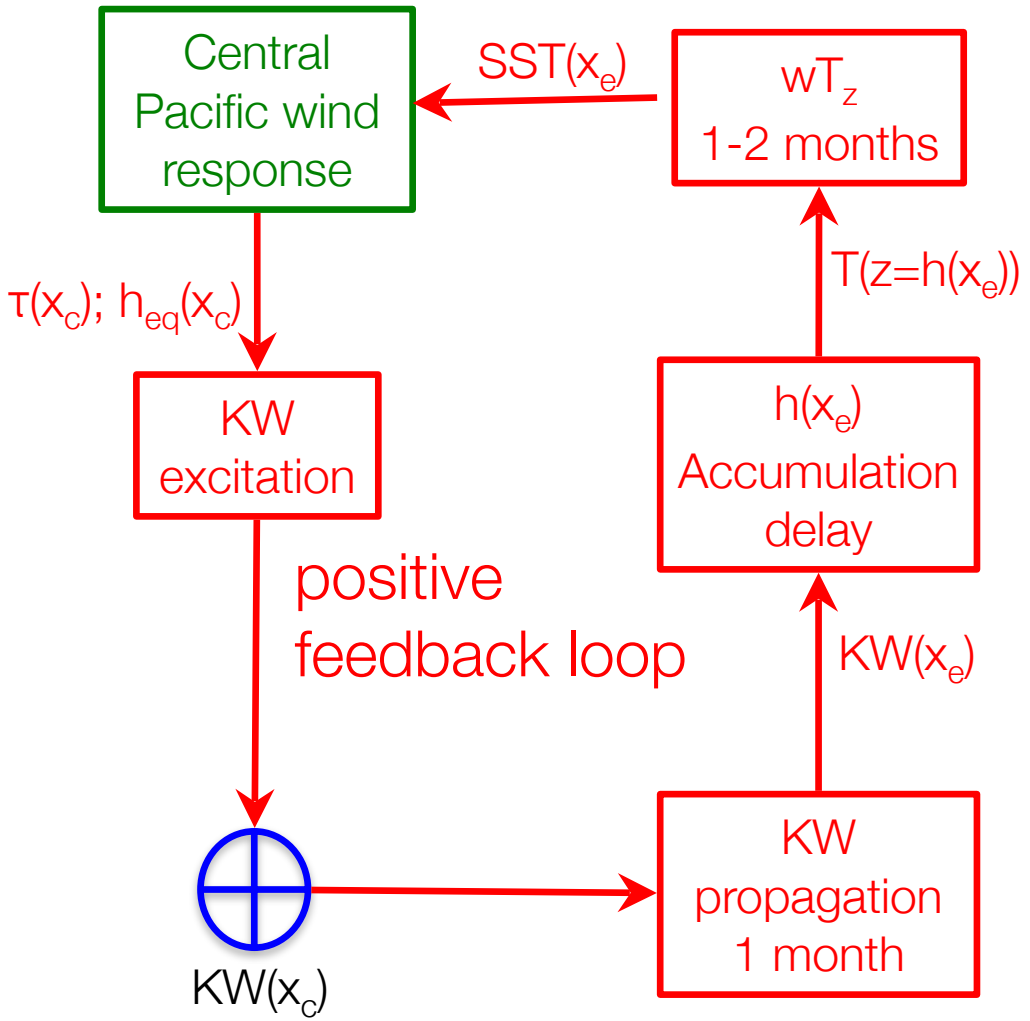

Each block represents a physical process relating input and output.

Right loop: eastern-Pacific positive feedback.

Left loop: negative feedback due to delayed Rossby waves.

Delay oscillator mechanism (Schopf-Suarez, Battisti, 1989)

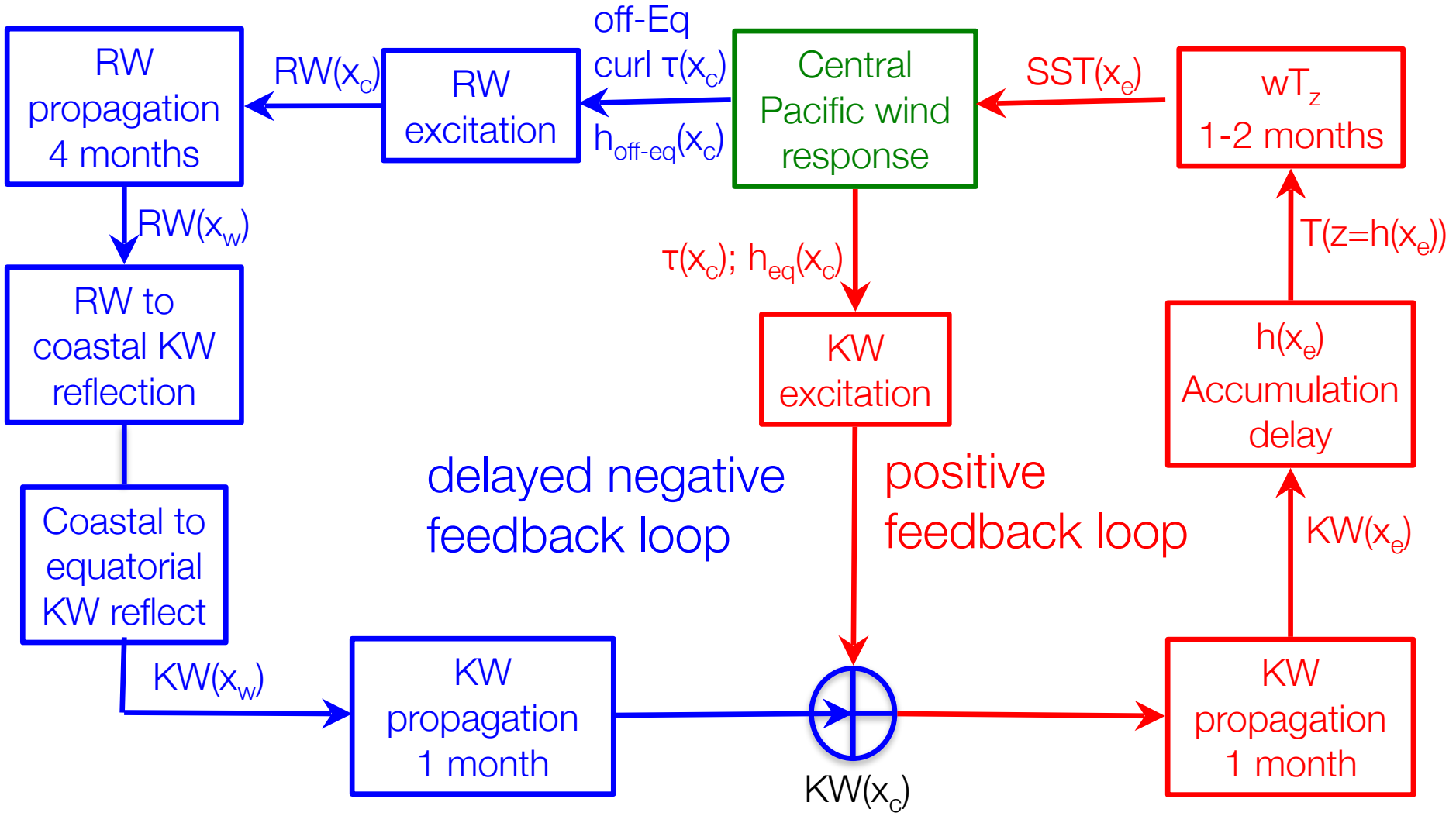

Each block represents a physical process relating input and output.

Right loop: eastern-Pacific positive feedback.

Left loop: negative feedback due to delayed Rossby waves.

Delayed oscillator analysis

neglect Kelvin delay for simplicity

$$\frac{dT(t)}{dt} = T(t) - \alpha T(t - \delta_T) - T^3(t).$$

Schopf & Suarez 1989

graduate level

Delayed oscillator analysis

neglect Kelvin delay for simplicity

$$\frac{dT(t)}{dt} = T(t) - \alpha T(t - \delta_T) - T^3(t).$$

steady states: $\bar{T} = 0, \pm\sqrt{1-\alpha}.$

Schopf & Suarez 1989

graduate level

Delayed oscillator analysis

neglect Kelvin delay for simplicity

$$\frac{dT(t)}{dt} = T(t) - \alpha T(t-\delta_T) - T^3(t).$$

steady states: $\bar{T} = 0, \pm\sqrt{1-\alpha}.$

Linearize: $T = \bar{T} + \tilde{T}$ to find $\frac{d\tilde{T}(t)}{dt} = \tilde{T}(t)(1-3\bar{T}^2) - \alpha\tilde{T}(t-\delta_T).$

Schopf & Suarez 1989

graduate level

Delayed oscillator analysis

neglect Kelvin delay for simplicity

$$\frac{dT(t)}{dt} = T(t) - \alpha T(t-\delta_T) - T^3(t).$$

steady states: $\bar{T} = 0, \pm\sqrt{1-\alpha}.$

Linearize: $T = \bar{T} + \tilde{T}$ to find $\frac{d\tilde{T}(t)}{dt} = \tilde{T}(t)(1-3\bar{T}^2) - \alpha\tilde{T}(t-\delta_T).$

Finding eigen solutions: $\text{Letting } \tilde{T} = e^{\sigma t} \text{ where } \sigma = \sigma_r + i\sigma_i$

Schopf & Suarez 1989

graduate level

Delayed oscillator analysis

neglect Kelvin delay for simplicity

$$\frac{dT(t)}{dt} = T(t) - \alpha T(t-\delta_T) - T^3(t).$$

steady states: $\bar{T} = 0, \pm\sqrt{1-\alpha}.$

Linearize: $T = \bar{T} + \tilde{T}$ to find $\frac{d\tilde{T}(t)}{dt} = \tilde{T}(t)(1-3\bar{T}^2) - \alpha\tilde{T}(t-\delta_T).$

Finding eigen solutions: Letting $\tilde{T} = e^{\sigma t}$ where $\sigma = \sigma_r + i\sigma_i$

need to solve transcendental equation: $\sigma = 1 - 3\bar{T}^2 - \alpha e^{-\sigma\delta_T}$

Schopf & Suarez 1989

graduate level

Delayed oscillator analysis

neglect Kelvin delay for simplicity

$$\frac{dT(t)}{dt} = T(t) - \alpha T(t-\delta_T) - T^3(t).$$

steady states: $\bar{T} = 0, \pm\sqrt{1-\alpha}.$

Linearize: $T = \bar{T} + \tilde{T}$ to find $\frac{d\tilde{T}(t)}{dt} = \tilde{T}(t)(1-3\bar{T}^2) - \alpha\tilde{T}(t-\delta_T).$

Finding eigen solutions: Letting $\tilde{T} = e^{\sigma t}$ where $\sigma = \sigma_r + i\sigma_i$

need to solve transcendental equation: $\sigma = 1 - 3\bar{T}^2 - \alpha e^{-\sigma\delta_T}$

solution

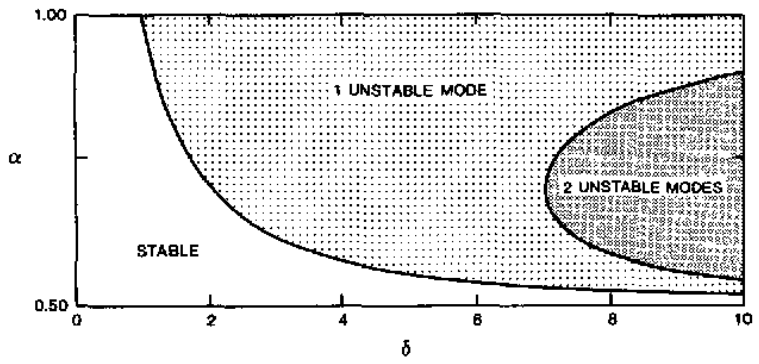

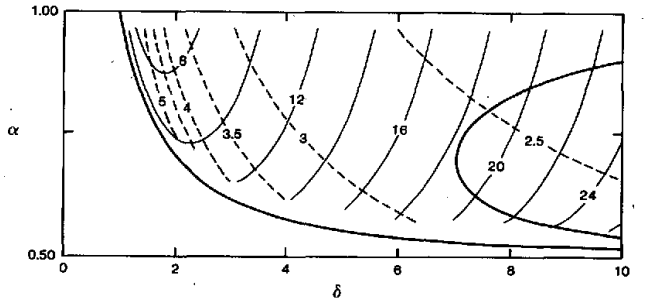

FIG. 5. The fundamental period of the nonlinear oscillator found numerically. The heavy solid lines are the neutral curves of the linear problem, reproduced from Fig. 2. The light solid contours give the period of the oscillation ($2\pi/\sigma_i$), while the dashed contours present the period in multiples of the delay.

Schopf & Suarez 1989

graduate level

The Recharge Oscillator mechanism for ENSO

Outline

1. Thermocline depth & East Pacific upwelling, temperature
2. Bjerknes feedback
3. Sverdrup balance
4. [Kelvin wave] (HW, section)
5. Recharge/discharge phases
6. The recharge oscillator mechanism
7. The recharge oscillator equations

(see next few slides)

F-F Jin 1997

graduate level

Bjerknes feedback

weaker easterlies

➡ reduced thermocline slope

➡ shallower east pacific thermocline

➡ warmer East Pacific

➡ weaker Walker cell

➡ weaker easterlies

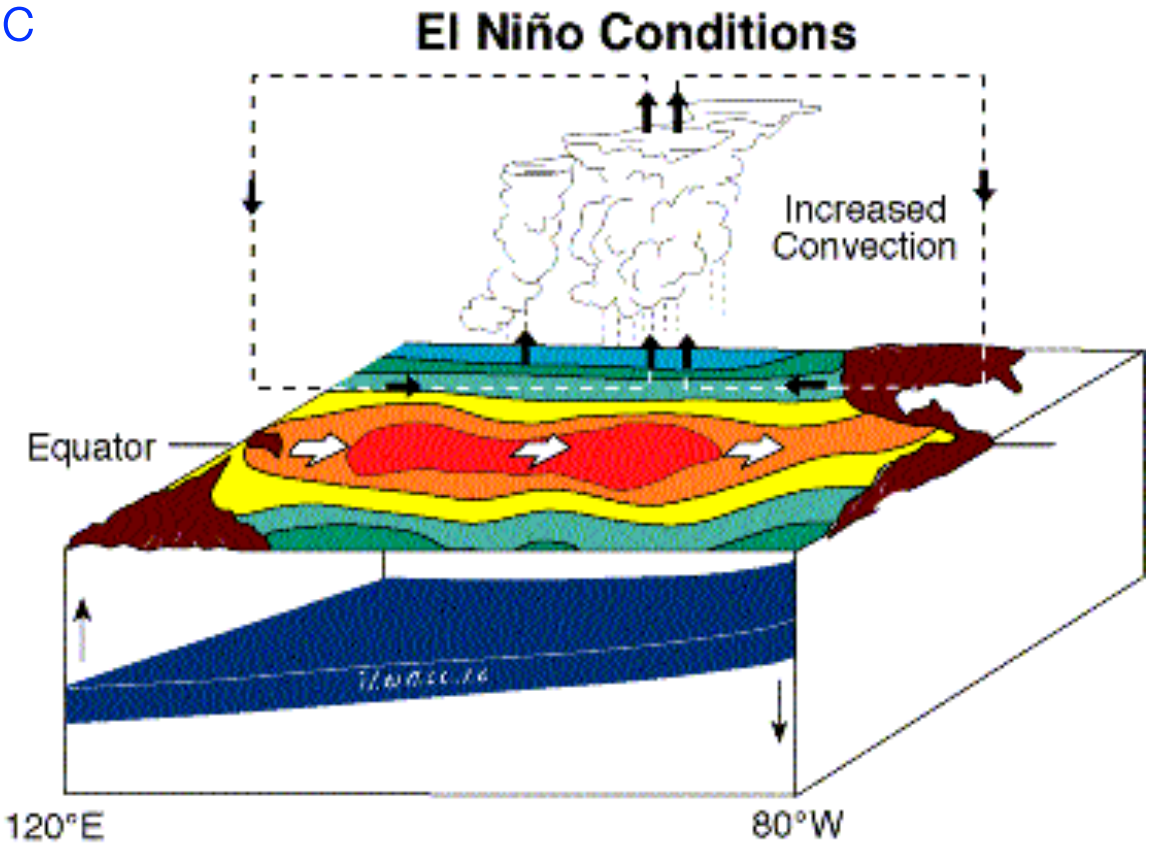

Sverdrup balance

1 Momentum equations for wind-driven circulation:

$$(1) \quad \frac{\partial u}{\partial t} - fv = -\frac{1}{\rho_0}\frac{\partial p}{\partial x} - ru$$

$$(2) \quad \frac{\partial v}{\partial t} + fu = -\frac{1}{\rho_0}\frac{\partial p}{\partial y} - rv$$

2 Beta plane:

$$\begin{aligned} f &= 2\Omega \sin\theta \approx 2\Omega \sin\theta_0 + 2\Omega \cos\theta_0 \,(\theta - \theta_0) \\ &= 2\Omega \sin\theta_0 + \frac{2\Omega}{R} \cos\theta_0 \, R(\theta - \theta_0) \\ &= f_0 + \beta y \end{aligned}$$

3 Vorticity: $\zeta = \dfrac{\partial v}{\partial x} - \dfrac{\partial u}{\partial y}$; for solid body rotation: $(v^r, v^\theta) = (0, \omega r), \quad \zeta = 2\omega$

planetary vorticity (solid Earth rotation): $f = 2\Omega \sin\theta$. Vorticity equation:

$$\frac{\partial (2)}{\partial x} - \frac{\partial (1)}{\partial y} \Rightarrow \frac{\partial \zeta}{\partial t} + \underline{\beta v} = -r\left(\frac{\partial v}{\partial x} - \frac{\partial u}{\partial y}\right) + \underline{\frac{1}{\rho_0 H}\left(\frac{\partial \tau^{(y)}}{\partial x} - \frac{\partial \tau^{(x)}}{\partial y}\right)}$$

Sverdrup balance

Discharge/Recharge phases

warm phase, westerlies (anomaly)

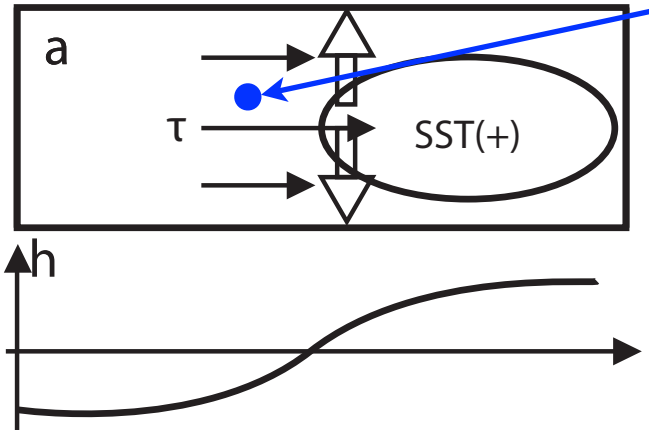

The westerly wind anomaly satisfies $\frac{\partial \tau^{(x)}}{\partial y} < 0$ and therefore the Sverdrup balance:

$$\beta v = \frac{1}{\rho_0 H}\left(\frac{\partial \tau^{(y)}}{\partial x} - \frac{\partial \tau^{(x)}}{\partial y}\right)$$

in the NH implies a $v > 0$, so transport anomaly *away* from the equator. Similarly in SH, $v < 0$.

➨ discharge!

F-F Jin 1997

graduate level

Discharge/Recharge phases

warm phase, westerlies (anomaly)

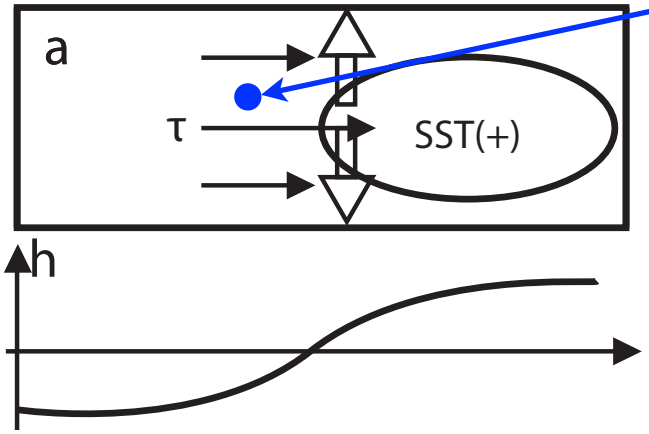

The westerly wind anomaly satisfies $\frac{\partial \tau^{(x)}}{\partial y} < 0$ and therefore the Sverdrup balance:

$$\beta v = \frac{1}{\rho_0 H}\left(\frac{\partial \tau^{(y)}}{\partial x} - \frac{\partial \tau^{(x)}}{\partial y}\right)$$

in the NH implies a $v > 0$, so transport anomaly *away* from the equator. Similarly in SH, $v < 0$.

➨ discharge!

Similarly, the cold phase implies an anomaly transport *toward* the equatorial,

➨ recharge!

cold phase

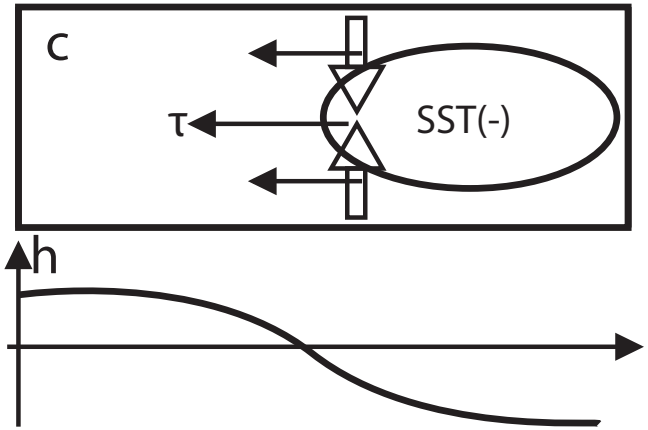

F-F Jin 1997

graduate level

Recharge oscillator

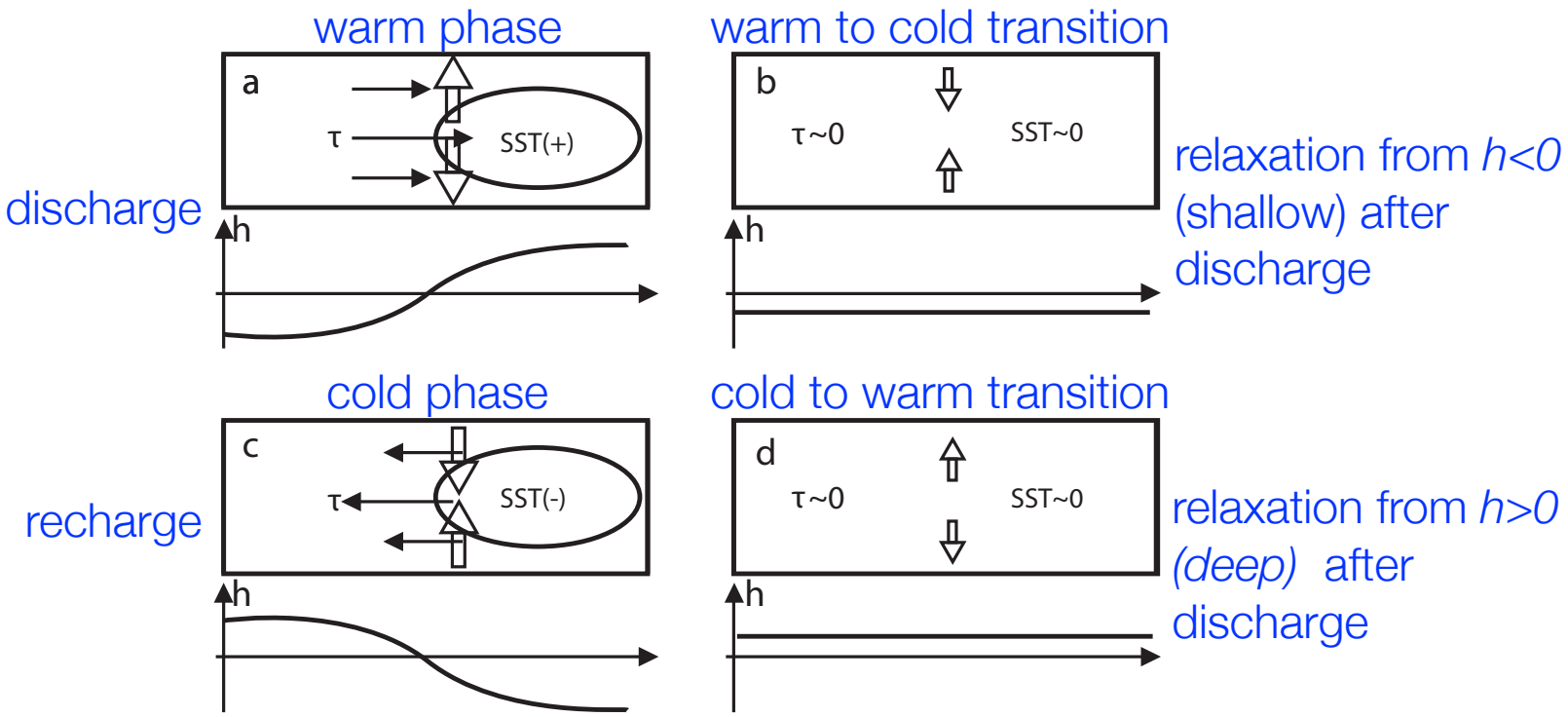

"The four phases of the recharge oscillation. Rectangular box represents the equatorial Pacific basin, ellipses: the SST anomaly, thin & filled arrows: wind stress anomaly associated with SST anomaly; thick unfilled arrows: the recharge/ discharge of equatorial heat content. Each panel also shows the distribution of the thermocline depth anomaly (h) along the equator."

F-F Jin 1997

graduate level

Recharge oscillator

Wind & thermocline tilt:

$$h_E = h_W + \hat{\tau},$$

Westerlies lead to discharge:

$$\frac{dh_W}{dt} = -rh_W - \alpha\hat{\tau}.$$

Damping, thermocline upwelling & wind-driven upwelling:

$$\frac{dT_E}{dt} = -cT_E + \gamma h_E + \delta_s \tau_E.$$

➡ shallow thermocline ($h_E < 0$) leads to cooling

Zonal Wind is driven by East Pacific temperature:

$$\hat{\tau} = bT_E, \ \tau_E = b'T_E,$$

Final equations:

$$\frac{dh_W}{dt} = -rh_W - \alpha b T_E$$

$$\frac{dT_E}{dt} = RT_E + \gamma h_W,$$

Where the Bjerknes feedback coefficient is:

$$R = \gamma b + \delta_s b' - c$$

F-F Jin 1997

graduate level

Recharge oscillator

Final equations in matrix form, with an added noise forcing:

$$\frac{d}{dt}\begin{pmatrix} h_w \\ T_E \end{pmatrix} = \begin{pmatrix} -r & -\alpha b \\ R & \gamma \end{pmatrix}\begin{pmatrix} h_w \\ T_E \end{pmatrix} + \nu(t)$$

Solution to $d\mathbf{x}/dt = A\mathbf{x}$ is $\mathbf{x}(t) = \mathbf{x}_0 e^{At} = \sum c_i \mathbf{e}_i e^{\lambda_i t}$

Calculating the eigenvalues $\lambda_{1,2} = \Re(\lambda) \pm i\Im(\lambda)$ of the matrix, the growth/damping rate $\Re(\lambda)$ and frequency $\Im(\lambda)$ are:

Growth/damping rate: $(R - r)/2$

Frequency: $\omega = \sqrt{\alpha b\gamma - (r + R)^2/4}$

F-F Jin 1997

graduate level

notes

Hopf bifurcation, see also next slide

Self-sustained vs damped ENSO: Delayed oscillator analysis

roots of linearized delayed oscillator equation:

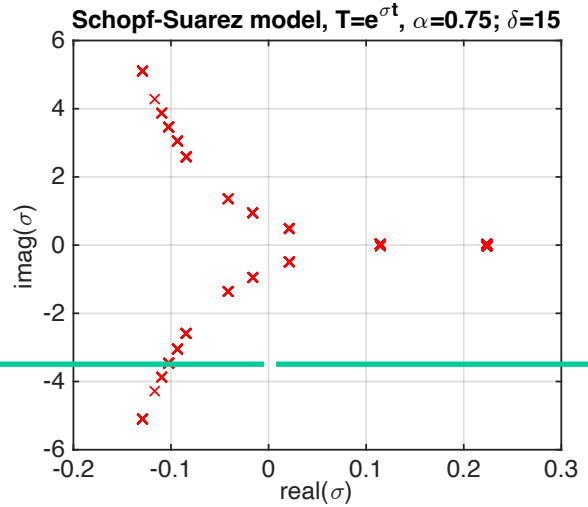

damped ⟵ ⟶ self-sustained

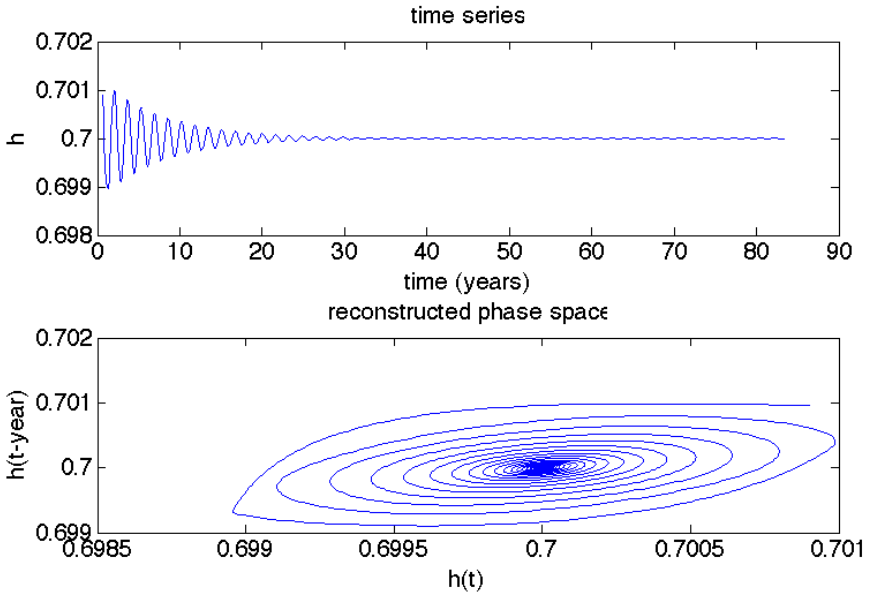

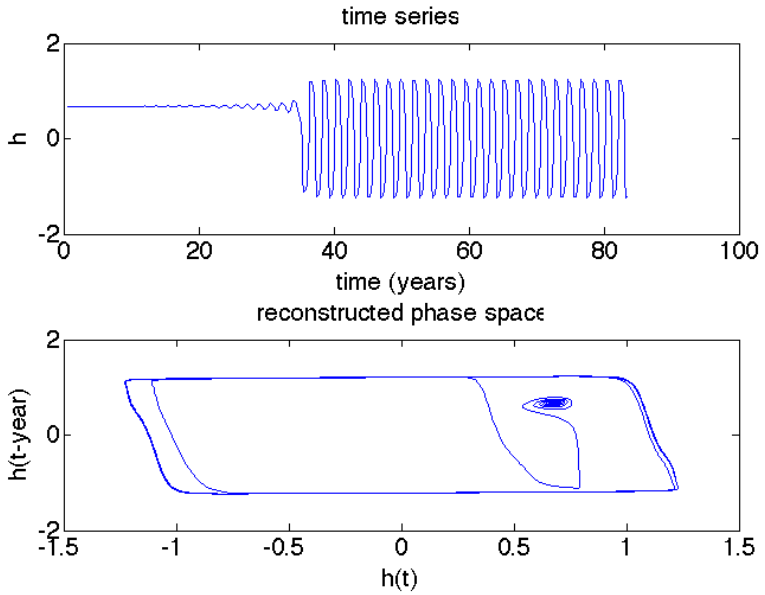

Time series and phase space of nonlinear solution, damped and self-sustained regimes

graduate level

In-class workshop

subcritical Hopf

graduate level

Irregularity: chaos

notes:

A. nonlinear synchronization example: fireflies (pp. 75,77)
B. nonlinear phase locking video in the following slide
C. circle map and quasi-periodicity route to chaos (pp. 79, 81)

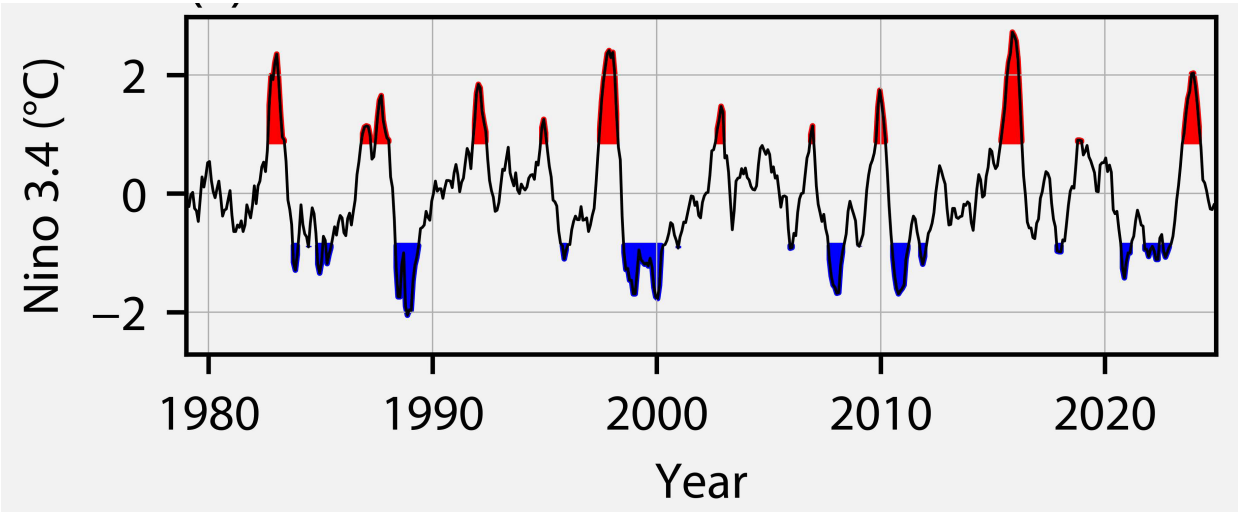

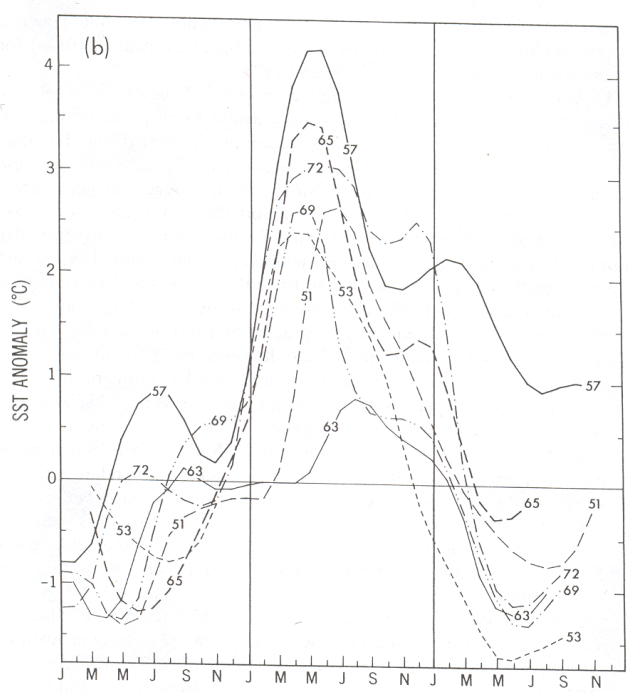

graduate level

Irregularity: chaos

Nonlinear phase locking

graduate level

Irregularity: chaos

Nonlinear phase locking

graduate level

Transition to chaos of an ENSO model

$(x, y, z) =$ (east,north,up) coordinates;

$[u, v, w]/[u_a, v_a]$: corresponding ocean water/atmospheric wind velocity;

$T(x, y, t)$ sea surface temperature; $h(x, y, t)$: depth of warm water.

- Ocean momentum and mass conservation:

$$\begin{aligned} u_t - \beta y v &= -g' h_x + \tau^{(x)}[u_a, v_a] - ru \\ \beta y u &= -g' h_y + \tau^{(y)}[u_a, v_a] - rv \\ h_t + H\nabla \mathbf{v} &= -rh. \end{aligned}$$

- Atmospheric momentum and mass:

$$\begin{aligned} \beta y v_a &= -\phi_x - r u_a \\ \beta y u_a &= -\phi_y - r v_a \\ \phi_t + H\nabla \mathbf{v} &= Q[T, \nabla \mathbf{v}_a] \end{aligned}$$

- Sea surface temperature equation:

$$T_t + \overline{\mathbf{v}}\nabla T + \mathbf{v}\nabla(\overline{T} + T) + w\overline{T}_z + (\overline{w} + w)T_z = -\alpha T \quad (1)$$

An "Intermediate" coupled ocean-atmosphere model, first to successfully predict El Niño events

graduate level

Transition to chaos of an ENSO model

SST

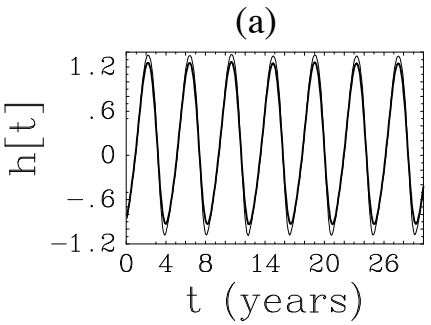

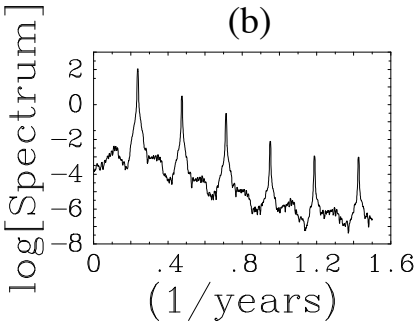

Spectrum

Delay coordinates reconstructed phase space

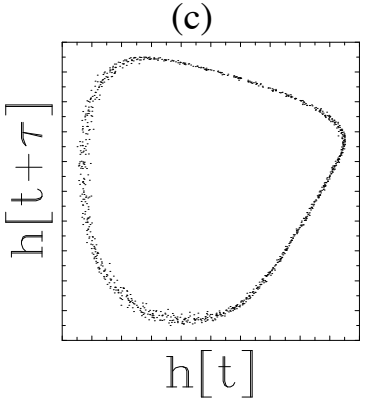

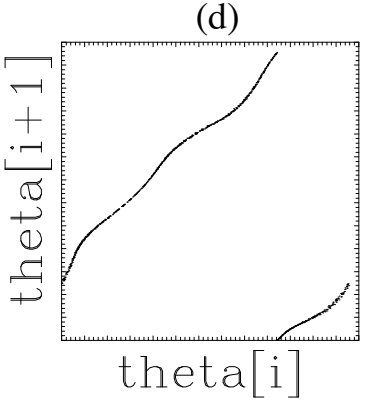

Number of events per month

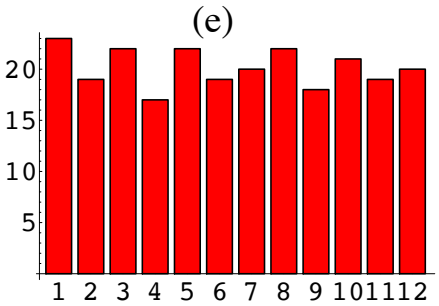

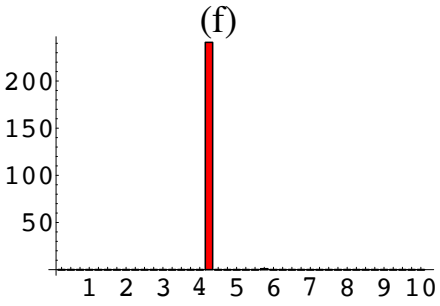

Time between events

Weak seasonal cycle: quasi-periodic, ENSO period is 4.X years

Transition to chaos of an ENSO model

SST

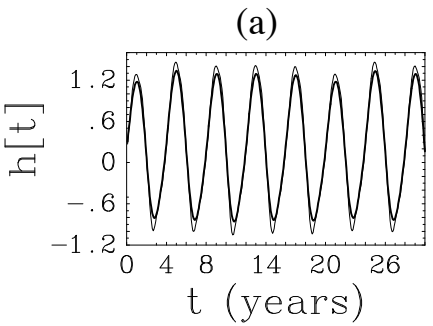

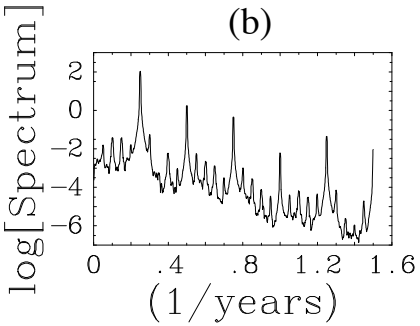

Spectrum

Delay coordinates reconstructed phase space

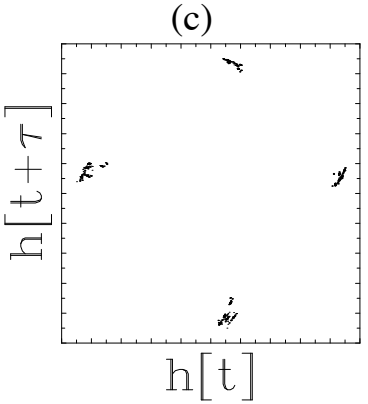

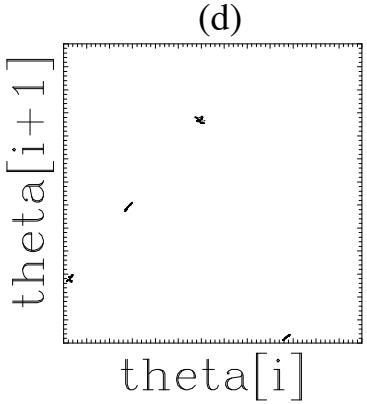

Number of events per month

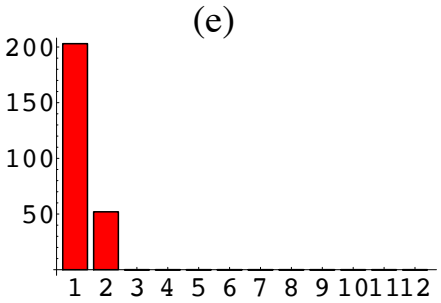

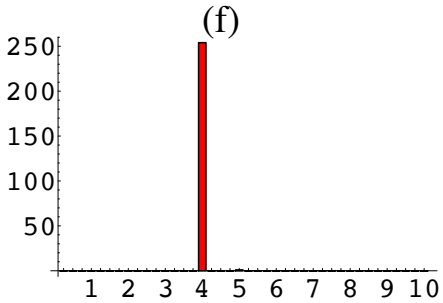

Time between events

Moderate amplitude seasonal cycle: phase-locked

graduate level

Transition to chaos of an ENSO model

SST

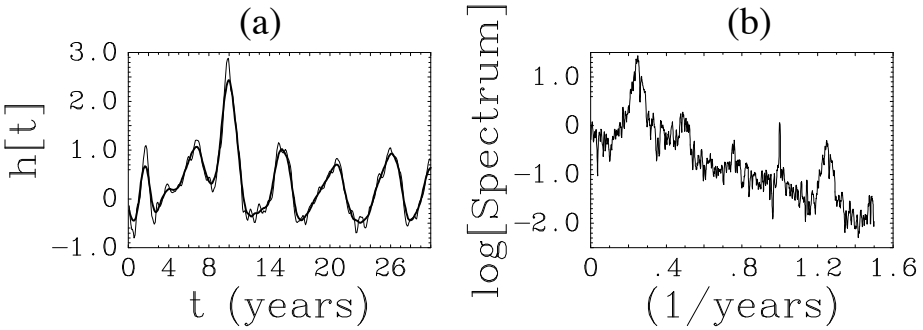

Spectrum

Delay coordinates reconstructed phase space

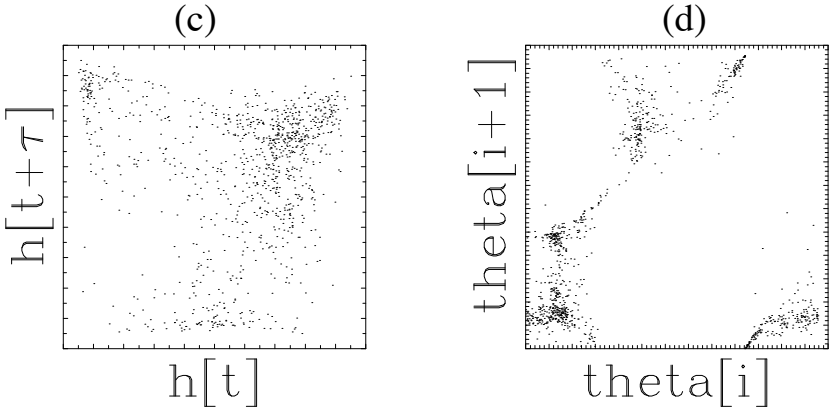

Number of events per month

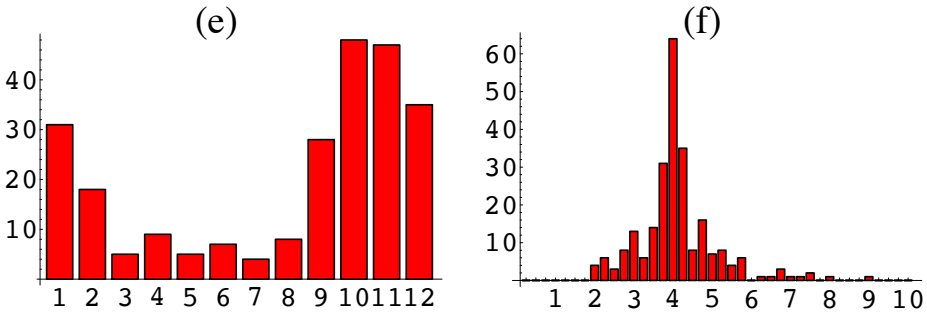

Time between events

Strong seasonal cycle: chaotic

graduate level

Irregularity: noise, transient growth

Outline:

1- notes: non-normal transient growth, optimal initial conditions
(stochastic optimals will be covered in AMOC section)

2- WWBs as stochastic optimals

3- WWBs are not purely stochastic, they depend on the mean state and occur more frequently during El Niño conditions

Irregularity: observed Westerly Wind Bursts

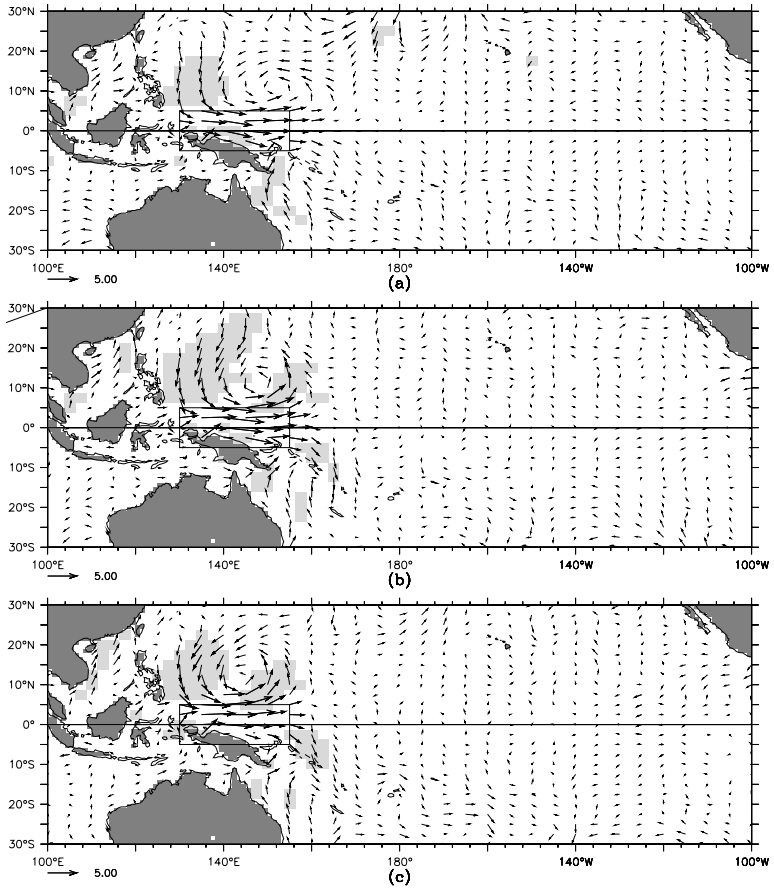

Figs 68, 69, 70: composite WWE 10-m wind anomaly vector map, for (a) day(–1), (b) day(0) and (c) day(1). The classifying region is indicated by the thin lined box. The scale vector is 5m/s. Zonal wind anomalies statistically significant at 99% are indicated by bold vectors, meridional wind anomalies significant at 99% are indicated by shaded background.

Vecchi and Harrison 1997

graduate level

Irregularity: observed Westerly Wind Bursts

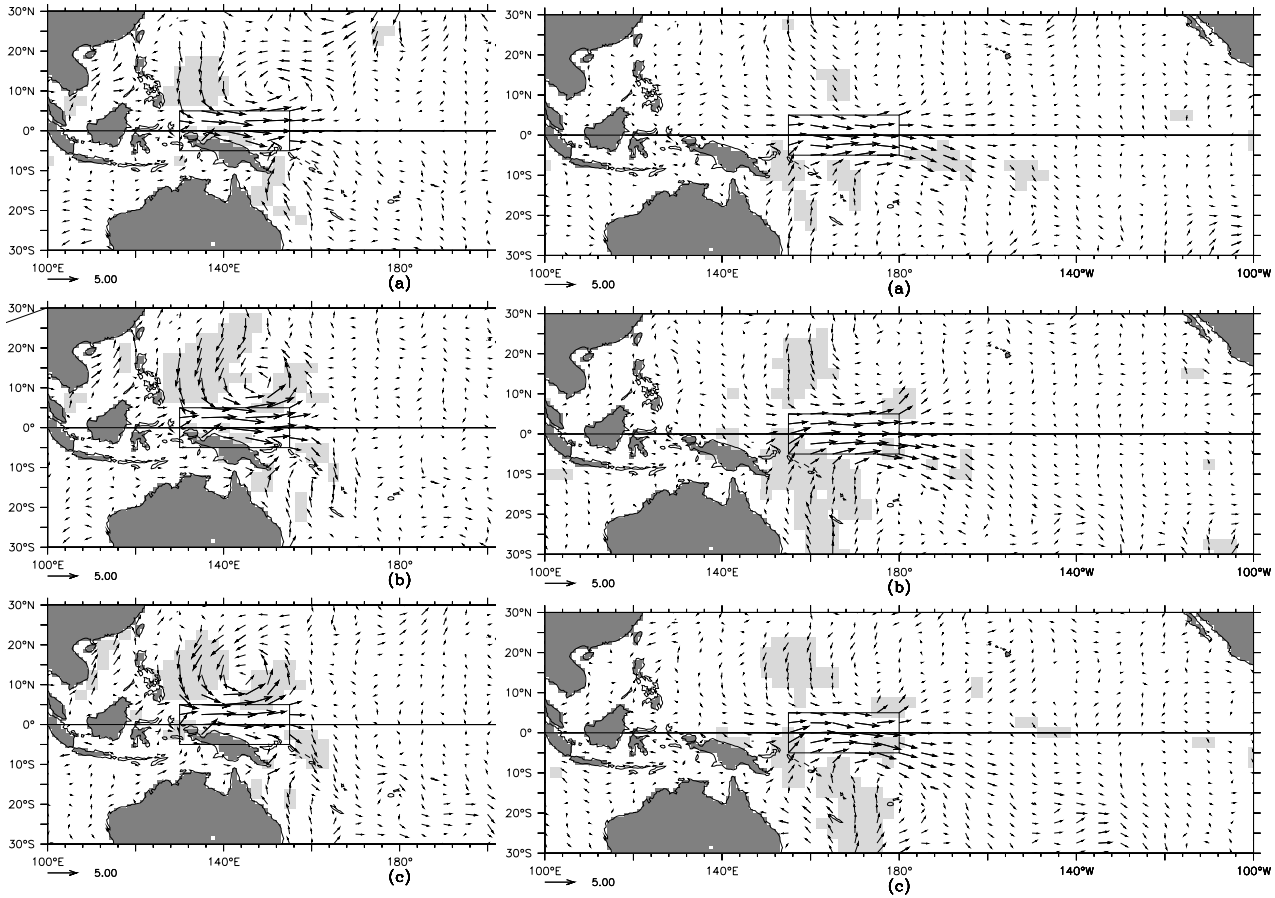

Figs 68, 69, 70: composite WWE 10-m wind anomaly vector map, for (a) day(–1), (b) day(0) and (c) day(1). The classifying region is indicated by the thin lined box. The scale vector is 5m/s. Zonal wind anomalies statistically significant at 99% are indicated by bold vectors, meridional wind anomalies significant at 99% are indicated by shaded background.

Vecchi and Harrison 1997

graduate level

Irregularity: observed Westerly Wind Bursts

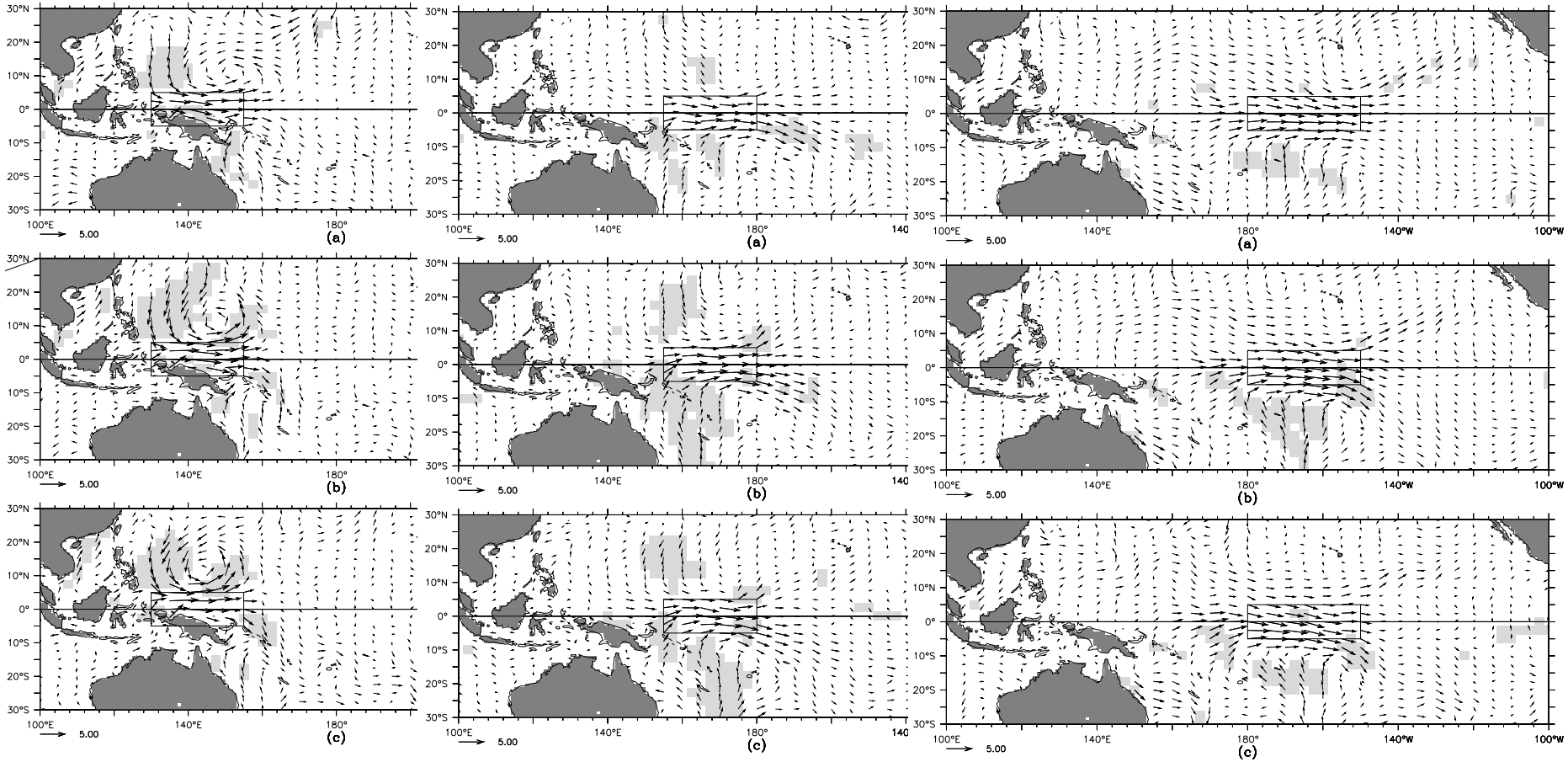

Figs 68, 69, 70: composite WWE 10-m wind anomaly vector map, for (a) day(–1), (b) day(0) and (c) day(1). The classifying region is indicated by the thin lined box. The scale vector is 5m/s. Zonal wind anomalies statistically significant at 99% are indicated by bold vectors, meridional wind anomalies significant at 99% are indicated by shaded background.

Vecchi and Harrison 1997

graduate level

Irregularity: Westerly Wind Bursts excite Kelvin waves

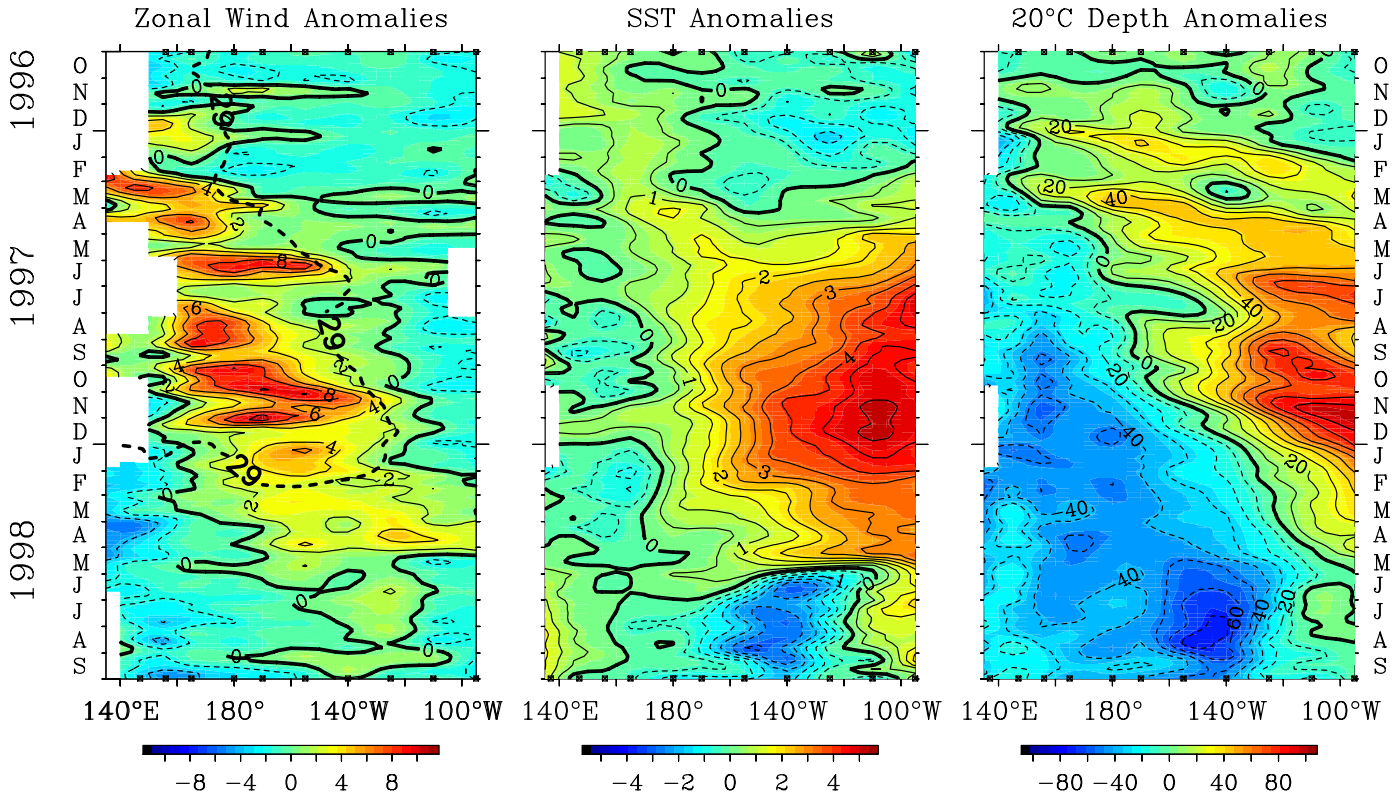

Figure 2. Heat content anomalies averaged between 2°N and 2°S along the equator from TAO data (in 10^{10} J m^{-3}, left), sea level anomalies along the equator from the TOPEX/Poseidon altimeter (in cm, middle), and modeled sea level anomalies along the equator (in cm, right). Temporal resolution is 5-days for TAO data and the model, 10-days for the altimeter data. A mean seasonal cycle has been removed from each time series.

McPhaden and Yu 1999

graduate level

Irregularity: WWBs precede major El Niños

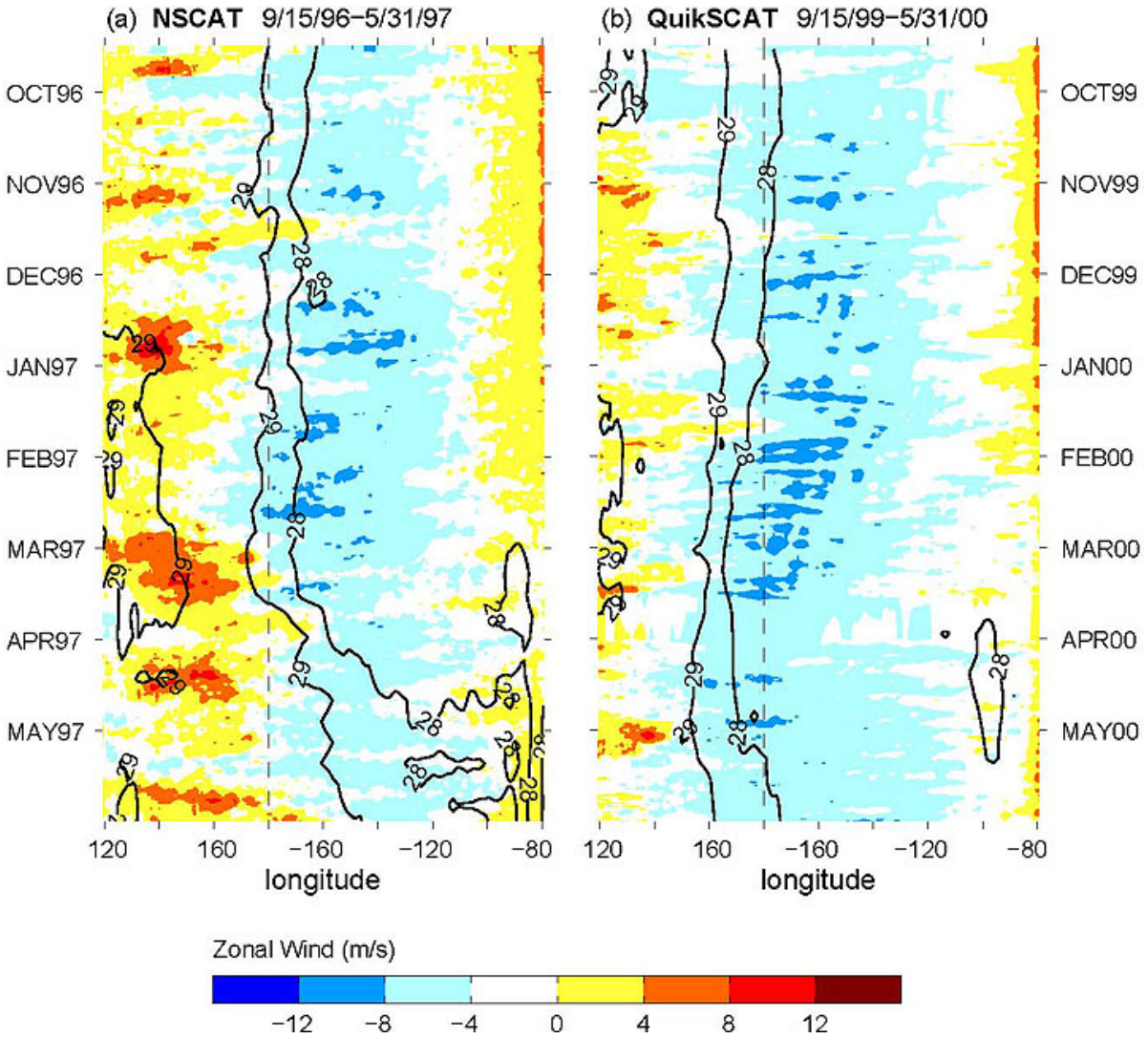

Lisan Yu: observed SST (contours) and WWBs (colors)

graduate level

Irregularity: Westerly Wind Bursts as optimal initial conditions

Figure 6: the structure of the fastest growing all terms singular factor (TAUSV) over the tropical pacific. during the July, August and September (JAS) quarter. Maps detailing the structure of the perturbation SST (delta T) , perturbation thermocline depth (delta h),perturbation zonal ocean current (delta u),equatorial perturbation vertical velocity (delta w),and vectors of the perturbation wind (delta U) are shown at the end of July and September. Light shading represents positive values of each quantity, while dark shading indicates negative values. Because the SVs are the result of a linear analysis, the scaling of the various fields is arbitrary.

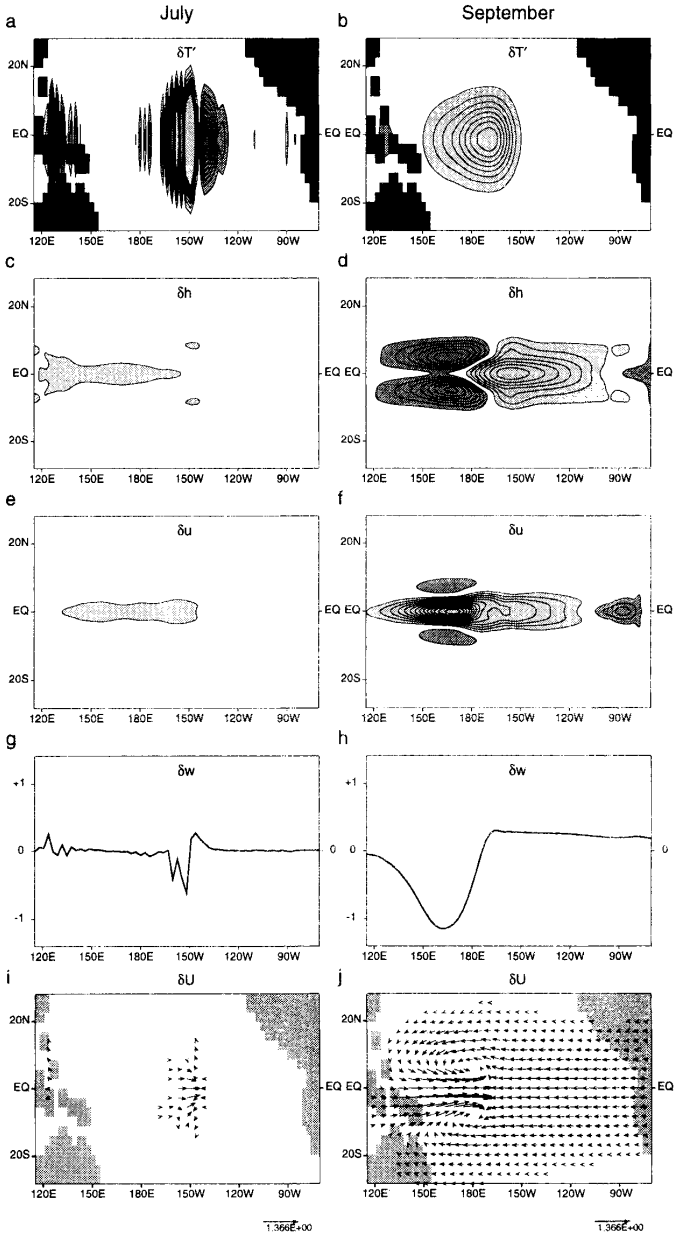

Moore and Kleeman 1997

graduate level

Irregularity: WWBs are not purely stochastic, depend on mean state

WWBs as a gaussian perturbation:

$$\tau = A \exp\left[-\frac{(x-x_0)^2}{L_{\mathrm{EW}}^2} - \frac{(y-y_0)^2}{L_{\mathrm{NS}}^2} - \frac{(t-t_0)^2}{T^2} \right].$$

with parameters:

$$\mathbf{R}(t) = (A, x_0, y_0, L_{\mathrm{EW}}, L_{\mathrm{NS}}, T, p)^{\mathrm{T}},$$

covariance matrix with SST

$$\mathbf{C}_{ij} = \frac{1}{N_{\mathrm{wwb}} - 1} \sum_{t=1}^{N_{\mathrm{wwb}}} T_i(t) \mathbf{R}_j(t).$$

and singular vectors are:

Tziperman and Yu 2007

graduate level

Irregularity: WWBs are not purely stochastic, depend on mean state

WWBs as a gaussian perturbation:

$$\tau = A \exp\left[-\frac{(x-x_0)^2}{L_{\mathrm{EW}}^2} - \frac{(y-y_0)^2}{L_{\mathrm{NS}}^2} - \frac{(t-t_0)^2}{T^2} \right].$$

with parameters:

$$\mathbf{R}(t) = (A, x_0, y_0, L_{\mathrm{EW}}, L_{\mathrm{NS}}, T, p)^{\mathrm{T}},$$

covariance matrix with SST

$$\mathbf{C}_{ij} = \frac{1}{N_{\mathrm{wwb}} - 1} \sum_{t=1}^{N_{\mathrm{wwb}}} T_i(t) \mathbf{R}_j(t).$$

and singular vectors are:

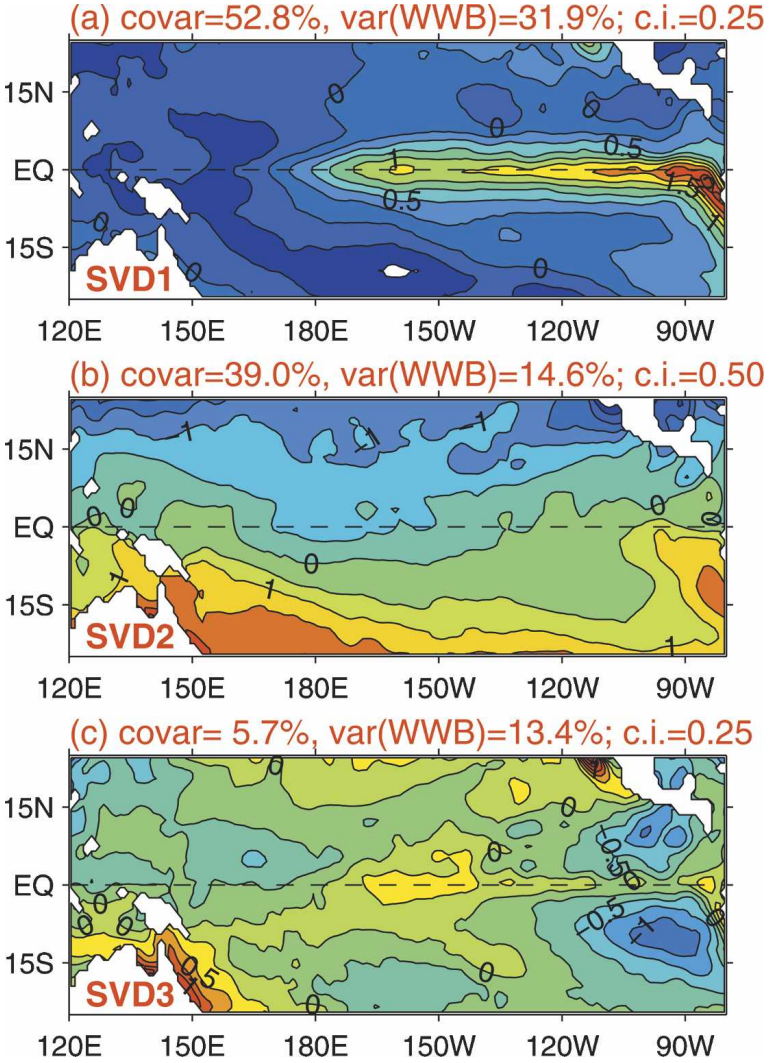

Tziperman and Yu 2007

graduate level

Irregularity: WWBs are not purely stochastic, depend on mean state

WWBs as a gaussian perturbation:

$$\tau = A \exp\left[-\frac{(x-x_0)^2}{L_{\mathrm{EW}}^2} - \frac{(y-y_0)^2}{L_{\mathrm{NS}}^2} - \frac{(t-t_0)^2}{T^2} \right].$$

with parameters:

$$\mathbf{R}(t) = (A, x_0, y_0, L_{\mathrm{EW}}, L_{\mathrm{NS}}, T, p)^{\mathrm{T}},$$

covariance matrix with SST

$$\mathbf{C}_{ij} = \frac{1}{N_{\mathrm{wwb}} - 1} \sum_{t=1}^{N_{\mathrm{wwb}}} T_i(t)\mathbf{R}_j(t).$$

and singular vectors are:

TABLE 1. The first seven rows of this table give the seven SVD vectors for the WWB parameters shown in Eq. (1). The entries are all multiplied by 100. The row marked "%covar" contains the percentage of the covariance between the SST and the WWB parameters explained by each SVD vector [using the singular values, Eq. (9)]. The last row, marked "%var(τ)," is the percentage of the variance of the WWB parameter vector explained by each SVD vector [using Eq. (11)].

	1	2	3	4	5	6	7
A	18	81	2	35	0	2	43
x_0	58	−20	27	−49	−23	0	51
L_{EW}	49	4	−7	17	−11	−75	−39
L_{NS}	11	−13	31	6	91	−15	14
T	27	1	67	30	−14	43	−43
P	47	−33	−56	43	11	38	8
y_0	−28	−41	27	57	−27	−29	44
%covar	53	39	6	1	1	0	0
%var(τ)	32	15	13	15	12	7	6

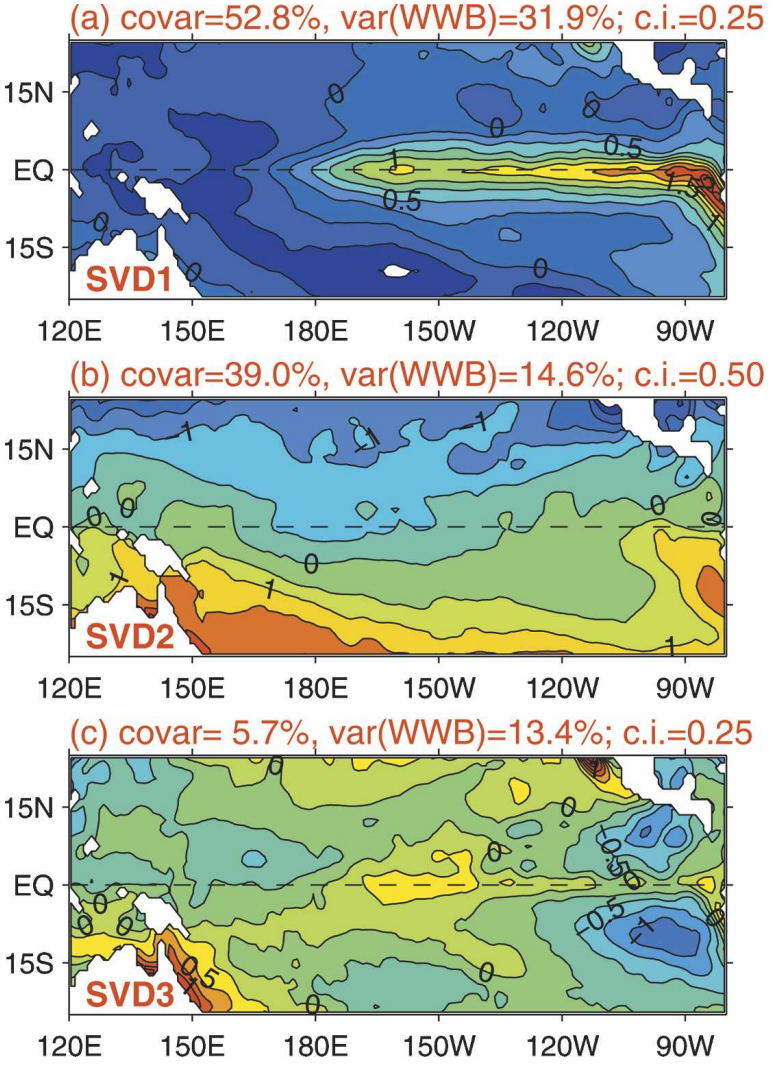

Tziperman and Yu 2007

graduate level

Summary of ENSO irregularity: Chaos or stochastic forcing
Why can't we predict El Niño well in advance?

Two possible paradigms

Chaos: the butterfly effect

- Irregularity from deterministic chaos driven by seasonal cycle

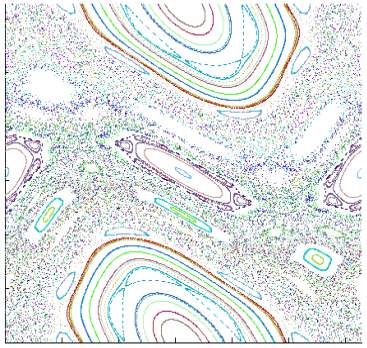

- ENSO oscillator irregularly jumps between nonlinear resonances with the seasonal cycle.
- reproduces major ENSO features
- Deterministic system but sensitive to initial conditions – 6-9 month predictability

Summary of ENSO irregularity: Chaos or stochastic forcing
Why can't we predict El Niño well in advance?

Two possible paradigms

Chaos: the butterfly effect

- Irregularity from deterministic chaos driven by seasonal cycle

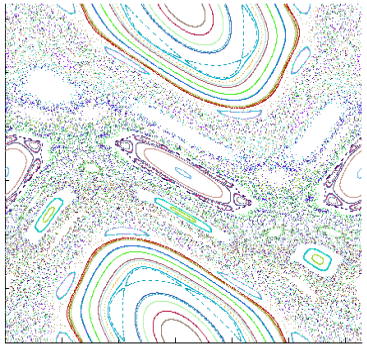

- ENSO oscillator irregularly jumps between nonlinear resonances with the seasonal cycle.
- reproduces major ENSO features
- Deterministic system but sensitive to initial conditions – 6-9 month predictability

Noise (Stochastic forcing):

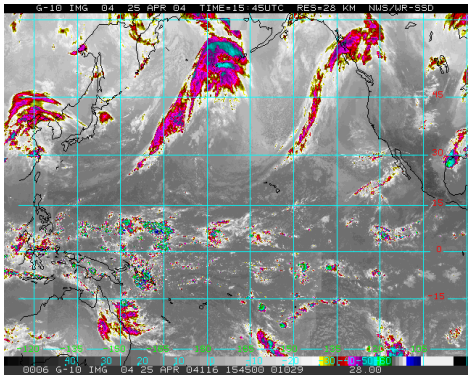

- Irregularity from weather forcing on inter-annually varying components
- Nonlinearity is not crucial. Damped oscillations are randomized by stochastic forcing
- non normal amplification!
- Models reproduce major ENSO features
- Insensitive to initial conditions, but stochastic forcing effects add up – 6-9 month predictability

graduate level

ENSO teleconnections

Reminder: ENSO teleconnections, precipitation:

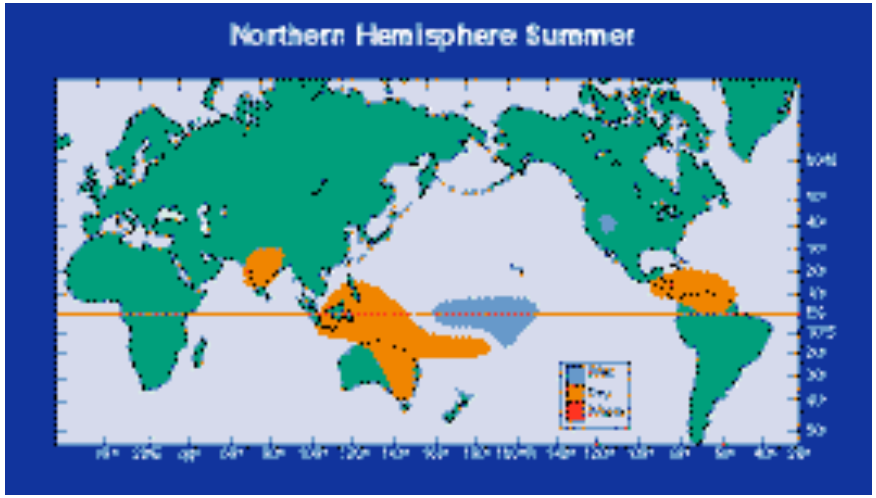

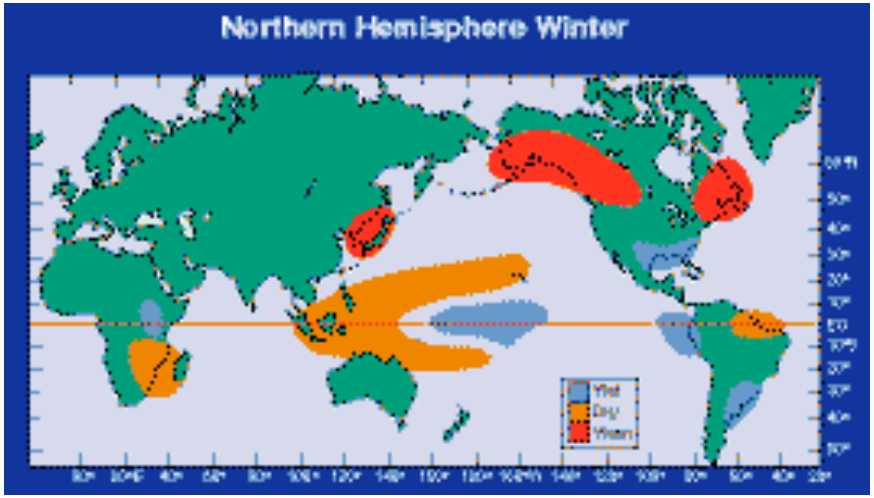

Precipitation anomalies during El Niño in (a) Summer and (b) Winter

http://www.pmel.noaa.gov/tao/elnino/impacts.html

graduate level

Atmospheric teleconnections: **Rossby wave** train forced by ENSO

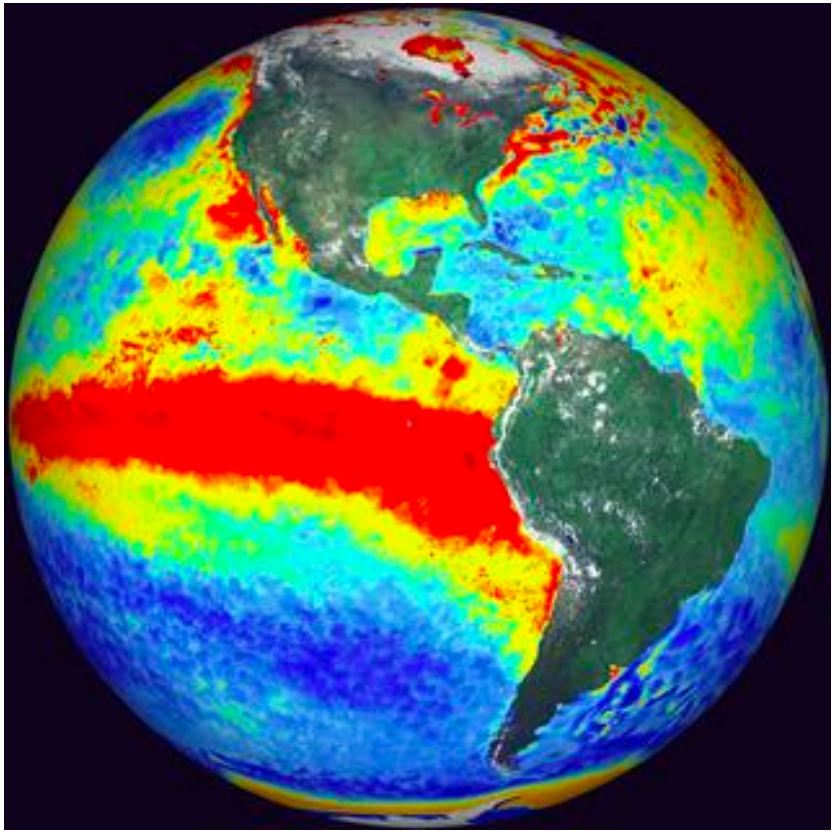

sea surface temperature anomaly during an El Niño event (https://snowbrains.com/noaa-el-nino-update-today/)

Atmospheric teleconnections: **Rossby wave** train forced by ENSO

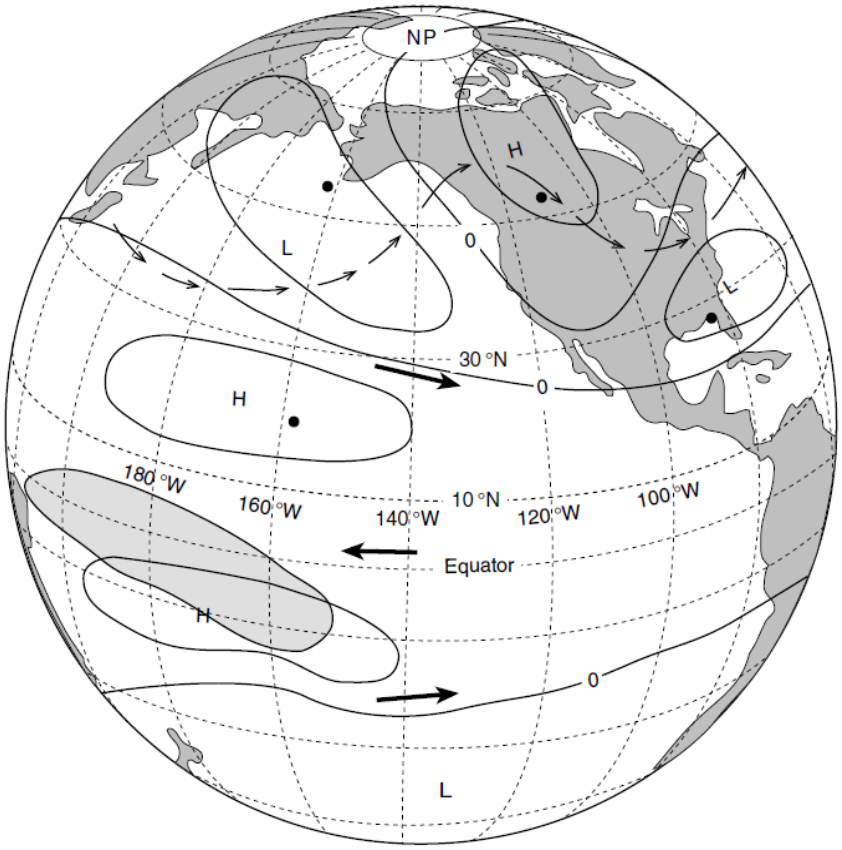

solid contours: schematic upper atmosphere geopotential height anomaly; shaded area at equator: enhanced cloudiness and rain. Light arrows: mid-tropospheric stream line distorted by wave pattern. (Horel & Wallace 1981)

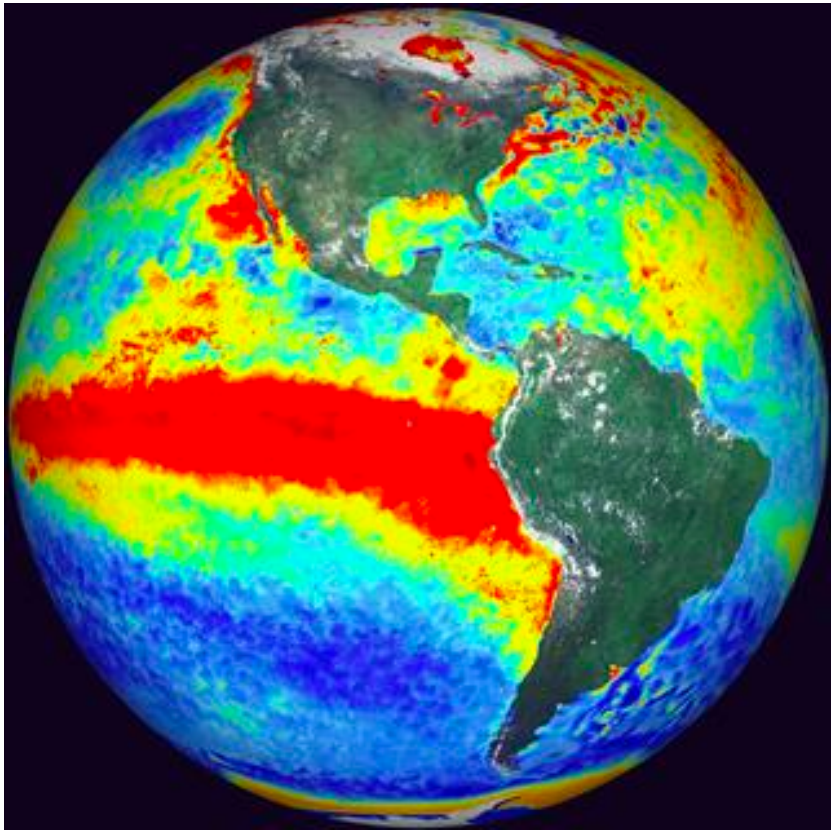

sea surface temperature anomaly during an El Niño event (https://snowbrains.com/noaa-el-nino-update-today/)

Atmospheric teleconnections: **Rossby wave** train forced by ENSO

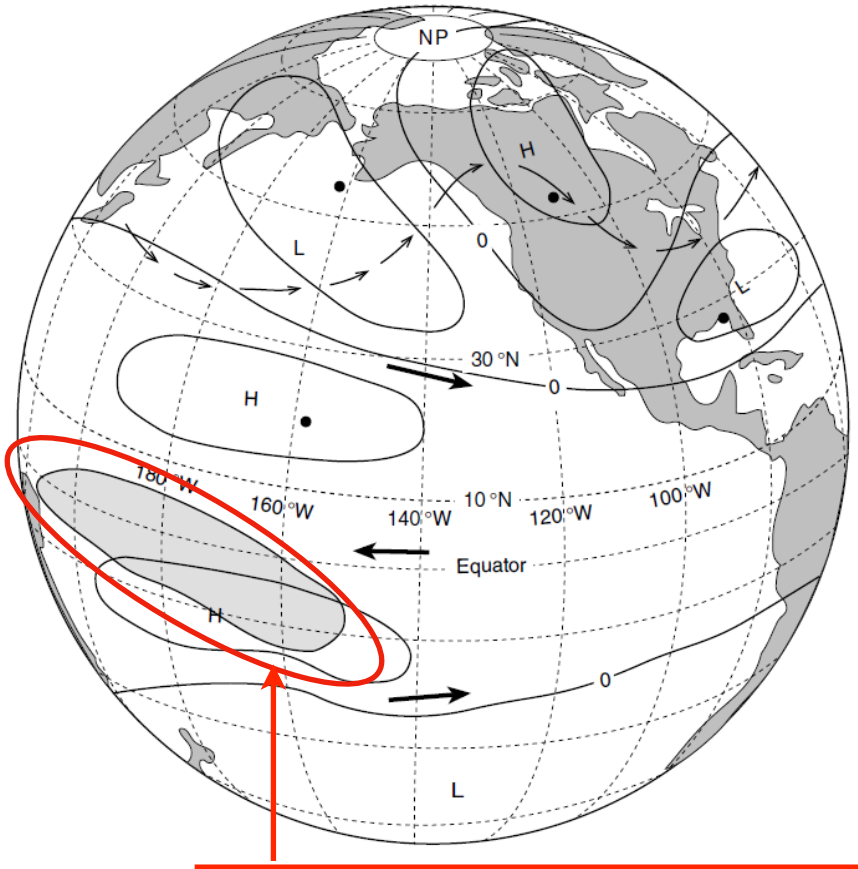

solid contou
atmosphere
shaded are
cloudiness
tropospheric stream line distorted by wave
pattern. (Horel & Wallace 1981)

precipitation and atmospheric heating due to El Niño, which forces atmospheric waves

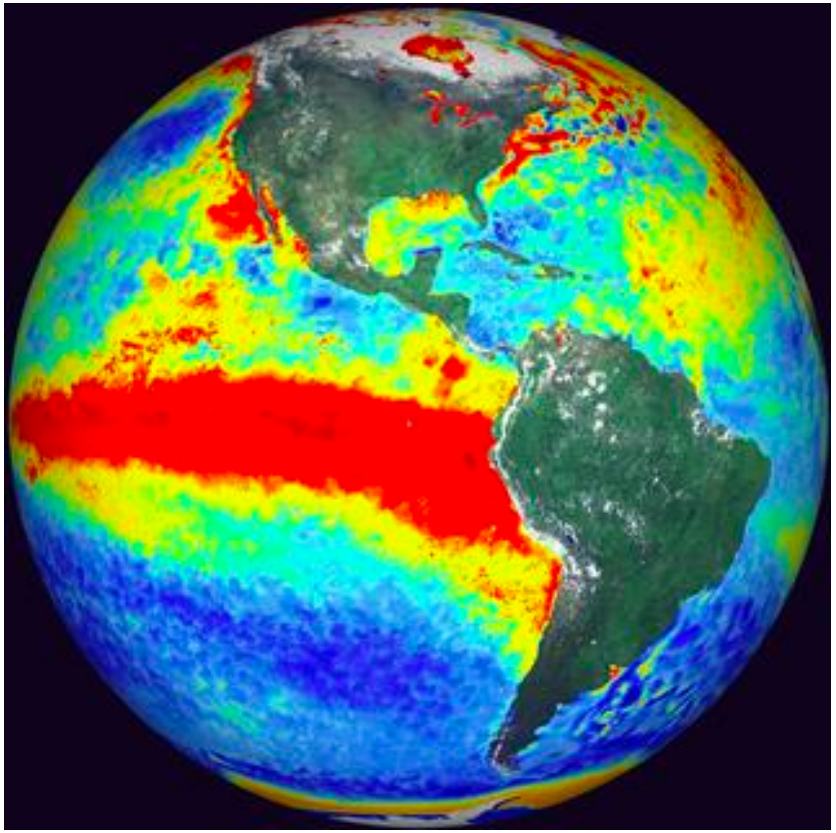

sea surface temperature anomaly during an El Niño event (https://snowbrains.com/noaa-el-nino-update-today/)

Atmospheric teleconnections: **Rossby wave** train forced by ENSO

Rossby wave

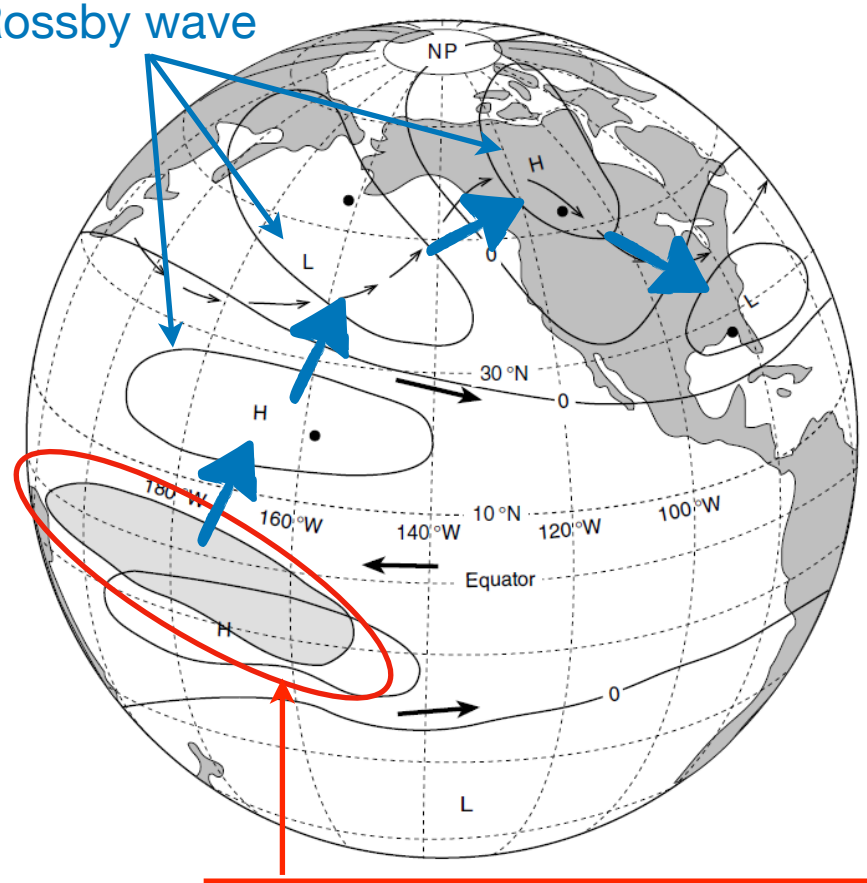

solid contou
atmosphere
shaded are
cloudiness
tropospheric stream line distorted by wave
pattern. (Horel & Wallace 1981)

precipitation and atmospheric heating due to El Niño, which forces atmospheric waves

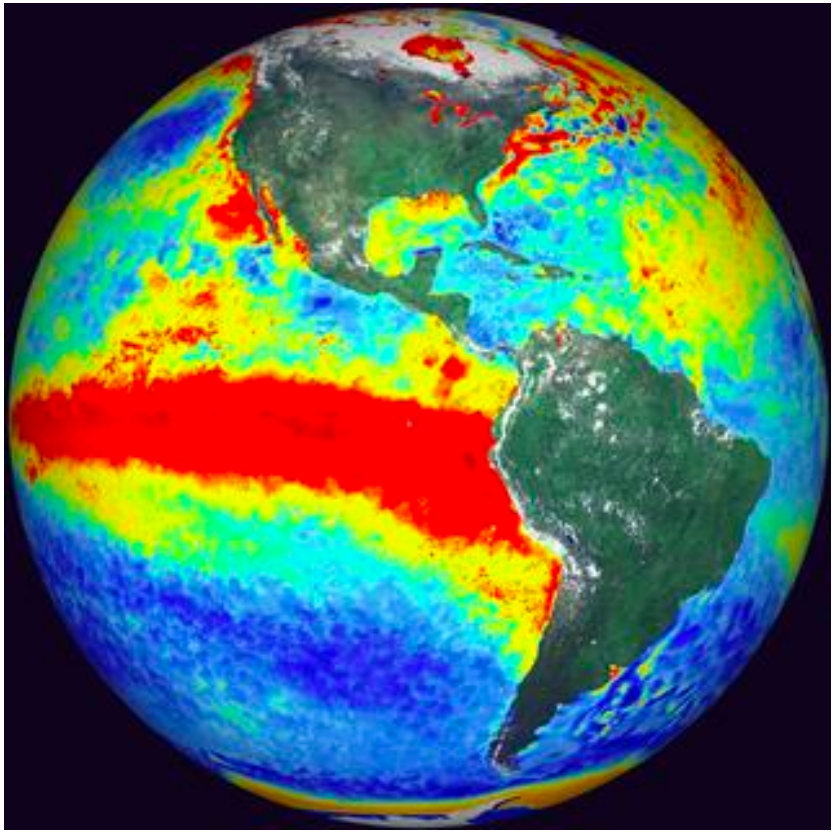

sea surface temperature anomaly during an El Niño event (https://snowbrains.com/noaa-el-nino-update-today/)

Atmospheric teleconnections: **Rossby wave** train forced by ENSO

Rossby wave

highs and lows affect precipitation locally

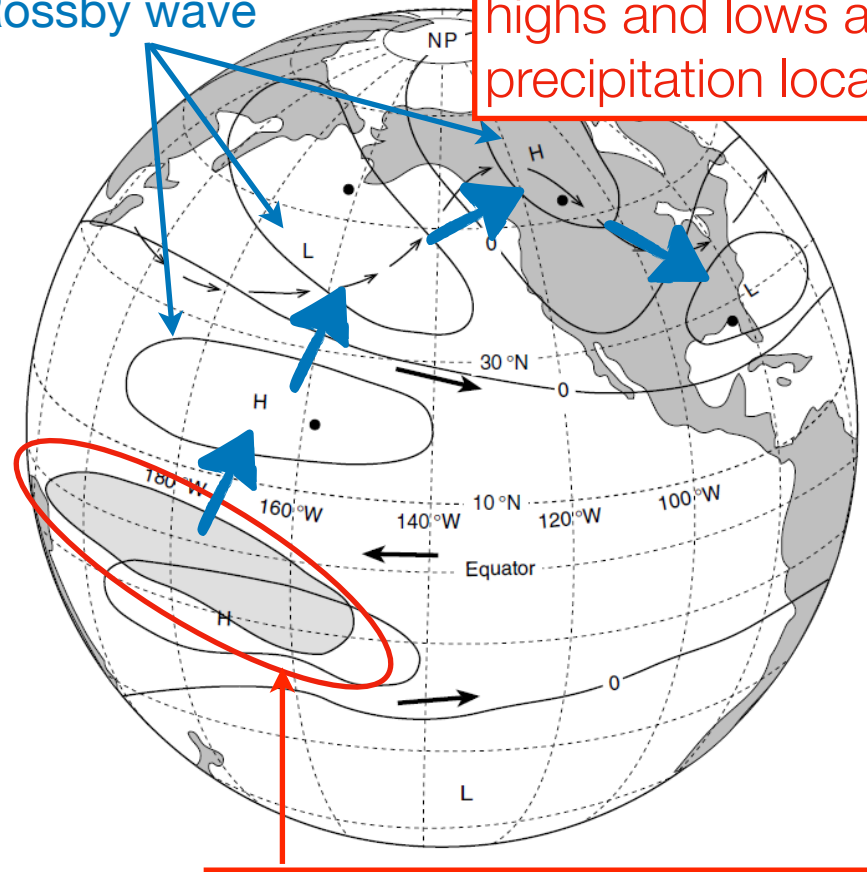

precipitation and atmospheric heating due to El Niño, which forces atmospheric waves

solid contou
atmosphere
shaded are
cloudiness
tropospheric stream line distorted by wave
pattern. (Horel & Wallace 1981)

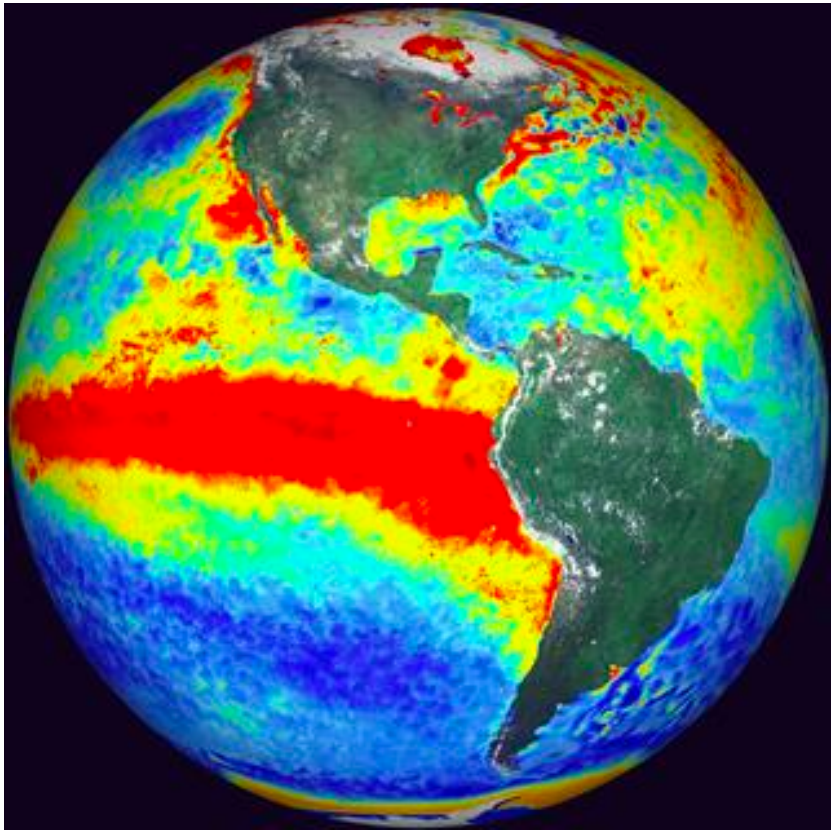

sea surface temperature anomaly during an El Niño event (https://snowbrains.com/noaa-el-nino-update-today/)

ENSO teleconnections

example wave teleconnection patterns

FIG. 3. Steady state, linear solution of a five-layer baroclinic model for a deep elliptical heat source at 15° perturbing the Northern Hemisphere winter zonal flow. Shown are (a) height field in a longitude-height section at 18.1°N (contour interval 1 dam), (b) 300 mb vorticity perturbation (contour interval 0.05Ω), and (c) 300 mb height field perturbation (contour interval 2 dam). The contour convention is as in Fig. 1 except that the zero contours in (a) are thick continuous lines. The center of the source is indicated by a cross in (a) and the region of heating larger than 0.5 K day^{-1} by hatching in (c). Tick marks in (a) are at 100, 300, 500, 700 and 900 mb in the vertical and every 30° of longitude.

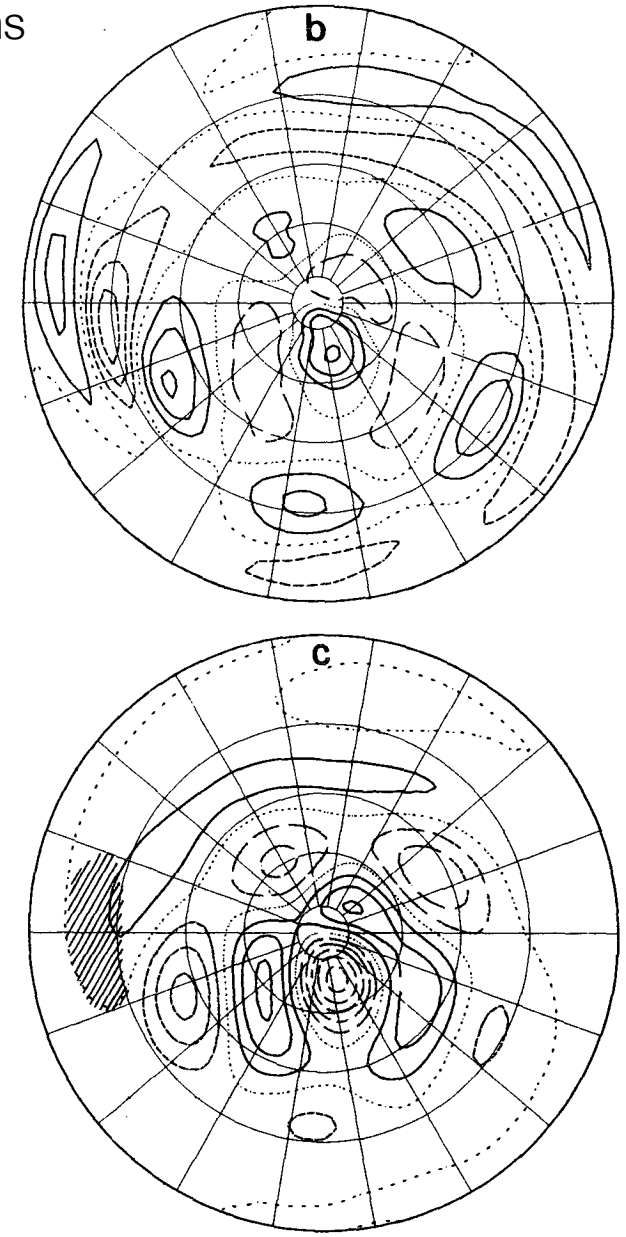

Hoskins and Karoly 1981

graduate level

ENSO teleconnections

notes, use also following slides

ENSO teleconnections: spherical coordinates, mercator projection

sphere. It is convenient to use a Mercator projection of the sphere (e.g., Phillips, 1973):

$$x = a\lambda, \tag{5.1}$$

$$y = a \ln[(1 + \sin\phi)/\cos\phi]. \tag{5.2}$$

Then

$$\frac{1}{a\cos\phi}\frac{\partial}{\partial\lambda} = \frac{1}{\cos\phi}\frac{\partial}{\partial x}, \tag{5.3}$$

$$\frac{1}{a}\frac{\partial}{\partial\phi} = \frac{1}{\cos\phi}\frac{\partial}{\partial y}, \tag{5.4}$$

$$\nabla^2 = \frac{1}{\cos^2\phi}\left(\frac{\partial^2}{\partial x^2} + \frac{\partial^2}{\partial y^2}\right), \tag{5.5}$$

$$\cos\phi = \operatorname{sech} y/a, \tag{5.6}$$

$$\sin\phi = \tanh y/a. \tag{5.7}$$

The Mercator basic zonal velocity

$$\bar{u}_M = \bar{u}/\cos\phi \tag{5.8}$$

is proportional to the angular velocity. The equation for the horizontal streamfunction perturbation ψ, on multiplying by $\cos^2\phi$, takes the form

$$\left(\frac{\partial}{\partial t} + \bar{u}_M\frac{\partial}{\partial x}\right)\left(\frac{\partial^2\psi}{\partial x^2} + \frac{\partial^2\psi}{\partial y^2}\right) + \beta_M\frac{\partial\psi}{\partial x} = 0, \tag{5.9}$$

where

$$\beta_M = \frac{2\Omega}{a}\cos^2\phi - \frac{d}{dy}\frac{1}{\cos^2\phi}\frac{d}{dy}(\cos^2\phi\bar{u}_M) \tag{5.10}$$

is $\cos\phi$ times the meridional gradient of the absolute vorticity on the sphere.

The dispersion equation for plane wave solutions $\exp i(kx + ly - \omega t)$ of (5.9)

$$\omega = \bar{u}_M k - \frac{\beta_M k}{k^2 + l^2}. \tag{5.11}$$

Hoskins and Karoly 1981

graduate level

In-class workshop

group velocity of barotropic atmospheric stationary Rossby waves

graduate level

ENSO teleconnections: steady-state view of Rossby ray bending

dispersion relation for stationary waves

$$0 = \omega = u_M k - \beta_M k/(k^2 + l^2)$$

define

$$K_s = (\beta_M/u_M)^{1/2} = k^2 + l^2$$

If $k > K_s$ then l must be imaginary. As the wave propagates northward from low latitudes, with a constant k while K_s gets smaller due to changes in mean flow and effective beta (Fig. 13 a,b), this implies evanescent behavior in latitude past a critical latitude, and trapping of the ray at the critical latitude.

Hoskins and Karoly 1981

graduate level

ENSO teleconnections

Ray tracing for idealized “constant angular momentum” mean flow:

Hoskins and Karoly 1981

graduate level

ENSO teleconnections

Ray tracing for idealized "constant angular momentum" mean flow:

$$\bar{u}_M = a\tilde{\omega} \quad \Rightarrow \bar{u} = \bar{u}_M \cos\phi = a\tilde{\omega}\cos\phi$$

$$\beta_M = \frac{2\cos^2\phi}{a}(\Omega + \tilde{\omega})$$

$$K_s \doteq (\epsilon a)^{-1}\cos\phi$$

and an analytic solution for wave ray path, $(x(t), y(t))$ is possible:

Hoskins and Karoly 1981

graduate level

ENSO teleconnections

Ray tracing for idealized "constant angular momentum" mean flow:

$$\bar{u}_M = a\tilde{\omega} \quad \Rightarrow \bar{u} = \bar{u}_M \cos\phi = a\tilde{\omega}\cos\phi$$

$$\beta_M = \frac{2\cos^2\phi}{a}(\Omega + \tilde{\omega})$$

$$K_s \doteq (\epsilon a)^{-1}\cos\phi$$

and an analytic solution for wave ray path, $(x(t), y(t))$ is possible:

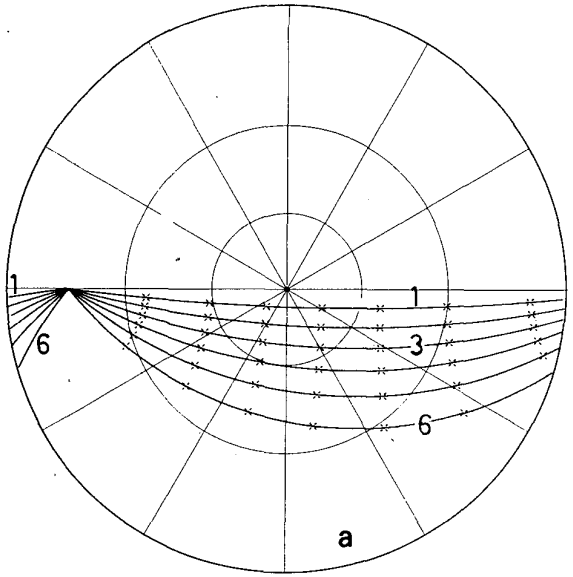

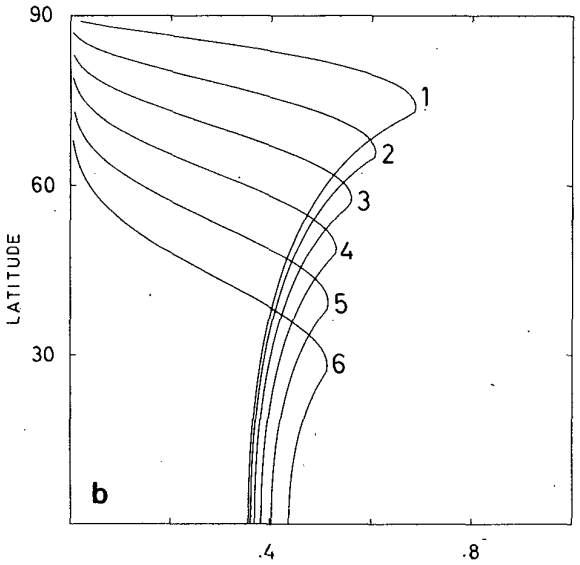

FIG. 12. (a) Rays and phases marked by a cross every 180° for a source at 15° in a super-rotation flow. If all wavelengths give a negative extremum at the source, the crosses mark the positions of successive positive and negative extrema. Lines of latitude and longitude are drawn every 30° and the zonal wavenumbers associated with the rays are indicated. (b) Amplitudes of the extrema on the rays for the different zonal wavenumbers, on the super-rotation flow shown as a function of latitude. The relative amplitudes of the different wavenumbers depend on the position and nature of the source.

Hoskins and Karoly 1981

graduate level

ENSO teleconnections

example teleconnection patterns

$\bar{u}_M/a,\ a\beta_M$ $\qquad$ $aK_s = \sqrt{\bar{u}_M/\beta_M}$

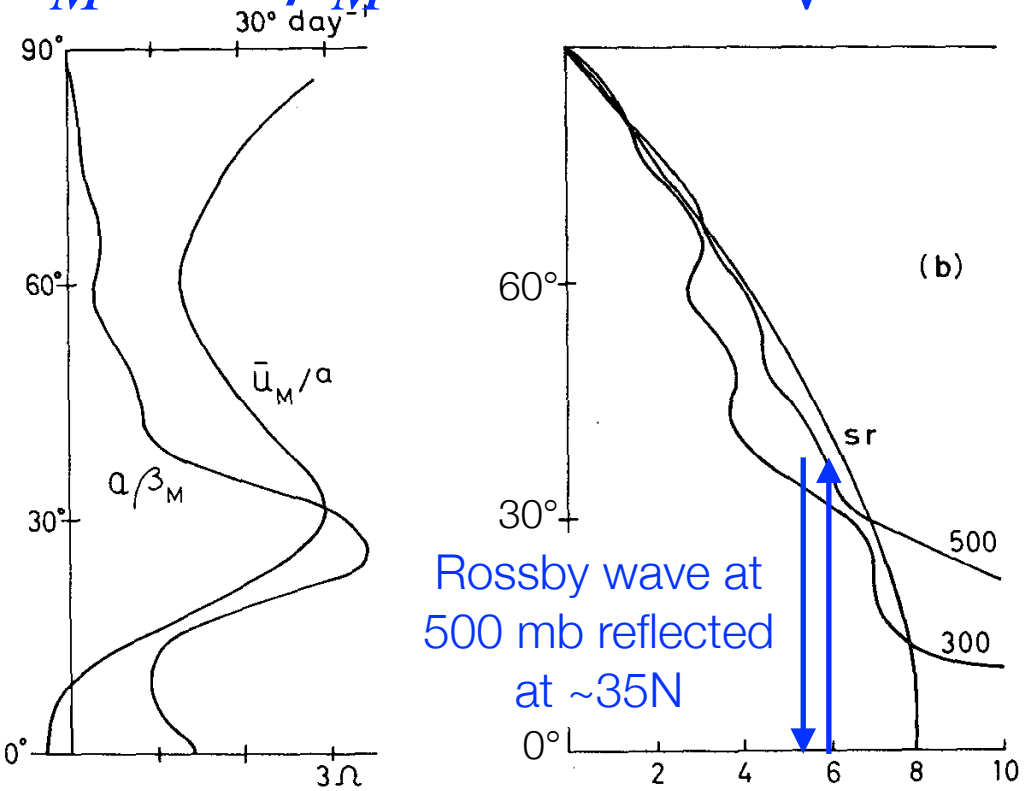

FIG. 13. (a) $\bar{u}_M/a$ (deg day^{-1}) and $a\beta_M$ for the 300 mb NH winter flow used in the model. (b) Stationary wavenumbers aK_s for the super-rotation flow, and the 500 and 300 mb NH winter flow.

Hoskins and Karoly 1981

graduate level

ENSO teleconnections

example teleconnection patterns

$\bar{u}_M/a,\ a\beta_M$ $\qquad aK_s = \sqrt{\bar{u}_M/\beta_M}$

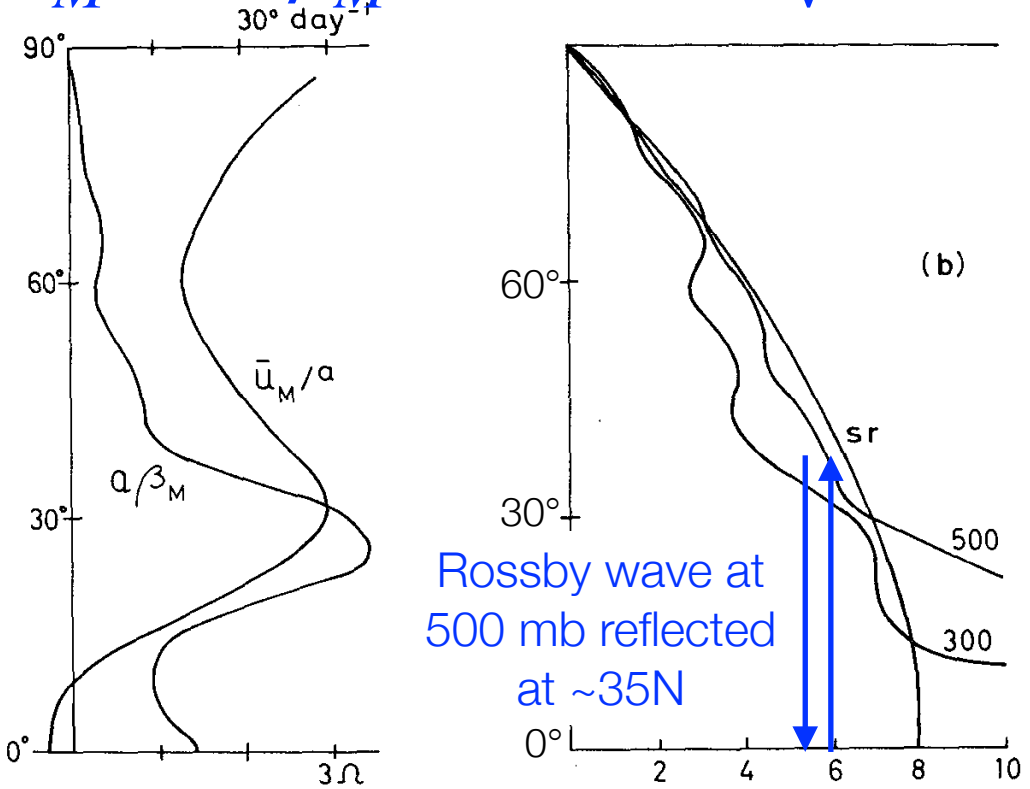

FIG. 13. (a) $\bar{u}_M/a$ (deg day^{-1}) and $a\beta_M$ for the 300 mb NH winter flow used in the model. (b) Stationary wavenumbers aK_s for the super-rotation flow, and the 500 and 300 mb NH winter flow.

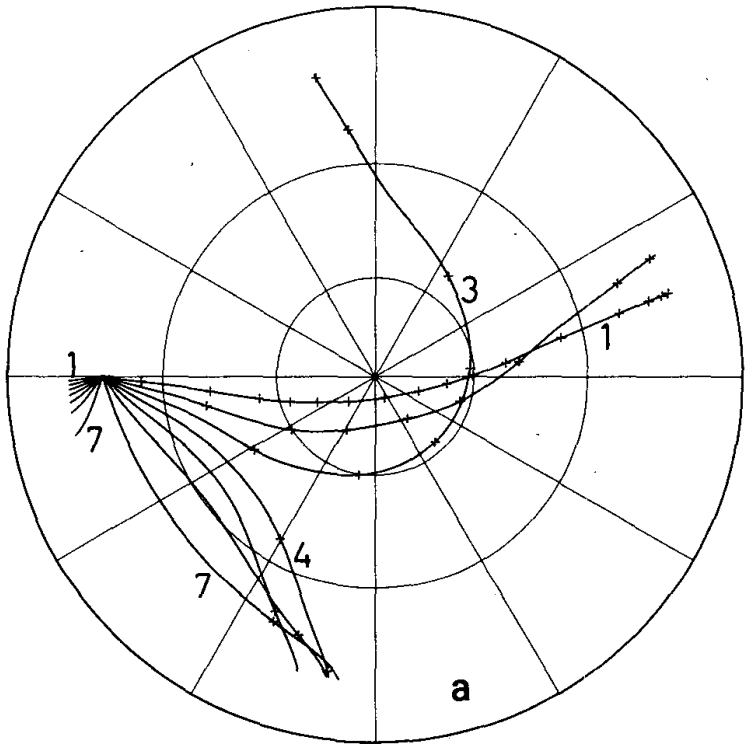

FIG. 15. A 15° source in the NH 300 mb zonal flow: (a) rays and propagation time marked by crosses every 2 days, and

Hoskins and Karoly 1981

graduate level

ENSO teleconnections

an example using the python code on course web page, should be useful for HW

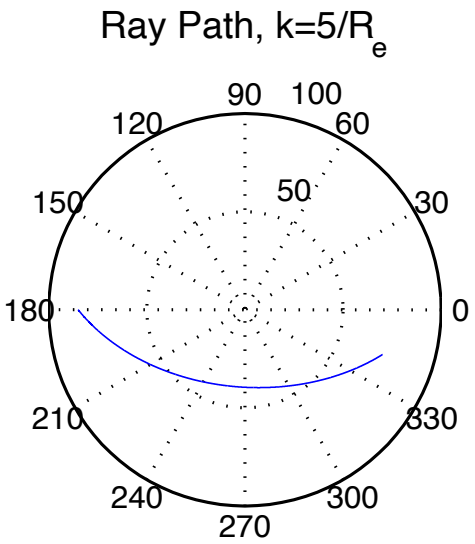

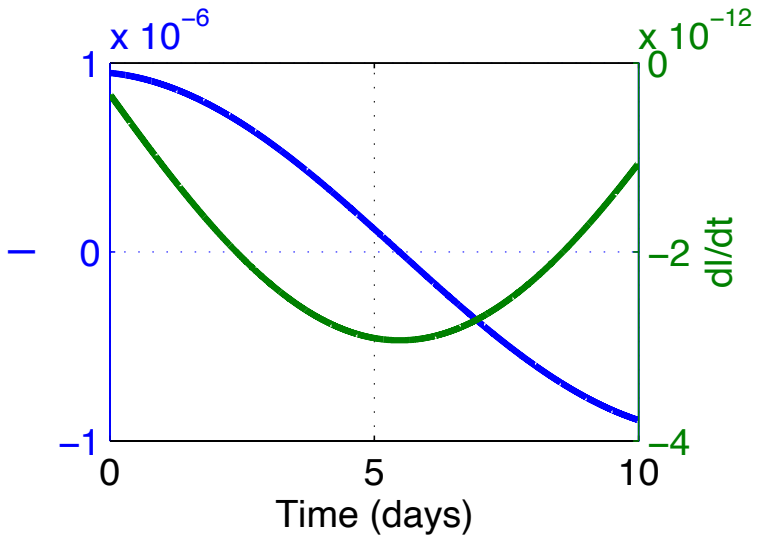

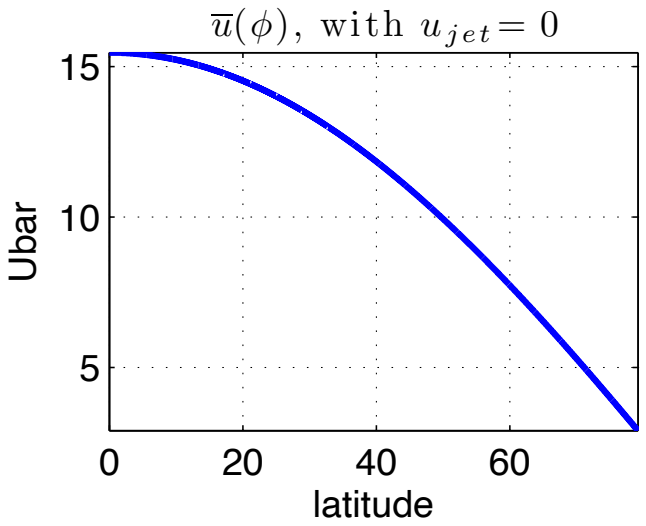

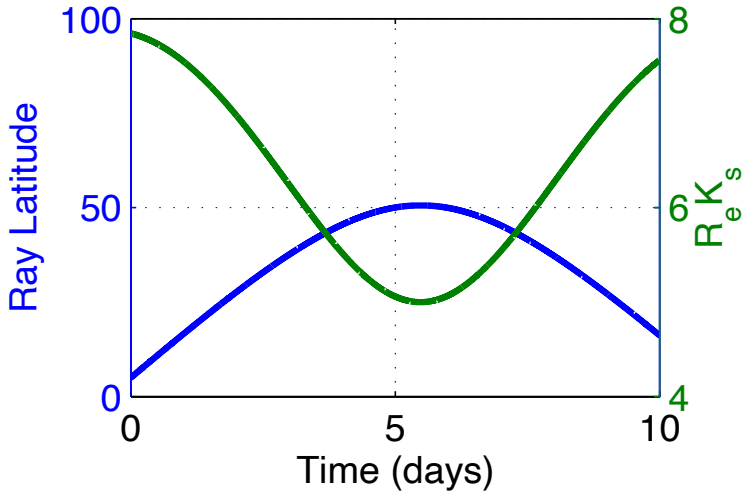

graduate level

ENSO diversity/ complexity

Examples of different El Niño/ La Niña types

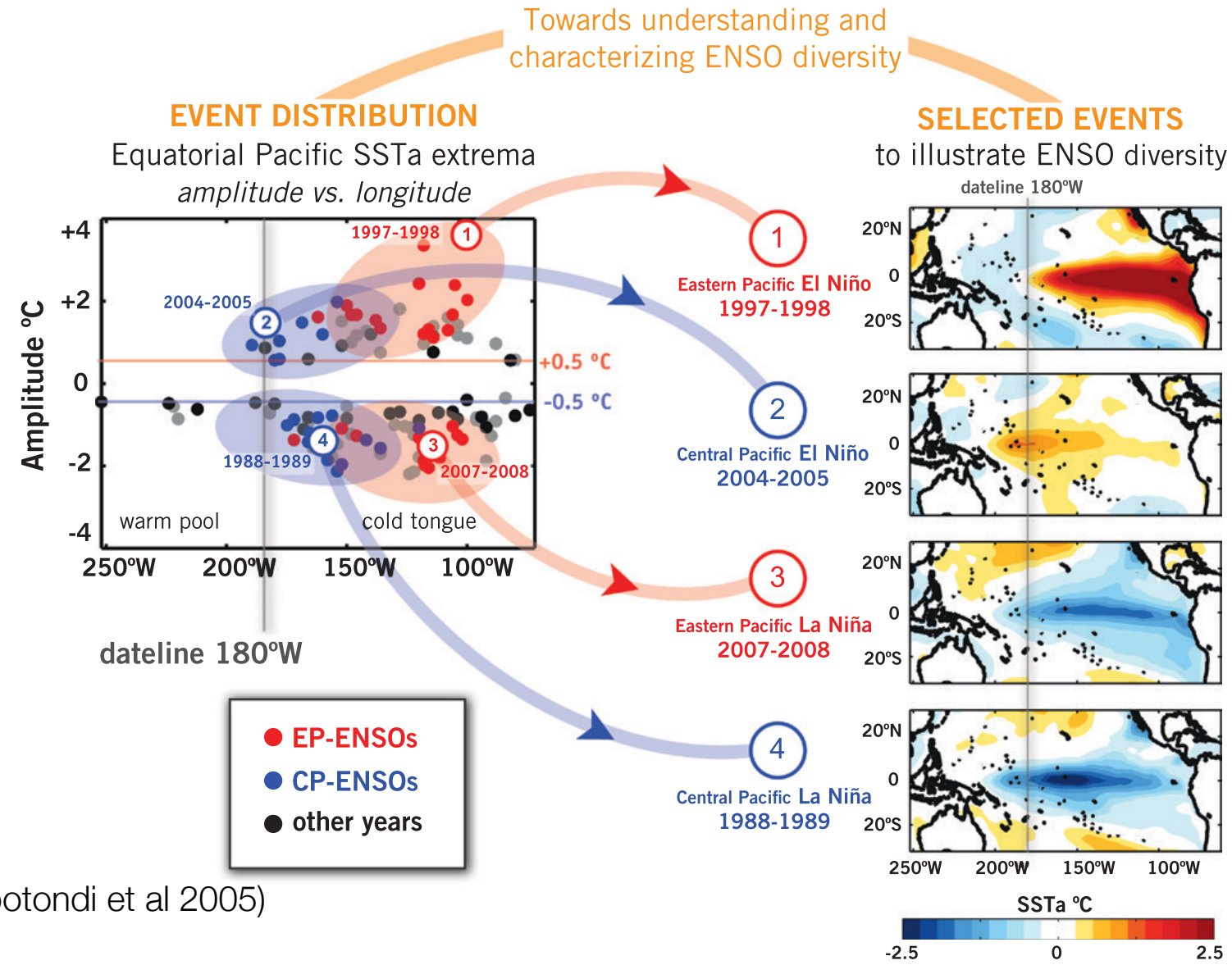

(Capotondi et al 2005)

Large events are EP (East Pacific) El Niños…

graduate level

Examples of different El Niño/ La Niña types

Fig. 1. (left) Distribution of boreal winter [Nov–Jan (NDJ)] SSTA extrema in the longitude–amplitude plane. Anomalies were obtained from the National Oceanic and Atmospheric Administration (NOAA) extended reconstructed SST dataset (Smith and Reynolds 2004) over the period 1900–2013, as departures from the 1945–2013 climatology. Each dot corresponds to the extreme positive or negative value over the NDJ of each year in the region 2°S–2°N, 110°E–90°W. Events prior to 1945 are colored in gray. Events after 1945 are considered EP (red dots) when the Niño-3 index exceeds one standard deviation. CP events are identified using the leading principal component of the SSTA residual after removing the SSTA regression onto the Niño-3 index. Blue dots in the left panel correspond to events for which the leading principal component (used as CP index) exceeds one standard deviation. (right) The spatial patterns of SSTA for specific warm and cold events of either type are shown, with a contour interval of 0.25°C.

(Capotondi et al 2005)

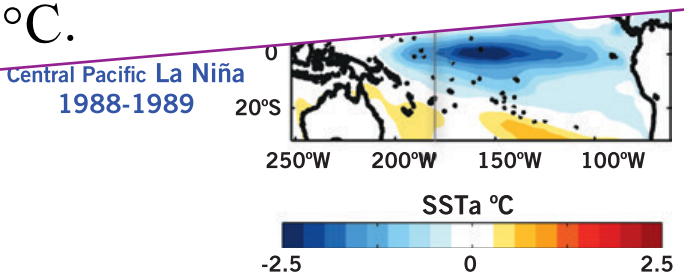

Large events are EP (East Pacific) El Niños…

graduate level

Thermocline feedback is weaker for CP (Central Pacific) events

Composite evolution of zonally averaged thermocline depth, as a func of latitude & time, for El Niño events in a 500-yr preindustrial simulation from CCSM4. The selected events peak in **(a)** Niño-3 region (5°S–5°N, 150°–90°W), **(b)** Niño-4 region (5°S–5°N, 160°E–150°W), & **(c)** 20° to west of the Niño-4 area.

(Capotondi et al 2005)

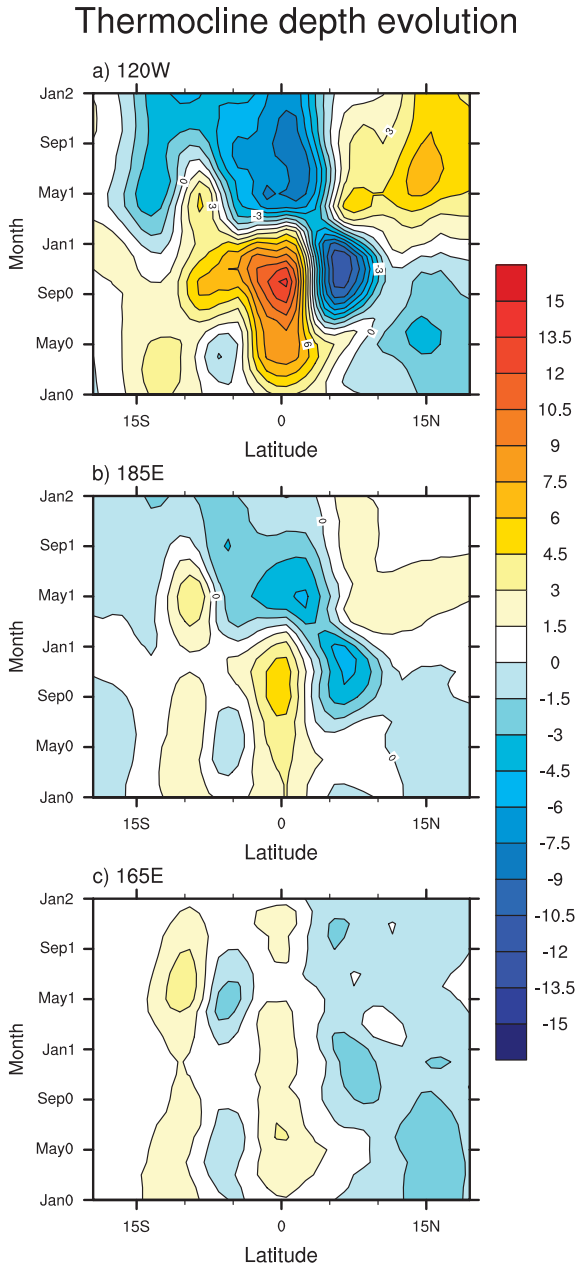

Zonal advective feedback: Positive feedback, particularly effective in the central Pacific, in which a positive (negative) equatorial SSTA weakens (strengthens) equatorial trade winds, reducing (enhancing) the oceanic transport of cold waters from the eastern Pacific. (Timmermann et al 2018)

EP & CP ENSO mechanisms: Thermocline vs zonal advection feedbacks

a, b, Leading two eigenmodes of SSTA & thermocline depth anomalies w/periods of 4 yr (QQ) and 2 yr (QB), from CZ model. Different roles of zonal advective feedback (ZAF) and thermocline feedback (TF).

[analysis: d**X**/dt=*A***X**, *A* has 2 main eigenmodes, rest are strongly damped]

c, Growth rates of 2 modes as func of mean thermocline depth H & mean wind strength. 2 dots: mean state for modes.

d–f, obs of SSTAs & 20°C depth for EP & CP El Niños & La Niñas, w/ key mechanisms: annual cycle (ACY), WWEs, South Pacific booster (SPB), North/South Pacific meridional modes (NPMM/ SPMM), tropical instabilty waves (TIW). Curly arrows: damping net surface heat flux (HF) feedback.

(Timmermann et al 2018; Xie and Jin 2018)

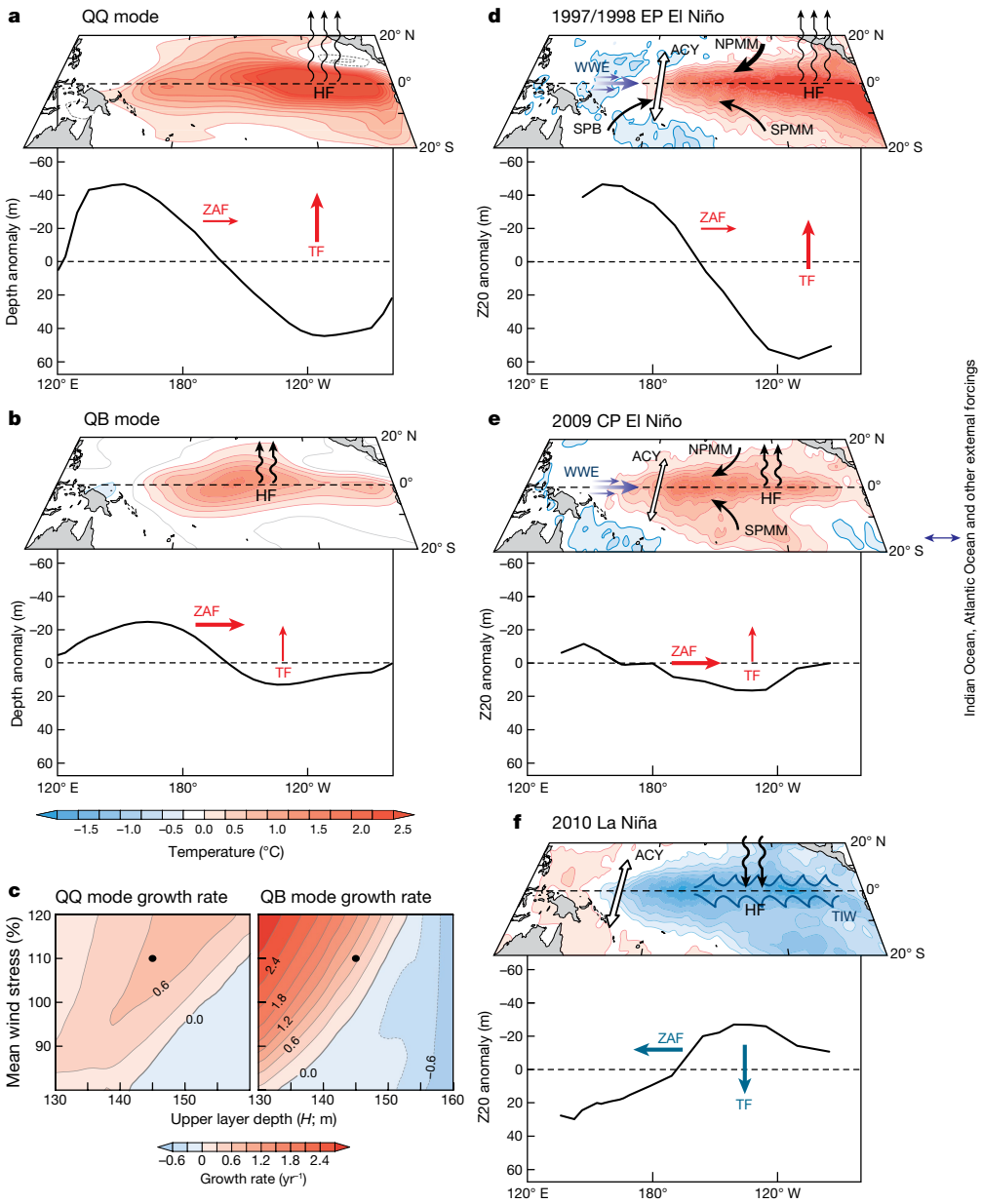

graduate level

Different teleconnections for EP and CP ENSOs

Composites of U.S. temperature anomalies during autumn [Sep–Nov (SON)] and winter (DJF) for conventional (i.e., EP) and dateline (i.e., CP) El Niños during 1950–2003.

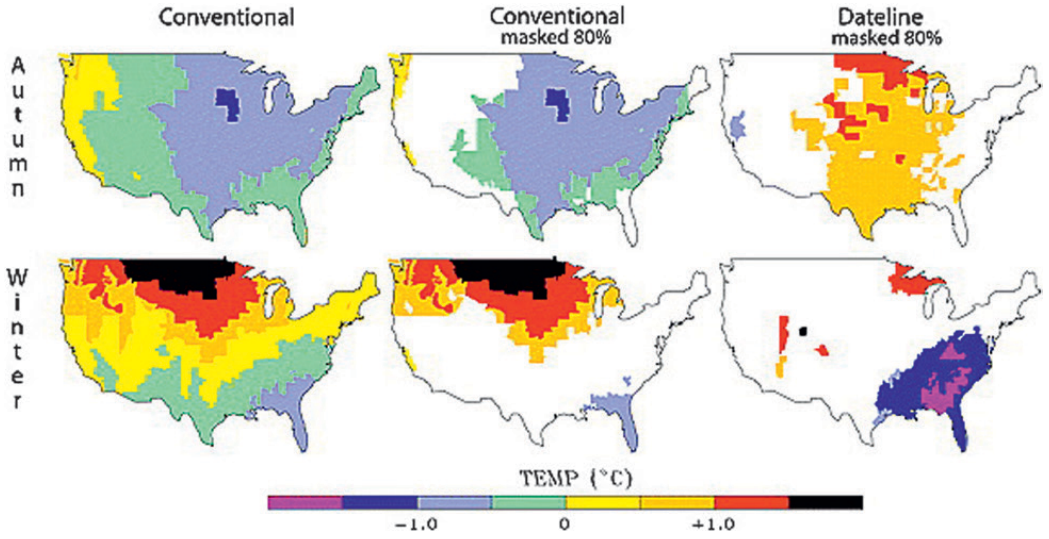

same, for U.S. precipitation anomalies.

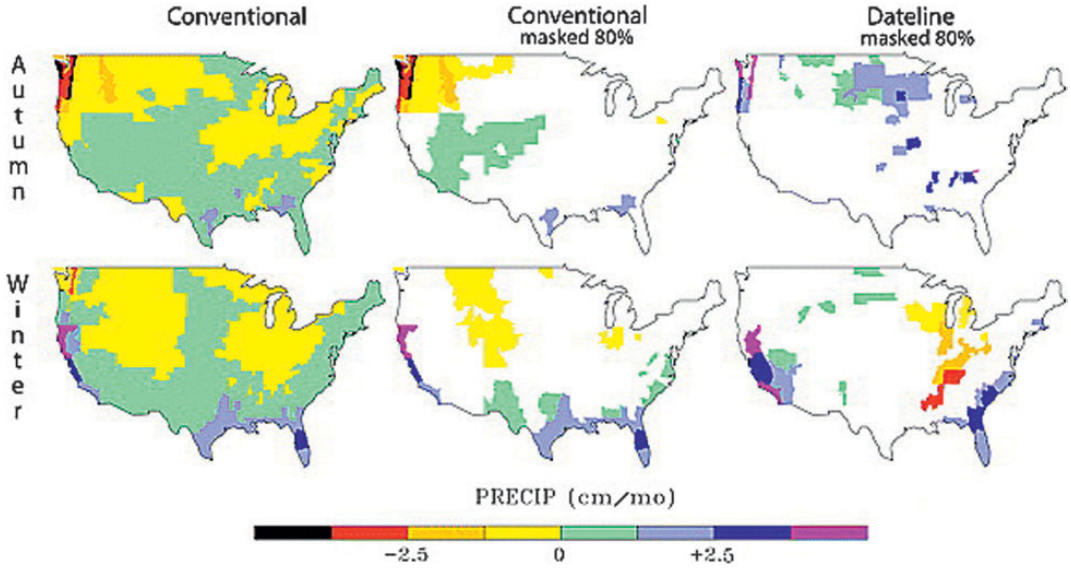

(Capotondi et al 2005)

graduate level

Summary

- Observed features of El Niño:

Eastern tropical Pacific warms & trade winds weaken for nearly a year, every 3-6 years; affects weather worldwide: fires in Australia, floods in South America, droughts in Africa, weather in the US

Summary

- Observed features of El Niño:

Eastern tropical Pacific warms & trade winds weaken for nearly a year, every 3-6 years; affects weather worldwide: fires in Australia, floods in South America, droughts in Africa, weather in the US

- Observations: moored buoy arrays, satellites, drifting buoys, ships

Summary

- Observed features of El Niño:

Eastern tropical Pacific warms & trade winds weaken for nearly a year, every 3-6 years; affects weather worldwide: fires in Australia, floods in South America, droughts in Africa, weather in the US

- Observations: moored buoy arrays, satellites, drifting buoys, ships

- Physical mechanism: El Niño starts due to a positive feedback between trade winds, Sea Surface Temperature and Kelvin waves/ thermocline tilt. El Niño ends due to delayed ocean adjustment through equatorial internal Rossby waves.

- Why is it irregular and difficult to predict?

Weather as stochastic forcing vs nonlinearity & large-scale chaos

Summary

- Observed features of El Niño:

Eastern tropical Pacific warms & trade winds weaken for nearly a year, every 3-6 years; affects weather worldwide: fires in Australia, floods in South America, droughts in Africa, weather in the US

- Observations: moored buoy arrays, satellites, drifting buoys, ships

- Physical mechanism: El Niño starts due to a positive feedback between trade winds, Sea Surface Temperature and Kelvin waves/ thermocline tilt. El Niño ends due to delayed ocean adjustment through equatorial internal Rossby waves.

- Why is it irregular and difficult to predict?

Weather as stochastic forcing vs nonlinearity & large-scale chaos

- ENSO diversity: CP vs EP, different mechanism & teleconnections

Summary

- Observed features of El Niño:

Eastern tropical Pacific warms & trade winds weaken for nearly a year, every 3-6 years; affects weather worldwide: fires in Australia, floods in South America, droughts in Africa, weather in the US

- Observations: moored buoy arrays, satellites, drifting buoys, ships

- Physical mechanism: El Niño starts due to a positive feedback between trade winds, Sea Surface Temperature and Kelvin waves/ thermocline tilt. El Niño ends due to delayed ocean adjustment through equatorial internal Rossby waves.

- Why is it irregular and difficult to predict?

Weather as stochastic forcing vs nonlinearity & large-scale chaos

- ENSO diversity: CP vs EP, different mechanism & teleconnections

- Future projections: unclear how frequency/ amplitude will change

The End